TRANSDERMAL DRUG DELIVERY ENHANCED BY MAGAININ PEPTIDE

A Thesis Presented to

The Academic Faculty

By

Yeu Chun Kim

In Partial Fulfillment of

the Requirement for

the Degree Doctor of Philosophy

in Chemical and Biomolecular Engineering

Georgia Institute of Technology

December 2007

TRANSDERMAL DRUG DELIVERY ENHANCED BY MAGAININ PEPTIDE

Approved by:

Dr. Mark R. Prausnitz, Advisor
School of Chemical & Biomolecular Engineering
Georgia Institute of Technology

Dr. Peter J. Ludovice, Co-advisor
School of Chemical & Biomolecular Engineering
Georgia Institute of Technology

Dr. Ronald W. Rousseau
School of Chemical & Biomolecular Engineering
Georgia Institute of Technology

Dr. William J. Koros
School of Chemical & Biomolecular Engineering
Georgia Institute of Technology

Dr. Christopher W. Jones
School of Chemical & Biomolecular Engineering
Georgia Institute of Technology

Dr. Ajay K. Banga
Department of Pharmaceutical Sciences
College of Pharmacy & Health Sciences
Mercer University

Date Approved: Octorber 12, 2007

To my wife and family…

ACKNOWLEDGEMENTS

I would like to give thanks to my two advisors, thesis committee members, funding sources, colleagues, friends, and family who have given me support and have helped make this thesis possible. First and foremost, I would like to thank my advisors at Georgia Tech; I appreciate Mark Prausnitz for his patience, intellect, passion, and thesis advice and, for giving me the opportunity to work in his lab and helping me grow as a researcher; I appreciate Pete Ludovice for his kindness, consideration, humor, brilliant ideas, and thesis advice as well as for giving me the opportunity to work in his lab and helping me grow as a researcher.

I would also like to thank Dr. Ronald W. Rousseau, Dr. William J. Koros, Dr. Christopher W. Jones, and Dr. Ajay K. Banga for serving as members of my thesis committee and for their scientific advice.

I would like to thank my funding source: the National Institutes of Health, U.S.

I would like to thank those past and present members of the Prausnitz's Drug Delivery Laboratory and Ludovice's Molecular Modeling Laboratory who have helped me in my research and for being such great colleagues and friends: Wijaya Martanto, Jason Jiang, Robyn Schlicher, Sean Sullivan, Harvinder Gill, Vladimir Zarnitsyn, Mangesh Deshpande, Esi Ghartey-Tagoe, Pavel Kamaev, Samantha

Andrews, Prerona Chakravarty, Ping Wang, Jeong-Woo Lee, Jung-Hwan Park, Samir Patel, Ying Liu, Jyoti Gupta, James Norman, Leonard Chu, Josh Hutcheson, Ayanna Bernard, Brett Brotherson, Derrick Callander, Andrew Swann, Wei Zhang.

I would especially like to thank the undergraduate researchers and collaborators who have helped with this work: Graham Thorsteinson, Andria Pate, Seong-O Choi, Sameer Late.

I would like to thank those at the IBB and Georgia Tech who have helped with this thesis: Donna Bondy for great support and kindness; Johnafel Crowe for confocal and flow cytometry expertise; Tracy Couse for her kind help with histology.

I would like to thank those at Emory Hospital for donating skin and helping with peptide synthesis.

I would like to thank the 'Georgia Tech Chemical and Biomolecular Engineering Korean Student Ascociation' members and proessor Jay Lee.

I would like to thank the 'Georgia Tech Korean Tennis Club' and the 'Georgia Tech Korean Soccer Club' members.

Most of all, I would like to acknowledge the family closest to me: my parents for their unconditional love and support. Their invaluable guidance provided the bearing in my life and I hope to continue in the example they have set. My father's wisdom and strict advice will always be remembered, and my mother's love and

confidence continues to inspire me. I want to especially thank my father-in-law for his attention and helpful research advice. I also thank my mother-in-law her belief and love.

I thank my two sisters for their love, support, and tolerance towards their little brother. I thank sister-in-laws and brother-in-laws for their affection.

Finally, but definitely not least, I would like to acknowledge Sonia Choy, my lovely wife, for being my best friend, my love, and my companion. Her words of encouragement and contribution in my life and work cannot be overstated. Without her support and sacrifice, none of this thesis would be possible.

TABLE OF CONTENTS

LIST OF TABLES

LIST OF FIGURES

LIST OF SYMBOLS AND ABBREVIATIONS

ANOVA	analysis of variance
ANTP	Antennapedia transduction sequence
AMP	antimicrobial peptide
CD	circular dichroism spectra
CMC	critical micelle concentration
DSC	differential scanning calorimetry
FDA	Food and Drug Administration
FT-IR	Fourier transform infrared spectroscopy
GRAS	Generally Recognized As Safe
LB	lipid bilayer lamellae
MG	magainin peptide
NLS	N-lauroylsarcosine
PBS	phosphate buffered saline
TDDS	transdermal drug delivery system
XRD	x-ray diffraction

SUMMARY

The world-wide transdermal drug delivery market is quite large, but only a small number of agents have FDA approval. The primary reason for such limited development of this market is the difficulty in permeating the *stratum corneum* layer of human skin. Compressed lipid bilayers comprise the continuum portion of this layer, which is the primary barrier in skin. Various physical and chemical methods have been tested to increase the permeability of the *stratum corneum* to drugs. However, few have succeeded in delivering relevant agents at the appropriate flux levels without causing notable skin irritation or damage.

In our study, we developed a novel percutaneous delivery enhancing approach. Magainin peptide was previously shown to disrupt vesicles which are made from lipid bilayer components representative of those found in human *stratum corneum* and this ability of magainin allows us to propose that magainin can increase skin permeability. Therefore, we tested the hypothesis that magainin, a peptide believed to form pores in bacterial cell membranes, can increase skin permeability by disrupting *stratum corneum* lipid structure. We further hypothesized that magainin's enhancement requires co-administration of a surfactant chemical enhancer to increase magainin penetration into the skin. In support of these hypotheses, synergistic enhancement of

transdermal permeation can be observed with magainin peptide in combination of N-lauroyl sarcosine (NLS) in 50% ethanol-PBS solution. The exposure to a known surfactant chemical enhancer, NLS, in 50% ethanol solution increased *in vitro* skin permeability to fluorescein 15 fold and the combination of magainin and NLS-ethanol synergistically increased skin permeability 47 fold. In contrast, skin permeability was unaffected by exposure to magainin without co-enhancement by NLS-ethanol.

The exact mechanism of this synergistic effect has not been elucidated, so several characterization methods such as differential scanning calorimetry, Fourier transform infrared spectroscopy, and X-ray diffraction were applied to investigate the mechanism of synergistic enhancement. These analyses showed that NLS-ethanol disrupted *stratum corneum* lipid structure and that the combination of magainin and NLS-ethanol disrupted *stratum corneum* lipids even further. Furthermore, confocal microscopy showed that magainin in the presence of NLS-ethanol penetrated deeply and extensively into *stratum corneum*, whereas magainin alone penetrated poorly into the skin. Together, these data suggest that NLS-ethanol increased magainin penetration into *stratum corneum*, which further increased *stratum corneum* lipid disruption and skin permeability.

In addition, we investigated the enhancement of modified magainin derivitives. The modification of magainin did not improve the transdermal enhancement

characterisitics of the peptide. The structure and lipid fluidization of peptides were not the main factors for percutaneous enhancement.

Finally, skin permeability was enhanced by changing the charge of magainin peptide via pH change and was dependent on the magainin concentration. We modulated pH from 5 to 11 to change the magainin charge from positive to neutral, which decreased skin permeability to a negatively charged model drug (fluorescein) and increased skin permeability to a positively charged drug (granisetron). This suggests that an attractive interaction between the drug and magainin peptide improves transdermal flux. Addition of salt above 1 M concentration caused the reduction of transdermal permeation, which indicated that permeation is reduced when magainin-fluorescein interactions are reduced at high ionic strength. Further modulation of pH to 12 increased skin permeability still further, which appeared to involve changes in intrinsic skin properties. Maximum skin permeability enhancement achieved in this study was 71 fold, which suggests these enhancers can be applied to transdermal drug delivery.

CHAPTER 1: INTRODUCTION

Over more than two decades, transdermal drug delivery has been developed to the stage where transdermal systems represent a feasible way of delivering clinically effective drugs. In the USA, out of 129 drug delivery candidate products under clinical evaluation, 51 are transdermal or dermal systems [1]. The worldwide transdermal market is currently more than US $ 4 billion and the annual US market for transdermal patches is more than US $ 3 billion. This technique represents the most successful non-oral systemic drug delivery system. Approximately 13 years ago, nicotine patches revolutionized smoking prevention. In addition, Nitroglycerin for angina, clondine for hypertension, scopolamine for motion sickness, and estradiol for estrogen deficiency are representative examples of successful transdermal patch products [2].

However, the major challenge in transdermal drug delivery system is to increase the variety of drugs which can be administered. This market is dispersed amongst only eighteen FDA-approved active agents: *scopolamine, nitroglycerin, clonidine, estradiol-norethindrone, fentanyl, nicotine, testosterone, ethinyl estradiol-norelgestromin, oxybutynin, 17-β estradiol, lidocaine, lidocaine-epinephrine, estradiol-levonorgestrel, lidocaine-tetracaine, fentanyl HCl, methylphenidate,*

selegiline, rotigotine, and rivastigmine. Only a small number of drugs are available using transdermal patch systems because of the low permeability of human skin (especially the outermost *stratum corneum* layer) which limits daily drug dosage to about 10 mg via an acceptable sized patch. Moreover, transdermal drug delivery is not suited to all drugs, nor is it justified for all therapies. Most of drugs transdermally administered should be small in molecular mass, highly lipophilic and require small dosages [1,3,4]. Only a limited number of drugs have been successfully delivered into the skin, so various methods such as iontophoresis, electroporation, sonophoresis, *stratum corneum* ablation, microneedles, and chemical enhancers have been investigated [5].

Conventionally, active agents are mostly administered to the body by periodic applications. In medical treatment, drugs are introduced in intervals by ingestion of pills, liquids or by injection and then circulate throughout the body. The concentration of the active agent rises and falls, therefore the initially high concentrations may be toxic and cause side effects both to the target organ and neighboring structures. When the concentration diminishes, which is hard to monitor, careful calculation of the amount of the residual active agent should be made to avoid overdosing. Due to natural metabolic processes, a second dose must be administered to prevent the concentration from dropping below the minimum effective level [6].

In transdermal administration of medication, the above problems can be largely eliminated because the drug diffuses over a prolonged period of time directly into the bloodstream. The advantages of transdermal delivery include therapeutic benefits like sustained plasma concentration profile, reduction of systemic side effects, improvement of patient compliance by reducing dosing schedule, avoidance of the first-pass metabolism, convenience, patient-friendliness, and non-invasive administration [7].

In spite of the abundant advantages of transdermal delivery systems, there are some obstacles to its widespread application. Transdermal transport of molecules is slow due to low permeability of the *stratum corneum*, the uppermost layer of the skin. Another serious obstacle to transdermal drug delivery is the possibility of adverse skin reactions known as contact allergic dermatitis [6].

In this study we tested the hypothesis that magainin, a peptide believed to form pores in bacterial cell membranes, can increase skin permeability by disrupting the *stratum corneum* lipid structure. We further hypothesized that magainin's enhancement requires co-administration with a surfactant chemical enhancer to increase magainin penetration into the skin. Additionally, we tested the hypothesis that greater increases in skin permeability can be realized by manipulating the charge properties of the magainin peptide by changing pH.

We believe this is the first study to demonstrate the use of a pore-forming peptide to increase skin permeability. This study also introduces the novel concept of using a first chemical enhancer to increase penetration of a second chemical enhancer into the skin to synergistically increase skin permeability to a model drug. We hope we will be able to propose the mechanism that the pore-forming peptide uses to increase skin permeability, based on all collected data in this study.

CHAPTER 2: BACKGROUND

2.1. Structure and anatomy of the human skin

Skin is one of the largest organs of the body. It consists of two parts: the cellular outermost layer, epidermis, and the inner connective tissue layer, dermis. Lying between these two layers is a microscopic structure, the basal lamina or basement membrane zone. (Figure 2.1)

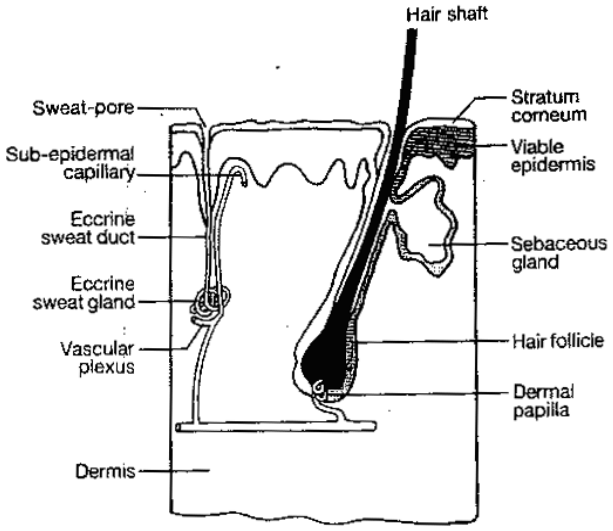

Figure 2. 1 Schematic representation of the skin. Reproduced from reference [8]

The epidermis is composed of two parts: the living cells of the Malpighian layer and the dead cells of the *stratum corneum* commonly referred to as the horny layer. The prime function of the viable cells of the epidermis is to move progressively

through a process of differentiation, eventually expiring to generate the barrier layer of *stratum corneum* [9]. The epidermis is a continually self-renewing, stratified squamous epithelium covering the entire outer surface of the body. (Figure 2.2) Over most of the body the epidermis ranges in thickness from 0.06 to 0.1 mm. The major cell of the epidermis is the keratinocyte and other important cellular elements include the melanocyte (the source of melanin pigment), the Langerhans cell which is part of the immune surveillance system, and the Merkel cell which functions as a mechanoceptor for the sensation of touch [10].

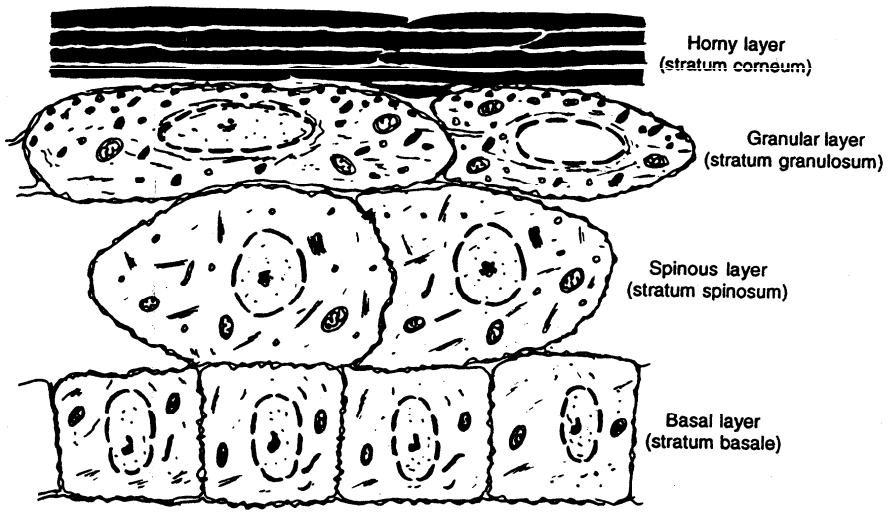

Figure 2. 2 Diagram of the different layers of epidermis. Reproduced from reference [8]

The *stratum corneum* is the end product of epidermal differentiation and consists of 15 to 25 cell layers over most of the body surface [11]. Change in the composition of the lipids during keratinization is shown in Table 2.1. The corneocyte is the largest cell in the *stratum corneum*, approximately 0.5 μm in thickness and 30 to 40 μm in width. It contains no organelles but is filled with protein, 80% of which is high molecular-weight keratin. The intercellular space is filled with lipids organized into multiple bilayers and these lipids are of unusual composition. Approximately 14 % of the *stratum corneum*, by weight, is lipids. In addition, *stratum corneum* has very low water content [12]. Formation of the *stratum corneum* is also accompanied by the deposition of a 15 nm thick band of protein on the inner surface of the plasma membrane, the cornified cell envelope, a structure unique to keratinocytes and a hallmark of the terminal differentiation [13].

The natural function of the skin is to protect the body against exogenous material, dehydration, and environmental stress. The major barrier towards inward and outward diffusion of compounds is the outermost layer of the skin, *stratum corneum* [14]. *Stratum corneum* consists of lipid-depleted and keratinized cells (corneocytes) embedded in a lamellar lipid-rich interstitium. Unique lipid arrangements which occupy the space of *stratum corneum*, play a critical role in

Table 2. 1 Change in the composition of the lipids during keratinization. Reproduced from referenc [15]

Percent ± SEM	Epidermis	*Stratum corneum*
Phospholipids	**45 ± 3.6**	**2.0 ± 0.5**
Cholesterol sulfate	**3 ± 0.5**	**1.5 ± 0.4**
Neutral lipids	**44 ± 1.8**	**66.0 ± 2.8**
Cholesterol	14 ± 1.8	32 ± 2.5
Free fatty acid	9 ± 1.5	20 ± 2.0
Triglycerides	12 ± 2.0	2 ± 0.5
Cholesterol esters	6 ± 1.0	10 ± 1.0
Squalene	3 ± 0.5	2 ± 0.5
Sphingolipids	**8 ± 1.5**	**30 ± 3.5**
Glucosylceramides	5.5 ± 0.5	traces
Ceramides	2.5 ± 0.5	30 ± 3.0

* SEM: standard error of the mean

establishing the barrier function and in maintaining cohesion between corneocytes [15].

The main lipid components of *stratum corneum* are ceramides, cholesterol, and free fatty acids, which make up approximately 50, 25, 10 percent of *stratum corneum* lipid mass [16]. The minor lipid components are glucosylceramides, cholesterol sulfate and cholesterol esters. In contrast with cellular membranes, ceramides located in the intercellular spaces cannot form bilayers by themselves, so cholesterol, free fatty acids, and cholesterol sulfate are required to form ordered structures. The lipid bilayer containing these components dramatically reduces skin permeability [17].

1) Ceramides

The ceramides in the *stratum corneum* can be separated into eight classes of different polarity, head-group architecture, and fatty acid chain length. The differences in chemical structure of the ceramides are assumed to be important for the characterisitic organization of *stratum corneum* lipids [17]. (Figure 2.3)

2) Cholesterol

Cholesterol decreases the interfacial line tension between phases, acting at the borders between different regions on the surface [18]. Cholesterol is the most

abundant individual lipid class in the *stratum corneum*, accounting for around 25% of the *stratum corneum* lipid mass [19].

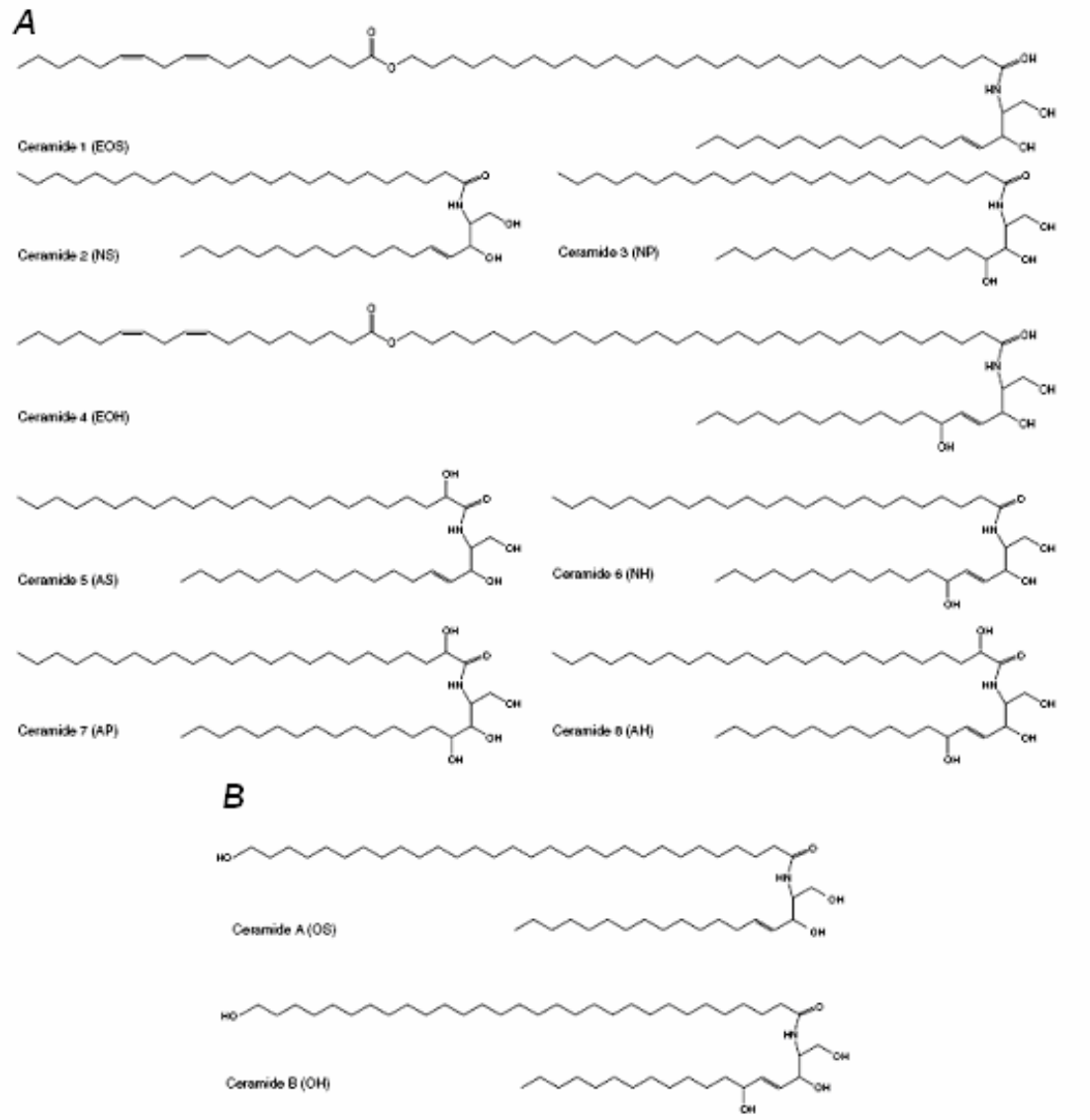

Figure 2. 3 Structures of the (A) eight major free ceramides and (B) two protein-bound ceramides of the human stratum corneum. A = α-hydroxy acid; E = ω-acyl-oxyacid or esterified ω-hydroxy acid; H = 6-hydroxysphingosine; N = nonhydroxyacid; O = ω-hydroxy acid; P = phytosphingosine; S = sphingosine. Reproduced from reference [20]

Cholesterol is capable of either fluidizing membrane domains or of making them more rigid depending on its concentration. The main role of cholesterol in the epidermal barrier is to provide a required degree of fluidity to what could otherwise be a rigid, possibly brittle membrane system [14].

3) Free fatty acids

Free fatty acids increase the lipid lattice density, which is critical for making an effective skin barrier [14]. The fatty acids are required for formation of a lamellar phase, since this is the principal ionizable lipid class in the *stratum corneum* [21]. Linoleic acid plays a direct role in the epidermial barrier function by incorporating two unique sphingolipids: acylglucosylceramide and acylceramide [15]. The fatty acid composition of the intercellular lipid plays an important role in the *stratum corneum* barrier and in the pH variations in the different *stratum corneum* layers [22].

4) Glucosylceramides

Glucosylceramides are the precursors of ceramides. Ceramide compounds are derived from the deglucosylation of polar glucosylceramides [23].

5) Cholesterol sulfate

Cholesterol sulfate is important for the desquamation process of skin. To inhibit certain enzyme activity in the lower layers in *stratum corneum* and maintain the elasticity of the skin, moderate levels of cholesterol sulfate in the intercellular regions are necessary. Also, in the presence of cholesterol sulfate, the solubility of cholesterol in the lipid mixtures increases [14,24].

2.2. *Stratum corneum* model

2.2.1 Brick and Mortar Model [25,26]

Elias depicted the *stratum corneum* skin barrier as a brick and mortar structure. The corneocytes represent the hydrophilic bricks and the intercellular lipids represent the hydrophobic mortar.

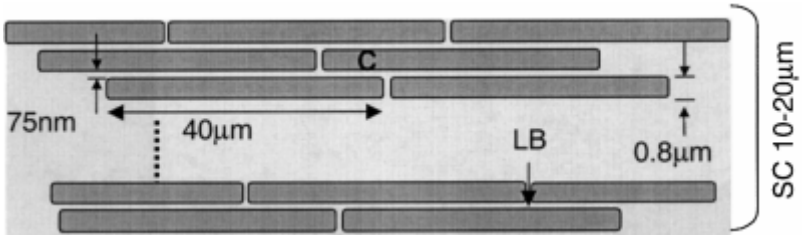

Figure 2. 4 Schematic illustration of the brick and mortar model of the SC. Reproduced from reference [27]

The corneocytes (C) are represented by the brick-like structures in the continuous phase of the lipid bilayer lamellae (LB) that comprise the intercellular space. In the *stratum corneum* - the first 10-20 μm of the skin - corneocytes have estimated dimensions of 40 μm in diameter and 0.8 μm in thickness, whereas the intercellular space thickness is estimated to be 75 nm [27]. (Figure 2.4)

2.2.2 Domain Mosaic Model [28,29]

Since the simplified "Brick and Mortar Model" cannot explain the complexity of the physical constraints on the lipid barrier, the "Domain Mosaic Model" was proposed. In the crystalline state, lipid aggregates corresponding to such mosaic domains are connected to each other by 'grain borders' within which the lipid units are actually in the fluid crystalline state.

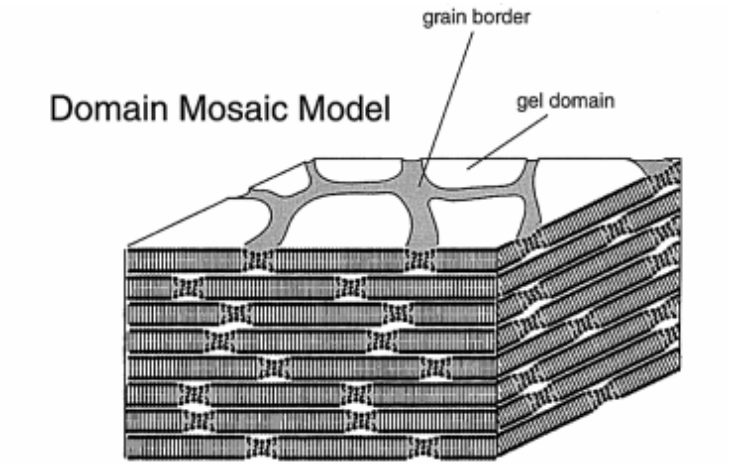

Figure 2. 5 Domain mosaic model. Note the presence of phase separation between liquid crystalline and gel domains. Reproduced from reference [30]

The bulk part of the barrier is mainly in the crystalline/gel state, which prevents water loss, and the fluid state grain borders allow some water to permeate the barrier towards the corneocytes for keratin pliability. This model provides the necessary mechanical properties permitting bending and stress imposed on the skin surface.

2.2.3 Sandwich Model [14,31]

The "Sandwich Model" was proposed in order to compensate for some flaws found in "Domain Mosaic Model". The "Domain Mosaic Model" requires the creation of new interfaces throughout the *stratum corneum.* Because liquid phase forms a narrow continuous pathway from the superficial *stratum corneum* layers down to the viable epidermis, substances would be able to diffuse only through this tortuous liquid phase, which might reduce the diffusional resistance of the skin. The "Sandwich Model" is based in the molecular arrangement of the lipids in the 13 nm phase. The liquid sublattice is located in the central part of the repeating unit and unsaturated linoleic acid, ceramide, and cholesterol are present in this central region. The liquid sublattice changes into a less mobile sublattice composed of hydrocarbon chains, which results in a densely packed lipid layer. Substances passing the *stratum corneum* lipid regions need to pass the crystalline lipid lamellae perpendicularly to the basal plane and permeate through two densely packed layers and one less densely

packed layer. So, the creation of liquid sublattice in the central layer keeps the skin barrier.

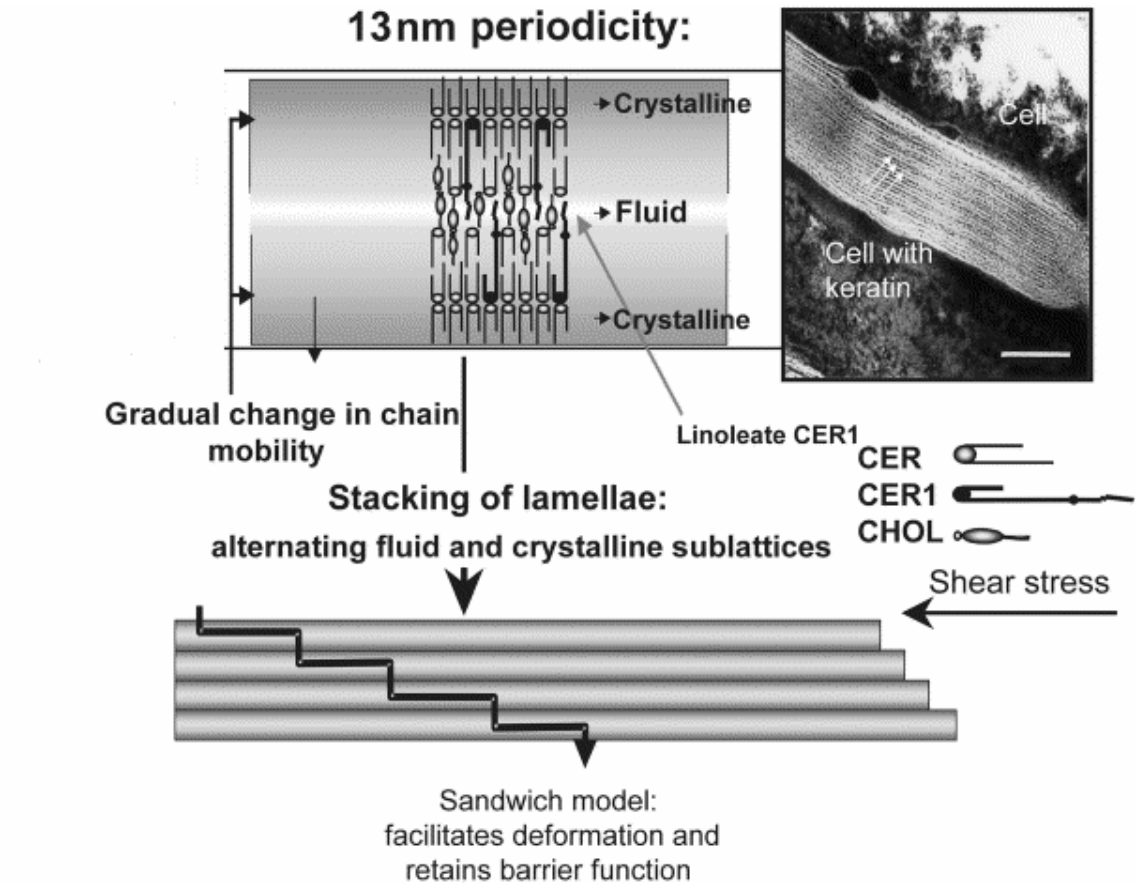

Figure 2. 6 Model for molecular arrangement of the long periodicity phase (LPP). The broad-narrow-broad pattern found in RuO_4 fixed *stratum corneum* is shown in right panel. A molecular model is presented in the middle panel, in which CER1 plays an important role in dictating the broad–narrow–broad sequence. Furthermore, the fluid phase is located in the central narrow band. In adjacent regions the crystallinity is gradually increasing from the central layer. Even in the presence of the central fluid layer the barrier function is retained while deformation as a consequence of shear stresses is facilitated. The latter might be of importance for the elastic properties of the skin. Reproduced from reference [31]

2.3. Transdermal drug delivery

Transdermal drug delivery systems (TDDS) deliver therapeutic quantities of drug through the skin and into the systemic circulation for their general effects. In such systems, the drug should penetrate across the skin to the underneath blood supply without drug accumulation in the dermal area. The drug initially penetrates through *stratum corneum* – the main rate limiting skin barrier – and then passes through the deeper epidermis and dermis. When drug reaches the dermal area, it becomes available for systemic circulation [32].

Some advantages of transdermal drug delivery are as follows [3,6,33].

- It can provide constant blood levels in the plasma for drugs with a narrow therapeutic window, thus minimizing the risk of toxic side effect or lack of efficacy.
- It can avoid first-pass metabolism in the gastrointestinal tract and liver, which allows drugs with poor oral bioavailability and short biological half-lives to be administered at most once a day, which can result in improved patient compliance.
- It can also avoid the problems of the gastrointestinal environment, such as chemical degradation of the drug and the resulting gastric irritation.

- It can provide a noninvasive alternative to parenteral, subcutaneous and intramuscular injections. The application of a patch-like device to the skin surface is a procedure that allows continuous intervention.
- It can provide predictable and extended duration of activity to reduce the frequency of dosage and minimize inter- and intrapatient variation.
- The large and readily accessible surface area (1-2 m^2) of skin allows many placement options for transdermal absorption.
- It is suitable for patients who are unconscious or vomiting and rely on self-administration

The transdermal drug delivery systems have disadvantages also. Only potent drugs are suitable candidates owing to the low permeability of skin and the potential of some drugs to cause skin irritation. The factors influencing the suitability of drugs for transdermal delivery using current technology are as follows [6,33].

- The daily systemic dosage must be below 20 mg.
- The molecular size of drug must be below 500 Da.
- The log P (lipophilicity) of drug should be in the range 1-3
- The melting point of drug should be below 200 ^oC.
- The drug should not irritate the skin
- The drug should not bring about immune response in the skin.

Table 2.2 describes some drugs currently using transdermal delivery. Although only a small numbers of drugs are currently used in transdermal systems, some other drugs being investigated recently include: diltiazem, isosorbide dinitrate, propranolol, nifedipine, mepindolo, verapamil, levonorgestrel/esradiol, physostigmine, xanomeline, naltrexone, methadone, buspirone, bupropion, and papaverine [32].

2.4. Percutaneous penetration enhancement

Penetration enhancers are substances that enhance the absorption of molecules through the skin by temporarily increasing its permeability. Ideal penetration enhancers should be pharmacologically and chemically inert, chemically stable, nontoxic, nonirritating, nonsenstizing, nonphototoxic, noncomedogenic, compatible with the drug and excipients, nonallergenic, ordorless, tasteless, colorless, cosmetically acceptable, and inexpensive. Further, they should have good solvent properties, a high degree of potency with specific activity, and produce reversible effects on skin properties. In addition, they should not lead to the loss of body fluids, electrolytes, and other endogenous materials [33].

Table 2. 2 Characteristics of several transdermally drugs delivered.

Reproduced from reference [2]

Active Ingredient	MW	Daily Dose	Type
Clonidine	230	0.1-0.3 mg	Reservoir
Estradiol	272	0.025-0.1 mg	Drug–in-Adhesive
Ethinyl Estradiol w/ Norelgestromin	296/328	0.15/0.02 mg	Drug–in-Adhesive
Fentanyl	337	Various	Reservoir / Martix
Lidocaine	234	Not stated	Drug–in-Adhesive
Nicotine	162	7-21 mg	OTC product Reservoir / Martix
Nitroglucerine	227	1.4-11.2mg	Drug–in-Adhesive /Reservoir
Scopolamine	303	0.33 mg	Reservoir
Testosterone	288	2.5-5 mg	Reservoir

2.4.1 Chemical percutaneous penetration enhancement

Chemical enhancers are assumed to operate in the intercellular spaces of the *stratum corneum*, which is the major diffusion route for lipophilic moieties. Although exact mechanisms have not been clearly elucidated, it is believed that they will have multiple effects once absorbed into the *stratum corneum*. Many different classes of chemical penetration enhancers have been investigated, including surfactants, fatty acids, esters, Azone, amines, amides, amino acetates, sulfoxides, urea, unsaturated cyclic ureas, terpenes, liposomes, and alcohols [34].

Azone (Figure 2.7) is a material that was developed specifically as a skin penetration enhancer to improve the absorption of topical agents [35]. Azone provokes dynamic structural disorder of the intercellular lamellar lipid structure throughout the *stratum corneum* and the creation of fluid domains involving the intercellular lipids, which was suggested by ^{2}H NMR assay [36]. Another mechanism was also proposed based on the alteration of the lateral bonding within *stratum corneum* lipid lamellae [37].

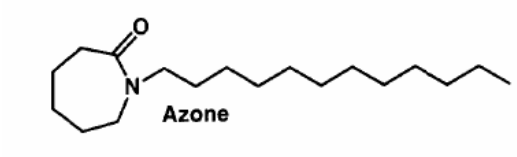

Figure 2. 7 Strucutre of Azone. Reproduced from reference [37]

Fatty acids have potential utility as skin permeation enhancers to improve the transdermal or topical delivery of drugs. In particular, oleic acid has been studied extensively [38]. The suggested mechanism of oleic acid–induced skin permeation includes lipid disordering, lipid fluidization, and phase separation deduced from *in vivo* [39] and *in vitro* [40] analysis.

Terpenes are hydroxyl cotaining dienes that are constituents of essential oils [41]. They are considered nontoxic with low irritancy and designated as Generally Recognized As Safe (GRAS) by the FDA [42]. The respective alcoholic terpenes, carvacrol, linalool and terpineol, were investigated in different solvents as transdermal enhancers: ethanol [43] and propylene glycol [44]. Those terpenes show high permeation of haloperidol in both solvents.

Ethanol was the good choice for the first enhancer to be incorporated into transdermal drug delivery. The interactions of ethanol with skin in terms of its permeation, primary irritation and cutaneous metabolism are better characterized than any other enhancer [45]. A permeation study of ethanol concentration demonstrated different result. Kurihara-Bergstrom showed 63 % is optimum [46], but Sznitowska found 25-50 % is the optimum concentration for skin permeability enhancement [47]. The mechanism of ethanol permeation enhancement was suggested as alteration of the

stratum corneum keratinized protein conformation, the extended hydrophilic domain between lipid polar head group, or lipid extraction [46].

Recently, a silicon-based transdermal penetration enhancer which was expected to show a low irritation to the skin was developed. This enhancer was considered to prevent inflammation even after penetration through the skin, because it would remain in the *stratum corneum* region owing to its high lipophilicity [48].

Surfactants as a chemical enhancer are discussed below.

2.4.2 Skin penetration enhancement by surfactant.

Many surfactants are capable of interacting with the *stratum corneum* to increase the absorption of drugs and other active compounds from products applied to the skin. Skin penetration measurements are valuable in quantifying these effects and observing the influence of surfactant chemistry and concentration.

A surfactant interacts with skin by depositing onto the *stratum corneum*, thereby disorganizing its structure. Then surfactant can solubilize or remove lipids or water-soluble constituents in or on the surface of the *stratum corneum*. Finally it can be transported into and through the *stratum corneum*. This last effect is related to the surfactant and *stratum corneum* protein interaction and epidermal keratin denaturation [8].

In general, anionic surfactants are more effective than cationic and nonionic surfactants in enhancing skin penetration of target molecules. Some anionic surfactants interact strongly with both keratin and lipids, whereas the cationic surfactants interact with the keratin fibrils of the cornified cells and result in a disrupted cell-lipid matrix. Nonionic surfactants enhance absorption by inducing fluidization of the *stratum corneum* lipids [49].

Scheuplein and Ross reported that the capacity of the *statum corneum* to retain significant quantities of membrane-bound water is reduced in the presence of sodium dodecanoate and sodium dodecyl sulfate [50]. This effect is readily reversible upon removal of the agents. These investigations proposed that anionic surfactants alter the permeability of the skin by acting on the helical filaments of the *stratum corneum*, thereby resulting in the uncoiling and extension of α-keratin filaments to produce β-keratin. Then they cause an expansion of the membrane, which increases permeability [50]. However, more recent findings suggest that impairment of the skin's barrier properties is unlikely to result from changes in protein conformation alone. Based on differential scanning calorimetry results, sodium lauryl sulfate (SLS) disrupted both the lipid and the protein components [51].

The amount of surfactant that penetrates the skin after the disruption of the skin barrier depends on the monomer activity and the critical micelle concentration (CMC).

Above the CMC, the added surfactant exists as micelles in the solution and micelles are too large to penetrate the skin.

The extent of barrier disruption and penetration enhancement of a surfactant is also strongly dependent on surfactant structure, especially alkyl chain length. In general, studies have shown that surfactants having 12 carbons in their alkyl chain cause more disruption to the skin barrier and allow drugs to penetrate more readily than those that have more or less than 12 carbons. The explanation for this optimum of 12 carbons is not known yet [8].

2.4.3 Physical percutaneous penetration enhancement

Physical methods use electrical or mechanical phenomena to increase skin permeability. Iontophoresis, electroporation, sonophoresis, *stratum corneum* ablation, and microneedles are most promising methods.

Iontophoresis can transport charged molecules into the skin by electrophoresis using the passage of a direct electric current through the electrolyte solution containing the charged molecules to be delivered [52].

Electroporaton applies a brief high-voltage electric field pulse to create transient aqueous pathways across the lipid bilayers of *stratum corneum* and thus enhance permeation across bilayer lipid membranes in the *stratum corneum* [53].

Sonophoresis is the application of ultrasound to increase the permeation of drugs through the skin. The mechanism appears to be disruption of *stratum corneum* lipid bilayer structure [54].

Stratum corneum ablation can be achived by micro-dermbrasion which use a stream of aluminum oxide crystals [55] and laser-ablation which use high powered thermal pulse to vaporize a *stratum corneum* [56]**.**

Microneedles can pierce the skin and create micrometer-scale pores. Channels of micrometer dimensions are much larger than macromolecules and dramatically increase skin permeability to large drug molecules [57].

In addition, magnetophoresis which use the ability of magnetic fields to deliver diamagnetic materials through skin [58] and photomechanical waves which enhance the drug penetration across the skin by irradiating a drug solution with laser pulse and stressing the *stratum corneum* with photomechanical [59] have also been investigated.

2.4.4 Metabolic percutaneous penetration enhancement

A limitation of conventional topical enhancement method was the usage of devitalized skin, because non-viable skin does not show metabolic response against barrier perturbation [60]. In case of *in vivo* skin, if the lipid - the determinant of skin

barrier function - was perturbed by chemical agents, the skin barrier recovery will be followed by lipid synthesis [61]. The concept of metabolic percutaneous enhancement method came from research that transdermal delivery enhancement by inhibition of critical metabolic sequence that restores skin barrier function. The classification of various metabolic percutaneous enhancement methods are as followings: lipid synthesis inhibitors, lamellar body secretion inhibitors, extracellular acidification inhibitors, sphingosine (precursor for ceramide) inhibitor, etc [60,62].

2.5. Antimicrobial and cell-penetrating peptide

Antimicrobial peptides have been shown to kill microbes with impressive potency and specificity and developed as therapeutic agents for infectious disease treatment. Permeating peptides can also be applied as carriers for delivery of foreign substances into microorganisms [63]. The natural antimicrobial peptides are normally 12-50 amino acids long and share two main characteristics. First, they are poly-cationic with positive net charge of more than +2. Second, they have the ability to form amphipathic structures with both positively charged and hydrophobic regions [63].

Microbial cell permeation by peptides can be seen as a three-step process. The first is an electrostatic attraction of the peptide to the membrane surface. (Figure 2.8) The second is membrane disruption, penetration and some reorganization of the peptide structure. Finally, peptide passes the membrane and gains access to the intracellular processes [64]. Within thes general framework, there are a number of more detailed models that describe the interaction of these peptides with cell membranes.

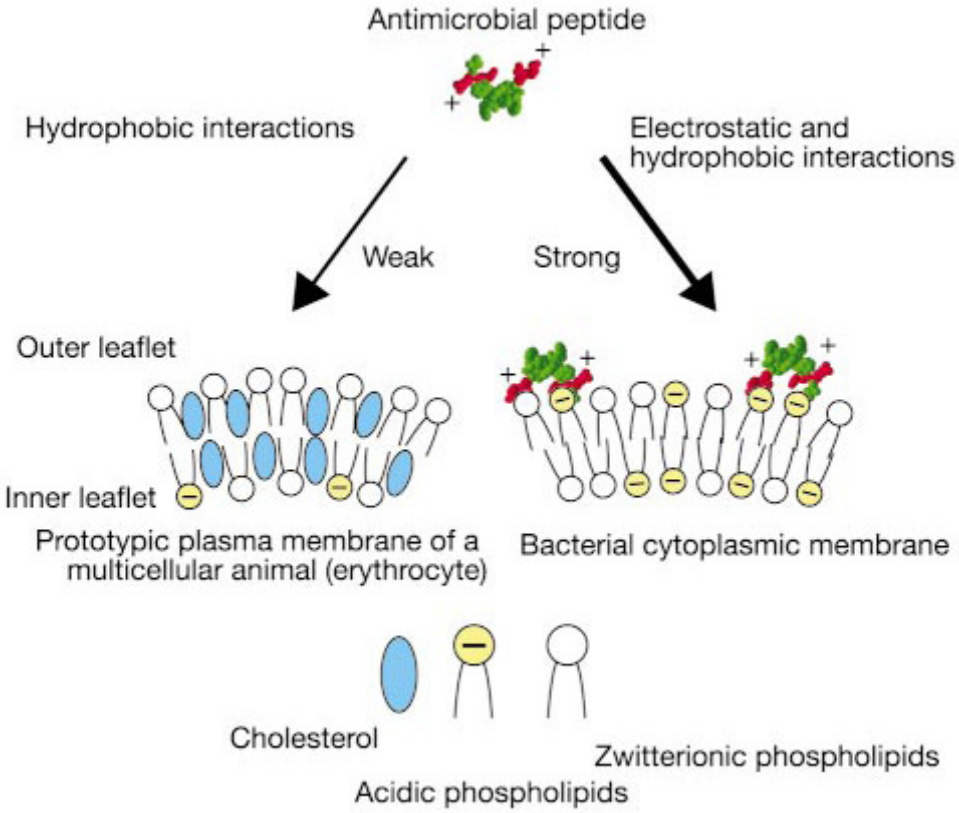

Figure 2. 8 The membrane target of antimicrobial peptides of multicellular organisms and the basis of specificity. Reproduced from reference [65]

1) Barrel stave model

The “Barrel stave” mechanism describes the formation of transmembrane pores by bundles of amphipathic α-helices, in which their hydrophobic surfaces interact with the lipid domain of the membrane and the hydrophilic surfaces point inward producing an aqueous pore [66]. (Figure 2.9)

This model involves four steps to form a transmembrane pore. ① Monomers bind to the membrane in an α-helical structure ② Molecules recognize the membrane-bound monomer at low surface density of bound peptide ③ At least two assembled monomers insert into the membrane to initiate the formation of a pore

④ Progressive recruitment of additional monomers increases the pore size

2) Carpet model

The carpet model describes a pore formation mechanism where amphipathic α-helical peptides bind to the surface of a membrane and cover it in a carpet-like manner. In contrast to the “Barrel stave model”, peptides are not inserted into the hydrophobic core of membrane, but instead bind to the phospholipids head-groups. Additionally, peptides do not need to adopt a specific structure for their binding.

This model involves four steps to form a transmembrane pore [67]. ① Peptide monomer has a tendency to bind to the phospholipids head group ② Alignment of the

peptide in the surface of membrane, their hydrophilic surface faces the phospholipids head group ③ Peptide rotation reorients them toward the hydrophobic core of membrane ④ Disintegration of membrane by disrupting the bilayer curvature

An early step before the membrane breakage includes the transient pore in the membrane.

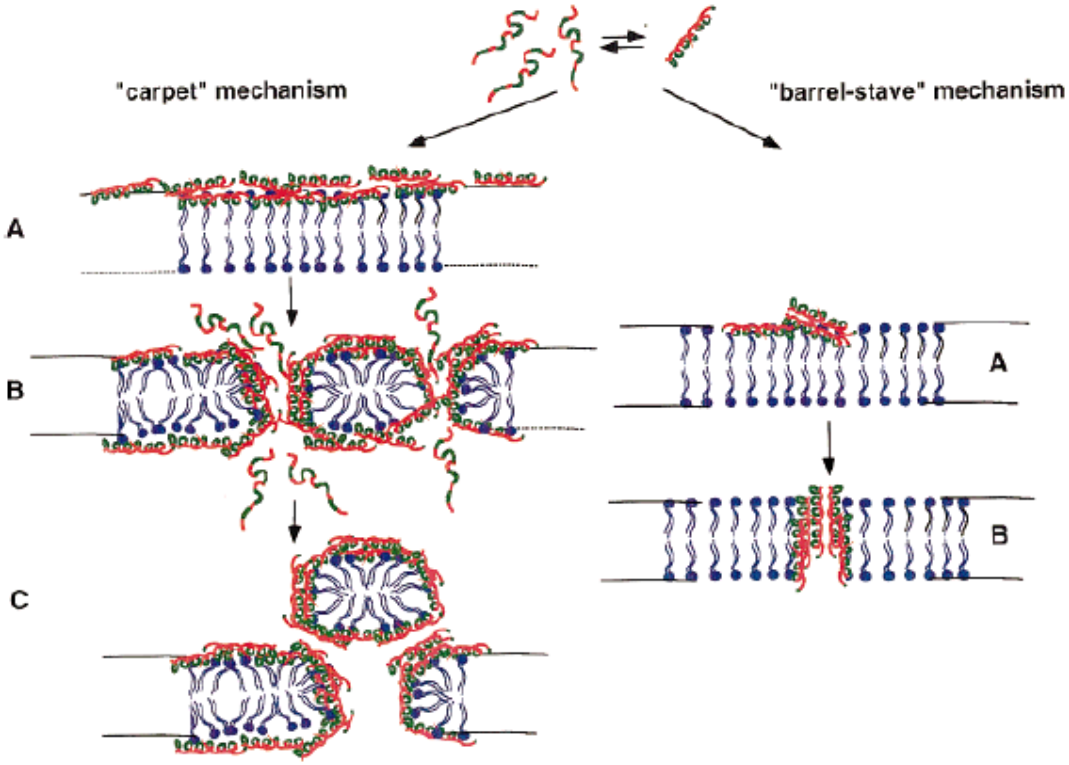

Figure 2. 9 Barrel-stave (to the right) and the carpet-like (to the left) models suggested for membrane permeation. Reproduced from reference [66]

3) Shai-Matsuzaki-Huang model

This model explains the activity of most antimicrobial peptides and proposes the interaction of the peptide with the membrane, displacement of lipids, alteration of membrane structure, and entry of the peptide into the inside of cell in a some cases [65].

① Carpeting of the outer leaflet with peptides ② Integration of the peptide into the membrane and thinning of the outer leaflet. The surface area of the outer leaflet expands relative to the inner leaflet, resulting in strain within the bilayer (jagged arrows). ③ Phase transition and `wormhole' formation. Transient pores are formed at this stage. ④ Transport of lipids and peptides into the inner leaflet. ⑤ Diffusion of peptides onto intracellular targets (in some cases). ⑥ Collapse of the membrane into fragments and physical disruption of the target cell's membrane.

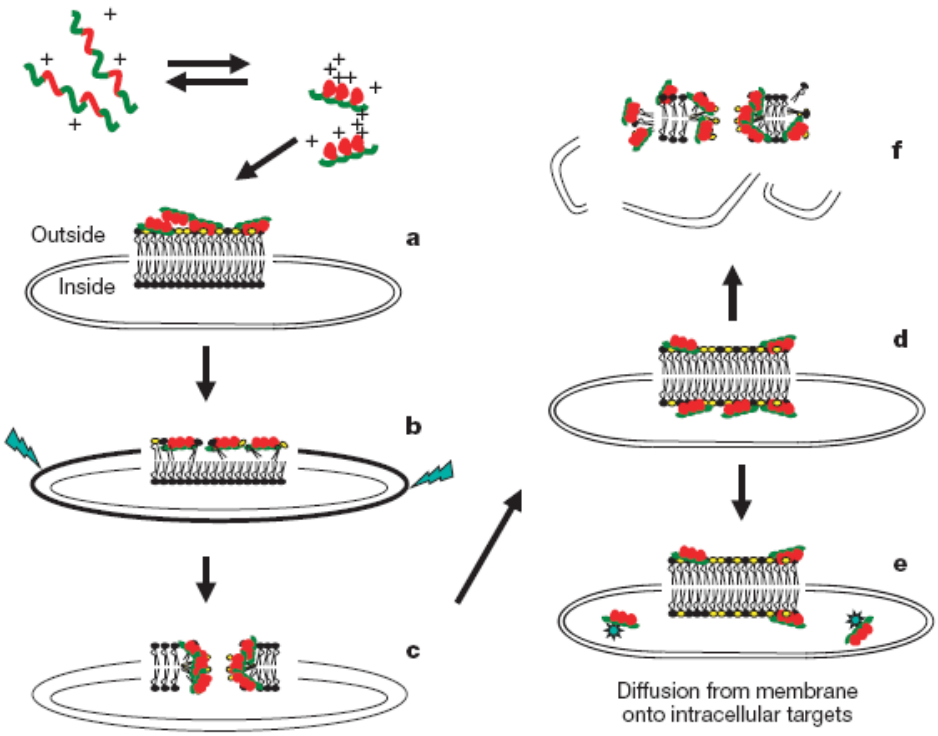

Figure 2. 10 The Shai-Matsuzaki-Huang model of the mechanism of action of an antimicrobial peptide. An α-helical peptide is depicted. Lipids with yellow head groups are acidic, or negatively charged. Lipids with black head groups have no net charge. Reproduced from reference [65]

A number of antimicrobial peptides have been discovered. These include Defensins from mammalian neutrophilies, Cecropins from insects, Melittin from bee venom, Tachyplesins from horseshoe crab hemolymph and Magainin from frogs [65].

Magainin 2 is a 23-residue helical peptide isolated from the skin granular gland of the African clawed frog named *Xenopus laevis* that exhibits a broad spectrum of antimicrobial activity as well as tumoricidal properties [68]. It has a net +4 charge at

physiological pH and binds to negatively charged phospholipid membranes with the aid of electrostatic interactions, forming an amphiphilic helix and permeabilizing the bilayers [69]. (Figure 2.11)

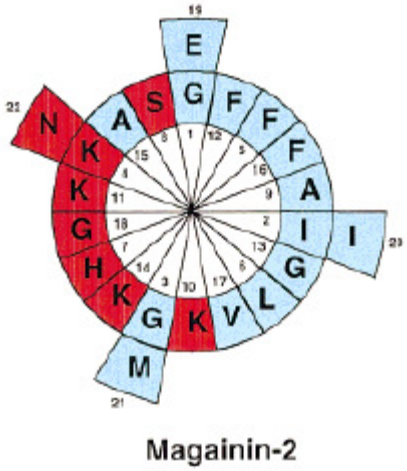

Figure 2. 11 Schiffer–Edmundson wheel projection of the N-terminal 22 amino acids of magainin-2. Number 1 represents residue 1 of the peptides. Blue indicates hydrophobic amino acids and red indicates hydrophilic amino acids. Reproduced from reference [66]

By now it is well established that magainin acts by disrupting cell membranes rather than by interacting with specific protein targets, subsequently causing an increase in membrane permeability and leading to cell lysis. The mechanism of magainin-lipid interactions have been proposed by Matsuzaki [69]. (Figure 2.12) Magainins take on an amorphous structures in aqueous solution and form an

amphiphilic helix on membrane binding. Electrostatic interaction between magainin and lipid membranes plays a critical part. The helix lies parallel to the membrane surface due to a balanced hydrophobic and hydrophilic angle. Five helices form a membrane-spanning pore consisting of a dynamic, peptide-lipid supra-molecular complex. Upon the disintegration of the pore, a fraction of the peptides translocate into the inner space [70].

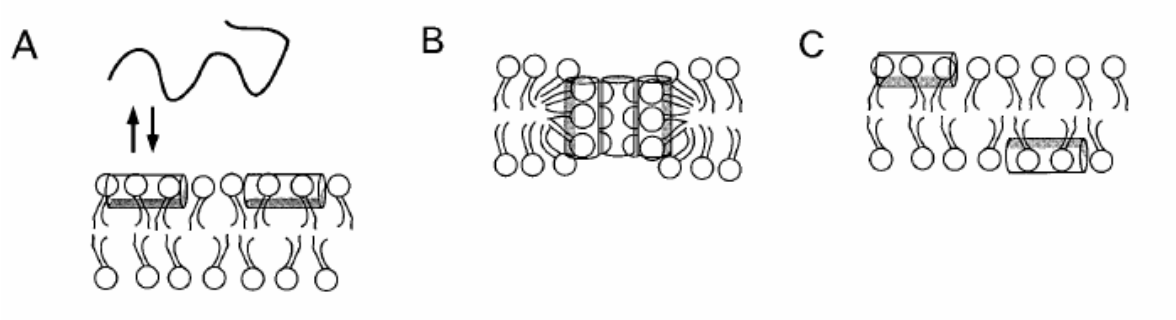

Figure 2. 12 A model for magainin 2-lipid bilayer interactions (A) Membrane binding accompanying helix formation. The shaded area represents the hydrophobic surface of the amphiphilic helix. (B) Formation of the pore composed of a dynamic, peptide-lipid supra-molecular complex. (C) Translocation of the peptide into the inner leaflet upon the disintegration of the pore. Reproduced from reference [70]

Magainin is considered as a good candidate for therapeutic agents because it is selectively active toward bacterial membranes. This selectivity originates from the

following factors. ① The outer membranes of eukaryotic cells are composed of zwitterionic lipids ② Eukaryotic cell membranes are rich in cholesterol which inhibit magainin – induced lysis ③ Bacterial cells have inside-negative transmembrane potentials causing magainin – induced lysis [71].

However, in most cases the detailed molecular mechanism of the antibiotic action is still unknown [72].

2.6. Peptide enhancement

Transdermal delivery of drug using peptides as enhancers has not been studied well and most of research was based on the conjugation of peptides with target molecules that we want to deliver. Protein transduction domains - a class of small peptides penetrating the plasma membrane of mammalian cells - were used as carriers to deliver peptide into the skin in therapeutic levels [73]. The conjugate of heptarginine oligomers to cyclosporine A was successfully delivered topically and even entered target tissue T-cells, which resulted in functional inhibition of cutaneous inflammation [74]. Antennapedia transduction sequence (ANTP) linked to an antigenic peptide was used as a peptide-based vaccine transdermally penetrated into the cells of the epidermis and dermis. Then, it derived a cytotoxic T-lymphocyte

(CTL) response [75]. TD-1 peptide was developed by the phage display technique and it delivered insulin into the skin. The mechanism behind this phenomenon has not been elucidated yet, but it is thought that TD-1 might create a transient pathway in the skin which enabled insulin to penetrate through the skin possibly via hair follicles and get to the systemic circulation [76].

2.7. Synergistic Enhancement

Whereas the aforementioned enhancement methods have shown enhancement of transdermal drug penetration, their combinations have been hypothesized to be more effective compared with each of them alone. In addition to transdermal drug penetration enhancement, a combination of enhancement methods should reduce the severity of the enhancers required to achieve the desirable flux of drug. However the effect of the enhancers that can be applied on the skin is limited by safety issues and irritation of skin. If we combine two or more enhancers, one can reduce the required concentration of individual enhancers. As a result, a combination of enhancers can increase the safety of enhancers and may increase the total enhancement [77].

Most synergistic enhancement applications have been carried out using a combination of a physical - especially electro-physical methods - and a chemical

enhancer. Iontophoresis showed great synergistic enhancement with chemical enhancers such as Azone [78], N-decylmethyl sulfoxide [79], oleic acid [80], lauric acid [81], linoleic acid -menthone in combination [82], and surfactant [83]. Electroporation with anionic lipid [84], heparin [85], sodium thiosulafe-urea [86], and surfactant [87] also showed synergistic enhancement. Finally, even ultrasound synergistically enhanced skin permeability with various chemical enhancers [88,89].

Synergistic effects between chemical enhancers have also been reported. Karande and coworkers investigated a huge number of binary mixtures of chemical enhancers using a high-throughput screening method studied and the mechanism of synergistic enhancement of a certain chemical enhancer mixture by FT-IR and NMR. [90,91] Combinations of chemcial enhancers and more polar co-solvents have also been reported, suggesting that the latter facilitate the solubilization of the former within the *stratum corneum*, thus amplifying the lipid-modulating effect [77]. The synergistic effects of occlusion, chemical enhancer and solvent on skin permeability have been studied [92].

2.8. Experimental Tools

2.8.1 Multi-photon excitation microscope analysis

In this study, to investigate the structure of human skin and the distribution of our model target drug (fluorescein) and magainin peptide (fluorescent-tagged magainin peptide) in the *stratum corneum*, multi-photon microscopy has been used.

While histological analysis has been widely used to study tissue morphology, some tissue information is not preserved due to the fixation and embedding process. In order to get 3-D information without loss of the sample, confocal microscoy was introduced. However, reflected confocal microscopy has limitations such as inability to get tissue biochemical information and image contrast which is generated by index of refraction mismatch. Therefore, multi-photon microscopy was developed, and this new tool has the following advantages over the original confocal method: more suitable for investigating thick tissue, higher light-detection efficiency, and less phototoxicity. A comparison of collection geometry between these two tools is shown in Figure 2.13 [93].

As mentioned above, multi-photon microscopy is a new tool for noninvasive biomedical diagnosis. It can directly visualize skin structural features and has been

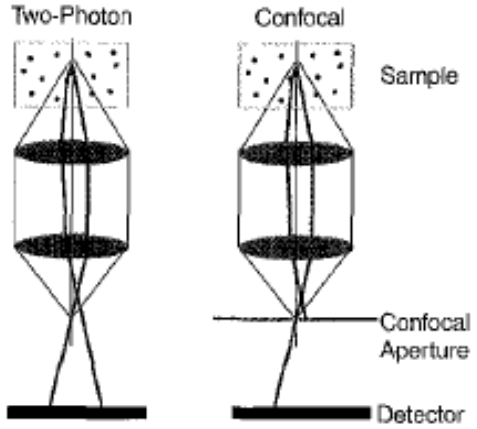

Figure 2. 13 A comparison between the collection geometry of two-photon and confocal detection schemes. In the two photon case, no detection pinhole is used, and the scattered photons can be better detected with a large area detector. Reproduced from reference [93]

used to visualize *in vitro* permeant spatial distributions across human cadaver skin. In addition, it can reduce sample photobleaching and increase three-dimensional depth discrimination [94].

Two-photon excitation is a good fluorescence technique to assess tissue structure down to the depth of several hundred micrometers. Tight focusing in a laser scanning microscope enables a dye molecule to simultaneously absorb two long-wavelength photons to reach its excited state. The long wave length photon source used in multi-photon microscopy has light penetrate into the media with a high degree of scattering. However the structural complexity of the *stratum corneum* poses a challenge to the

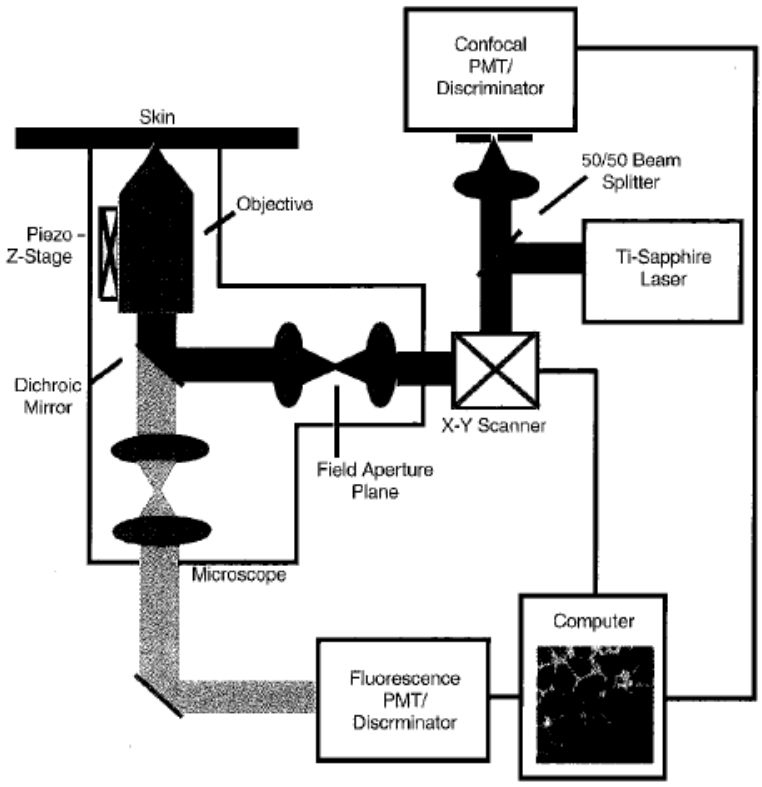

Figure 2. 14 Schematics of a simultaneous two-photon fluorescence and confocal reflected light microscope. Reproduced from reference [93]

quantitative analysis of average transport properties in the skin [27]. Figure 2.14 shows a typical multi-photon microscopy design.

2.8.2 FT-IR (Fourier Transform InfraRed Spectroscopy)

The technique of Fourier Transform InfraRed (FT-IR) spectroscopy has been used extensively to study the phase of lipid membranes. The lipids of the *stratum corneum* can be studied by this technique. Unlike other membrane systems where

samples are suspended in water, *stratum corneum* samples are evaluated as intact sheets [95].

A typical FTIR spectrum of porcine *stratum corneum* is shown in Figure 2.15. The peaks caused by carbon-hydrogen stretching vibrations have been extensively investigated and these two prominent peaks occur near 2920 and 2850 cm^{-1} for the asymmetric and symmetric C-H vibrations of the long chain hydrocarbons of lipids. Because the height and area of these two bands are proportional to the amount of the lipids present, any extraction of lipids from *stratum corneum* results in a decrease of peak height and area [96]. Fluidization of *stratum corneum* lipids also enhances the permeation of drugs. The shift of C-H stretching peaks to higher wave number and increase in their peak width indicate fluidization of *stratum corneum* lipids [97].

Conformational change of *stratum corneum* protein can be explained by FT-IR spectroscopy. The bands located between 1800 and 1500 cm^{-1} correspond to protein absorption. Denaturation of protein is correlated with amide I band (1700-1600 cm^{-1}) which is sensitive to the protein conformation. This band provides information on four different protein structures: α-helices (1660-1650 cm^{-1}), β-sheets (1640-1620 cm^{-1}), random coils (1650-1640 cm^{-1}), and antiparallel β-sheets and β-turns (1695-1660 cm^{-1}) [98,99].

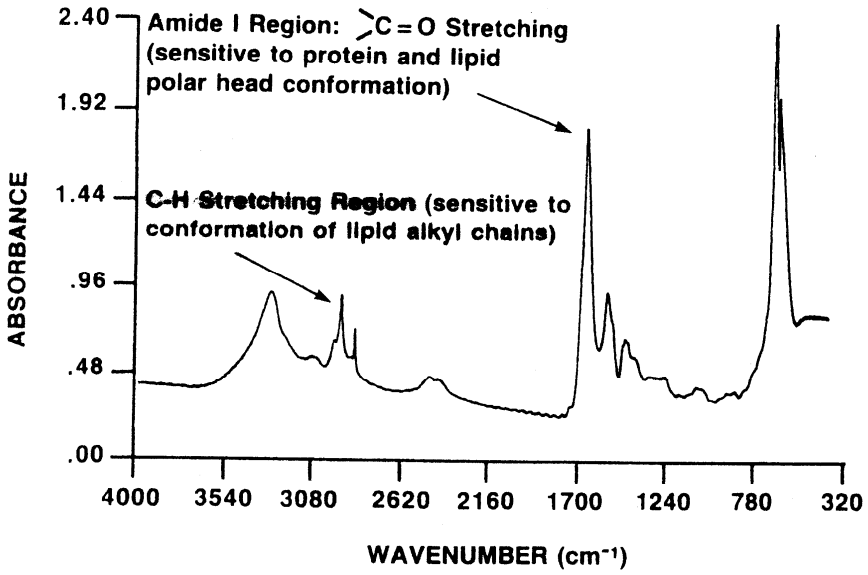

Figure 2. 15 The typical infrared (IR) spectrum of *stratum corneum.* Reproduced from reference [95]

2.8.3 DSC (Differential Scanning Calorimetry)

Differential scanning calorimetry (DSC) is employed to measure directly the effects of transdermal permeation enhancers on the thermal phase properties of *stratum corneum* [40].

Human *stratum corneum* is characterized by four transitions in the 20-120 ^{o}C range. Three major phase transitions occur near 65, 80 and 95 ^{o}C. (Figure 2.16) In addition, a small peak which is not present in all samples occurs near 35 ^{o}C [100]. From thermal reversibility, extraction and other assay tools, four peaks can be ascribed to structural changes associated with various components as follows: 35 ^{o}C –

lipid, 65 °C – lipid, 80 °C – lipid & protein, 95 °C – protein. Wide angle X-ray experiments with thermal analysis have shown that this first peak is due to a change in lipid packing. The fourth peak is assumed to be the intracellular keratin denaturation. In case of the third peak, it has been interpreted as protein-lipid associated thermal behavior or complete destruction of the lipid bilayer structure. The second peak is interpreted as the stacking of the lamellae in the *stratum corneum*.

Interaction of a chemical or peptide enhancer with lipids or protein is shown as a change in transition temperature or shape in DSC graph. For example, the decrease of both the 2nd and 3rd transition temperatures indicate fluidized states of *stratum corneum* lipid.

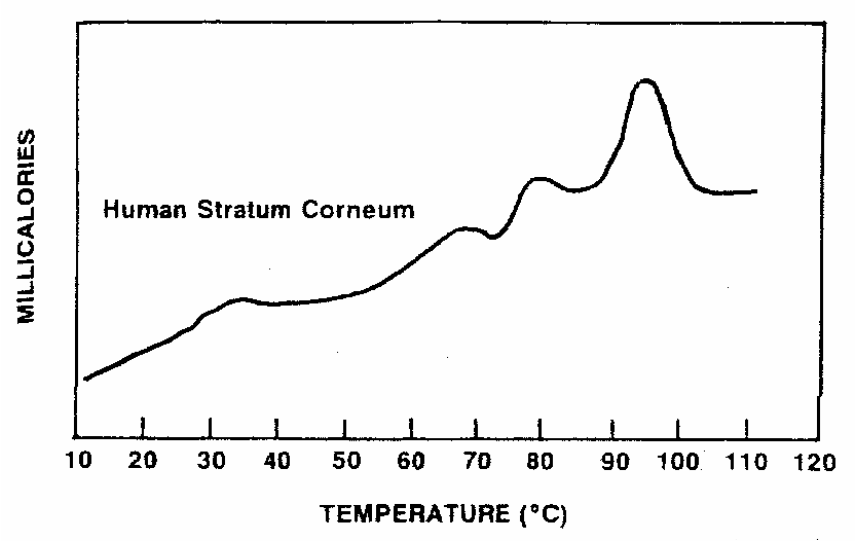

Figure 2. 16 The DSC thermal profile of Human *stratum corneum.* Reproduced from reference [100]

2.8.4 X-Ray Diffraction

The main diffusion barrier of *stratum corenum* is the intercellular lipid domains. Exploring physical properties and molecular structure of these domains is critical in the transdermal delivery study. X-ray diffraction analysis is a very useful tool to obtain structural information on lipid domains which are well-structured arrays [101]. Two X-ray diffraction methods have been used: small and wide angle X-ray diffraction. Small angle X-ray diffraction (SAXD) has been demonstrated to be useful to study the structure of the residual tissue after treatments, in particular, the intercellular lipids [102]. This method shows structural knowledge with large repeat distances on the order of 50-150Å and reveals that the *stratum corneum* lipids are organized in lamellar phases with two periodicities of approximately 6 nm (short periodicity phase) and 13 nm (long periodicity phase) [103]. Wide angle X-ray diffraction (WAXD) has been shown to be useful in determining the components of the disaggregated fraction and the type of links existing between them. This method provides structural information using a small repeat distance on the order of 3-10Å. White et al. found that intact *stratum corneum* from the hairless mouse gave sharp wide angle X-ray reflections at 0.38 nm and 0.46 nm [103].

The use of this strategy provides new knowledge of the structural *stratum corneum* modifications associated to disaggregation, possibly related to the

desquamation process [13]. In the damaged *stratum corneum* prepared by treatment with sodium dodecyl sulfate, small-angle diffraction peaks disappear and only the wide maxima remain around 1^{st}, 2^{nd} and 3^{rd} order diffraction peaks. These facts indicate that in the normal *stratum corneum,* the lamellar structure is ordered and in the damaged *stratum corneum,* the lamellar structure is disordered [104].

CHAPTER 3: SYNERGISTIC ENHANCEMENT OF SKIN PERMEABILITY BY N-LAUROYLSARCOSINE AND ETHANOL

3.1 Introduction

While most drugs are administered orally, there are numerous advantages to the transdermal route. These advantages include the potential for sustained release, controlled input kinetics, improved patient compliance, and avoidance of first-pass metabolism in the gastrointestinal tract. However, human skin is a very effective barrier and severely limits the transdermal delivery of drugs [4]. Corneocytes embedded in a lipid bilayer matrix comprise the unique hierarchical structure of the *stratum corneum* that provides the skins barrier properties. Only a few drug molecules of optimal physicochemical properties can penetrate the skin sufficiently to be therapeutically efficient. Intercellular lipids in the human *stratum corneum* principally consist of ceramides, fatty acids, cholesterol, and cholesteryl sulfate that are assembled into multi-lamellar bilayers [106]. [105]

In order to improve transdermal drug delivery, various penetration enhancers which disrupt the aforementioned structural hierarchy to decrease the barrier resistance of the *stratum corneum* have been investigated previously. Many

compounds have been used as penetration enhancers, including Azone derivatives, fatty acids, fatty esters, sulphoxides, alcohols, pyrrolidones, glycols, surfactants, and terpenes [106]. Among the various chemical enhancers, surfactants have been widely investigated as transdermal permeation enhancers, and also have a long history of use as emulsifiers, stabilizers, and suspending agents in many topical pharmaceutical formulations [107].

Many surfactants can interact with the *stratum corneum* to increase the penetration of drugs applied to skin [108]. Anionic surfactants have been shown to disrupt the intercellular lipid lamellae and to cause selective loss of intercellular lipids [109]. Among the various anionic surfactants, N-lauroylsarcosine (NLS) has been used as a permeation enhancer and has shown a synergistic improvement of transdermal flux when used in combination with other enhancers, such as squalene and vitamin E [111]. [110]When mixed with sorbitan monolaurate, the formulation exhibited not only synergistic transdermal flux enhancement, but also reduction of skin irritation [91].

Synergistic effects between chemical enhancers and various solvents have also been reported. A combination of surfactant and 50% propylene glycol showed strong synergistic effects on skin permeability [111]. Polar solvents, such as ethanol, have been reported not only to have direct effects on skin permeability, but also to facilitate

the solubilization of enhancers within the *stratum corneum,* thus further amplifying the lipid-modulating effect [3]. Ethanol is a known enhancer for the transdermal delivery of lipophilic drugs and is currently commercialized in transdermal systems for estradiol and fentanyl [112].

Given the observations that formulations combining lipid-disrupting penetration enhancers and appropriate solvents can be especially effective to increase skin permeability, we sought to study the mechanism by which this enhancement occurs using mixtures of NLS and ethanol as a model system. We hypothesize that NLS and ethanol synergistically increase skin permeability by increasing the fluidity of *stratum corneum* lipid structure. This hypothesis was tested by measuring the effect of NLS and ethanol concentrations on skin permeability to the model fluorescent probe fluorecein.

The mechanism of action was further investigated using skin resistance measurements, differential scanning calorimetry (DSC) and Fourier transform infrared spectroscopy (FTIR). Measurement of skin resistance can be used as a 'generic' measure of skin permeability that does not depend on the specific characteristics of target molecules such as hydrophobicity and charge. DSC and FTIR measurements allow us to probe the intercellular lipid domain of the *stratum corneum* to provide information especially on lipid fluidization.

3.2. Materials and Methods

3.2.1 Skin preparation

Human cadaver skin was obtained from the National Disease Research Interchange (Philadelphia, PA, USA) or Emory University School of Medicine (Atlanta, GA, USA) and stored at -75 ^{o}C until use for permeation studies with approval from the Georgia Tech Institutional Review Board. Immediately prior to a diffusion experiment, whole skin was thawed in deionized water at 30 ^{o}C for 1 h. Epidermis was isolated from dermis using a heat separation method [113], in which the skin was immersed in deionized water for 2 min at 60 ^{o}C. The epidermis was then carefully peeled away from the dermis with a spatula and used for the diffusion or other experiments.

For experiments on isolated *stratum corneum*, a *stratum corneum* sheet was isolated from human epidermis by trypsin digestion. The epidermis was incubated in phosphate-buffered saline (Sigma Aldrich, St.Louis, MO, USA) containing 0.25% trypsin (Mediatech, Herndon, VA, USA) and 0.0l% gentamicin (Clonetics, Walkersville, MD, USA) at 32 ^{o}C for 24 h. The isolated *stratum corneum* then was rinsed with distilled water three times and stored on polymer-coated paper (Fisher

Scientific, Waltham, MA, USA) under vacuum (KNF Neuberger, Trenton, New Jersey, USA) overnight at room temperature, 23 - 24 ^{o}C [46].

3.2.2 Transdermal flux measurements

Transdermal flux experiments consisted of three steps. The first step was the pretreatment of skin with a chemical enhancer formulation in a vertical Franz diffusion glass cell apparatus (PermeGear, Bethlehem, PA, USA). This Franz cell was used to hold epidermis samples (0.7 cm^2 exposed skin surface area) between the donor (upper) and receiver (lower) chambers during an *in vitro* permeation experiment. The *stratum corneum* side was exposed to 0.3 ml of the enhancer formulations in the donor chamber. Solutions of varying NLS (98%, Fluka, Buchs, Switzerland) concentrations in solvents of various ethanol (Sigma Aldrich, St.Louis, MO, USA) concentrations was placed in the donor chamber, and the Franz cell was kept in the refrigerator at 4 ^{o}C for 12 h for pretreatment. The concentration of NLS solution used in the penetration experiment was 2 % (w/v) and the concentration of ethanol was 50 % (v/v) in water, unless otherwise noted.

The second step was an equilibration step. The Franz cell was placed in a heater/stirrer block (PermeGear) maintained at 37 ^{o}C and stirred at 455 rpm for 3 h.

For the final step, the chemical enhancer formulation was removed from the donor chamber and 0.3 ml of 1 mM fluorescein (Sigma Aldrich, St. Louis, MO, USA) in PBS buffer solution was placed in the donor chamber. The amount of fluorescein in the receiver chamber was measured by calibrated fluorescence spectroscopy (Photon Technology International, Birmingham, NJ, USA) every hour for 5 h to determine the transdermal fluorescein flux. At each sample time, all of the solution in the receiver chamber was removed and replaced with fresh PBS.

3.2.3 Skin resistance measurements

The electrical resistance across the epidermis was measured by a Keithley 3322 LCZ meter (Keithley Instruments, Cleveland, OH, USA). A Ag/AgCl disk electrode (In Vivo Metric, Healdsburg, CA, USA) was inserted into the receiver chamber through the sampling outlet of a vertical Franz diffusion cell apparatus and another Ag/AgCl electrode was placed in the donor chamber.

3.2.4 Differential scanning calorimetry

DSC was used to characterize the thermal transitions in *stratum corneum* samples that were either untreated or treated with a chemical enhancer formulation. Thermal analysis employed a DSCQ100 differential scanning calorimeter fitted with a

refrigerated cooling system (TA Instruments, New Castle, DE, USA). Several pieces of *stratum corneum* were each soaked in various chemical enhancer formulations for 24 h at 4 ^{o}C and then washed with PBS solution. The *stratum corneum* samples were desiccated under vacuum for 12 h, and were hermetically sealed within an aluminum holder (PerkinEelmer, Wellesley, MA,USA). Samples were heated from 0 ^{o}C to 120 ^{o}C at a heating rate is 10 ^{o}C /min.

3.2.5 Fourier transform infrared spectroscopy

Prior to spectral analysis by FTIR, several pieces of *stratum corneum* were treated as described for DSC samples, but were not desiccated. Using a Magma-IR 560 FTIR spectrometer (Nicolet, Thermo Electron Corporation, Waltham, MA, USA), all spectra (4/cm^{-1} resolution, representing the average of 64 scans) were obtained in the frequency range 4000 - 1000 cm^{-1}. OMNIC professional software (Thermo Electron Corporation, Waltham, MA, USA) was used to determine the peak position.

3.2.6 Statistical Analysis

The transdermal flux of fluorescein, skin resistance, DSC spectra, and FTIR spectra were measured using at least three skin specimens each, from which the mean and standard error of the mean were calculated. A two-tailed Student's t-test (α=0.05)

was performed when comparing two different conditions. When comparing three or more conditions, a one-way analysis of variance (ANOVA, α=0.05) was performed. In all cases, a value $p<0.05$ was considered statistically significant.

3.3. Results and discussion

3.3.1 Effect of NLS and ethanol concentration on transdermal flux

To better understand the mechanism by which NLS increases skin permeability, we first measured the effect of NLS concentration on transdermal fluorescein delivery across human cadaver skin. Fluorescein is a moderately large (332.31 Da) and hydrophilic (octanol-water partition coefficient: logP = -1.22) molecule that serves as a model drug that is normally difficult to deliver across the skin. As shown in Figure 3.1A, accumulated fluorescein delivered across the skin increased approximately linearly with time (ANOVA, $p<0.05$), indicating steady state behavior. The accumulated amount delivered over the 5 h experimental period and the corresponding skin permeability is shown in Figure 3.1B. These data demonstrate that skin permeability increased with increasing NLS concentration (ANOVA, $p<0.05$) and did not show saturation over the range of conditions studied. At the highest NLS concentration studied, the presence of NLS increased skin permeability to fluorescein

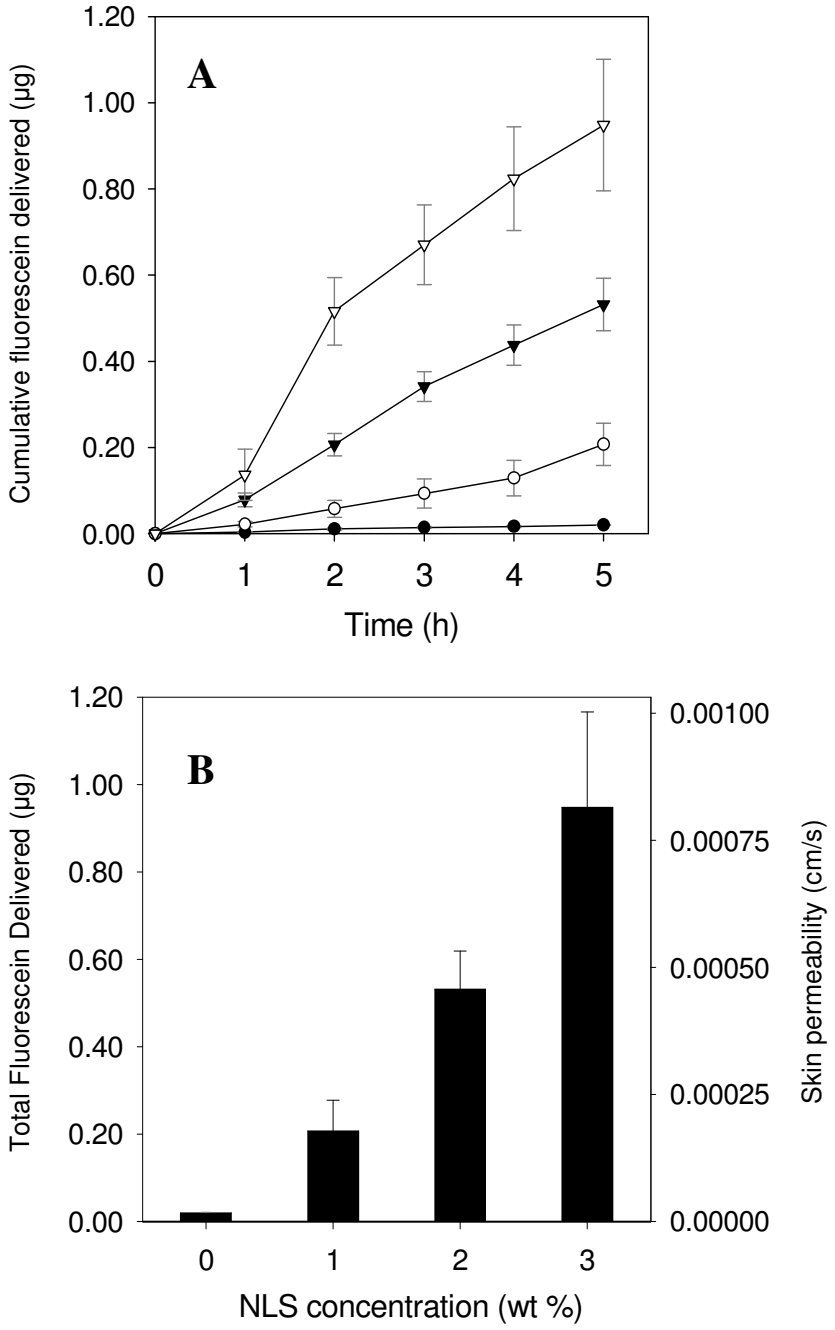

Figure 3. 1 Transdermal delivery of fluorescein across human cadaver epidermis as a function of NLS concentration. (A) Cumulative fluorescein delivered across the skin as a function of time from a formulation containing (●) 0%, (○) 1%, (▼) 2%, and (▽) 3% (w/v) NLS in 50% (v/v) ethanol. (B) Total fluorescein delivered and skin permeability after 5 h as a function of NLS concentration. Data were taken from part (A). Data points show the average of n≥3 replicates and error bars correspond to the standard error of the mean.

47 fold relative to the control sample without NLS (Student's *t* test, $p<0.01$).

Because NLS has poor water solubility, the above experiments were carried out in an aqueous solution containing 50% ethanol. In addition to increasing NLS solubility, the presence of ethanol is also known to increase skin permeability itself. We therefore examined the effect of ethanol concentration on transdermal fluorescein delivery. As shown in Figures 3.2A and 3.2B, skin permeability exhibited a complex dependence on ethanol concentration. In the absence of ethanol, the addition of NLS did not significantly enhance skin permeability (0% ethanol without NLS vs. 0% ethanol with NLS, Student's *t* test, $p<0.01$). Skin permeability in the presence of NLS with 25% and 50% ethanol increased skin permeability by a factor of 20 and 24, respectively, relative to the control sample with NLS in 0% ethanol (Student's *t* test, $p<0.01$). There was no statistical difference between the permeability measured at 25% and 50% ethanol (Student's *t* test, $p>0.05$). Skin permeability at 75% and 100% ethanol were progressively lower, but were still 6 and 3 times greater, respectively, than the control sample with NLS in 0% ethanol (Student's *t* test, $p<0.05$). Altogether, we conclude that NLS in the absence of ethanol does not enhance skin permeability, NLS with high concentration of ethanol (i.e., 75% or 100% ethanol) is a weak enhancer, and NLS with moderate concentration of ethanol (i.e., 25% or 50% ethanol) is a strong enhancer.

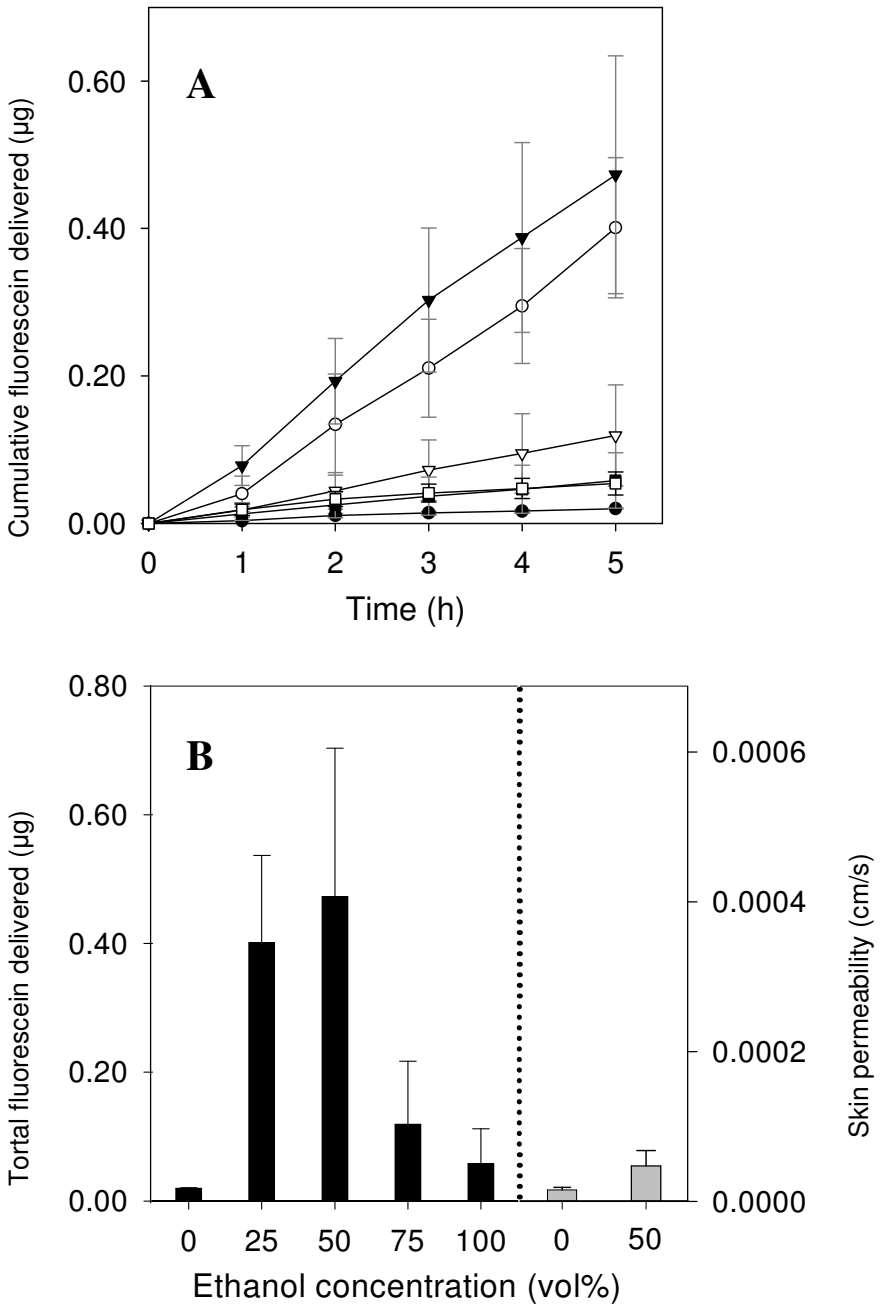

Figure 3. 2 Transdermal delivery of fluorescein across human cadaver epidermis as a function of ethanol concentration. (A) Cumulative fluorescein delivered as a function of time from a formulation containing 2% (w/v) NLS in (●) 0%, (○) 25%, (▼) 50%, (▽) 75%, and (■) 100% (v/v) ethanol in PBS or a formulation containing (□) 50% ethanol without NLS. (B) Total fluorescein delivered and skin permeability after 5h as a function of ethanol concentration either (■) with or (▒) without 2% NLS. Data were taken from part (A). Data points show the average of n≥3 replicates and error bars correspond to the standard error of the mean.

To facilitate better interpretation, we ran an additional control experiment using 50% ethanol in the absence of NLS, which can decouple the direct effects of ethanol on enhancement from the synergistic effects of ethanol and NLS together. In this case, ethanol increased skin permeability by a factor of 3 relative to the control sample without ethanol or NLS, but this was not significant (Student's *t* test, $p=0.08$). This increase in skin permeability due to ethanol alone was also not statistically different from that caused by NLS either in the absence of ethanol or in the presence of 75% or 100% ethanol (Student's *t* test, $p>0.1$). In contrast, skin permeability in the presence of NLS and 25% or 50% ethanol was significantly greater than for 50% ethanol alone (Student's *t* test, $p<0.01$). This indicates a synergistic interaction between ethanol and NLS, because the sum of the permeability enhancement from NLS alone (non-significant) and ethanol alone (3 fold) are much less than the enhancement caused by their combination (24 fold).

The reasons for this mechanistic enhancement at 25-50% ethanol concentrations will be further investigated below. At 75-100% ethanol concentrations, the reduced enhancement may be explained in part by dehydration of the *stratum corneum*. Previous results have shown that exposure to high ethanol concentrations can substantially dehydrate the outer layer of the *stratum corneum* and thereby decrease

skin permeability [114]. Dehydration has also been shown to shrink the keratins of the *stratum corneum*, which similarly decreases skin permeability [96].

3.3.2 Skin resistance measurement

To further validate the synergistic effects of NLS and ethanol of skin barrier properties, we examined the effect of ethanol concentration on the electrical resistance of skin. Skin's electrical resistance is generally considered a marker of skin permeability and changes in skin resistance due to exposure to different chemical enhancers has been shown to correlate with increased skin permeability to model drug compounds [115,116]. Moreover, because skin resistance can be easily measured on a continuous basis, electrical measurements permit better characterization of the kinetics of skin permeability changes.

Figure 3.3 A shows skin resistance over time for different formulations. Skin samples exposed to 50% ethanol, without NLS, showed a small and insignificant (Student's *t* test, $p>0.1$) drop in resistance over the 24-h experimental period. However, the combination of NLS and ethanol decreased skin resistance more rapidly and to a greater extent, where NLS in 50% ethanol had the greatest effect (Student's *t* test, $p<0.01$); NLS in 25 and 75% ethanol had similar, but lesser effects (Student's *t* test, $p<0.01$); and NLS in 100% ethanol had much less effect, but still more than the

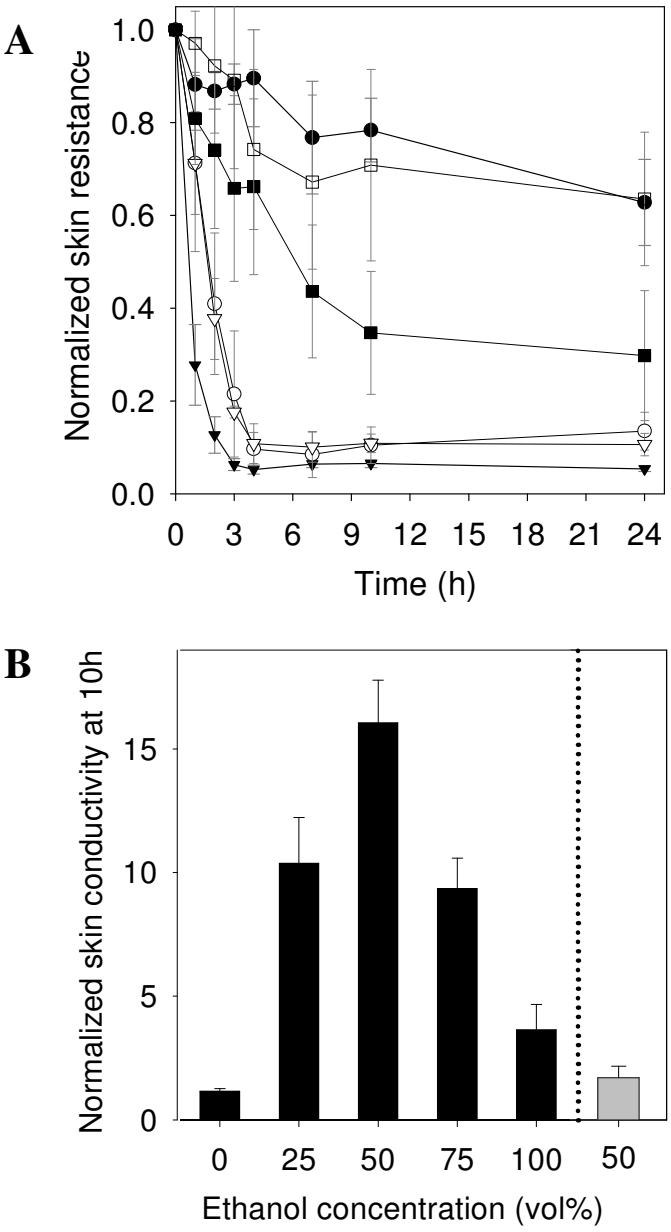

Figure 3. 3 Skin electrical resistance and conductivity as a function of ethanol concentration. (A) Normalized electrical resistance of human cadaver epidermis treated with a formulation containing 2% NLS in (●) 0%, (○) 25%, (▼) 50%, (▽) 75%, and (■) 100% ethanol in PBS and a formulation containing (□) 50% ethanol without NLS. Resistance values were normalized relative to their pretreatment levels. (B) Normalized electrical conductivity (i.e., the inverse of resistance) of human epidermis after 10 h of treatment (■) with and (▒) without NLS as a function of ethanol concentration. Data were taken from part (A). Data points show the average of n≥3 replicates and error bars correspond to the standard error of the mean.

NLS-only or ethanol-only controls (Student's *t* test, $p<0.05$).

Figure 3.3B summarizes these data and replots them as electrical conductivity, which is the inverse of electrical resistance and is known to correlate directly with skin permeability. [115] The dependence of changes in skin resistance and conductivity on ethanol concentration is strongly consistent with the dependence found in measurements of skin permeability to fluorescein (Figure 3.2B), which further validates the findings and suggests that these decreases in skin barrier properties may be broadly applicable to many drugs.

From a mechanistic viewpoint, skin's electrical resistance is known to be governed primarily to the highly ordered, lipophilic barrier of the *stratum corneum* lipid bilayers [117]. Therefore, changes in skin resistance are a sensitive measure of changes in *stratum corneum* lipid bilayer integrity. These measurements suggest that the combination of NLS and ethanol act by disrupting *stratum corneum* lipid bilayer structure.

A final observation of the skin resistance data concerns the kinetics of action. Changes in skin resistance are seen to occur with a lag time of one or more hours (Figure 3.3A), which suggests a kinetic barrier that may be a diffusive transport limitation. Lag times for transdermal diffusion of small drugs can similarly be a few hours [4], which suggests that the lag time observed for NLS-based enhancement

may be limited by the time it takes for NLS to diffuse into and throughout the *stratum corneum*.

3.3.3 Differential scanning calorimetry

To further explore the effects of NLS and ethanol on the skin barrier, we are guided by the hypothesis that NLS and ethanol increase skin permeability by increasing the fluidity of *stratum corneum* lipid structure. To test this hypothesis, DSC was employed to investigate the potential fluidizing effects of NLS in ethanol solution on the thermal properties of human *stratum corneum* (Figure 3.4 and 3.5). DSC analysis of negative control samples of human *stratum corneum* exposed to PBS without NLS or ethanol showed two major endothermic transition peaks, T_{m1} and T_{m2}, that occur near 75 and 90 ^{o}C, respectively. T_{m1} is known to correspond to lipid structure transformation from a lamellar to disordered state and T_{m2} corresponds to protein-associated lipid transition from gel to liquid form [118]. It should be mentioned that a commonly observed, lower-temperature transition peak (at 35-40 ^{o}C) [100] is not easily observed and an additional transition peak (at 105-120^{o}C), representing changes in *stratum corneum* protein conformation, is also not seen, because it requires a skin water content of at least 15% [119] and our *stratum corneum* samples were desiccated before DSC analysis.

The effect of NLS concentration on the thermal profiles of *stratum corneum* is shown in Figures 3.4A and 3.4B. These data show that increasing NLS concentration (in the presence of 50% ethanol) significantly decreased both of the transition temperatures, T_{m1} and T_{m2}, by as much as 9 and 11^{o}C respectively (Student's *t* test, $p<0.01$). These lipid transitions involve decreased packing order relative to the initial state of the *stratum corneum,* such that the observed decreases in T_m reflect thermal transitions starting from less ordered and more fluidized states of *stratum corneum* [120]. These changes in transition temperatures therefore suggest that incorporation of NLS into the *stratum corneum*, with the aid of the ethanol solution, leads to increased lipid disorder or fluidization. Moreover, the changes in T_{m1} and T_{m2} as a function of NLS concentration scale with the corresponding changes in skin permeability (Figure 3.1B), which suggests that increased skin permeability correlates the effect of NLS-ethanol mixtures on *stratum corneum* lipids, DSC analysis showed increased *stratum corneum* lipid fluidization. To further investigate the fluidizing effect of NLS-ethanol mixtures on *stratum corneum* lipids, DSC analysis was performed as a function of ethanol concentration. Figures 3.5A and 3.5B indicate that the lipid transition temperatures are reduced by the addition of ethanol and that the largest reduction is found at 25% and 50% ethanol (Student's *t* test, $p<0.01$),

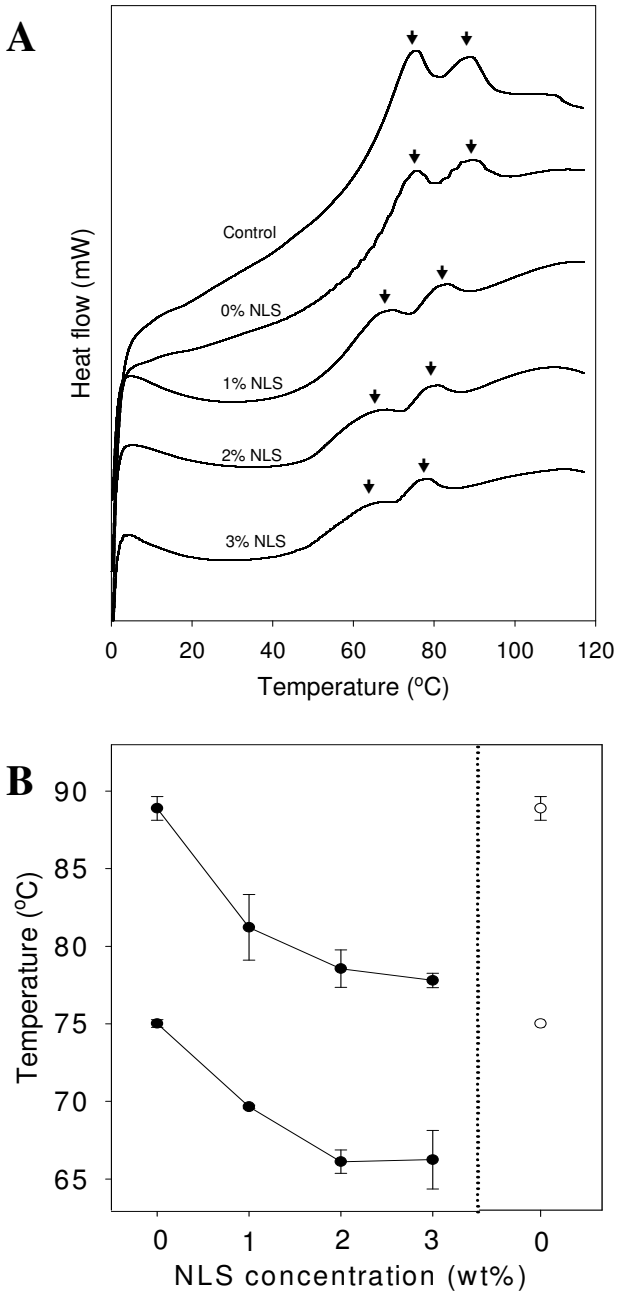

Figure 3. 4 Differential scanning calorimetry (DSC) analysis of human *stratum corneum* as a function of NLS concentration. (A) DSC thermograms of *stratum corneum* treated with various concentrations of NLS in 50% ethanol and negative control thermogram for untreated skin (i.e., no NLS and no ethanol) (B) Peak temperature of two characteristic order-disorder transitions associated with *stratum corneum* lipids as a function of NLS concentration (●) and for the negative control skin (○). Data were taken from part (A).

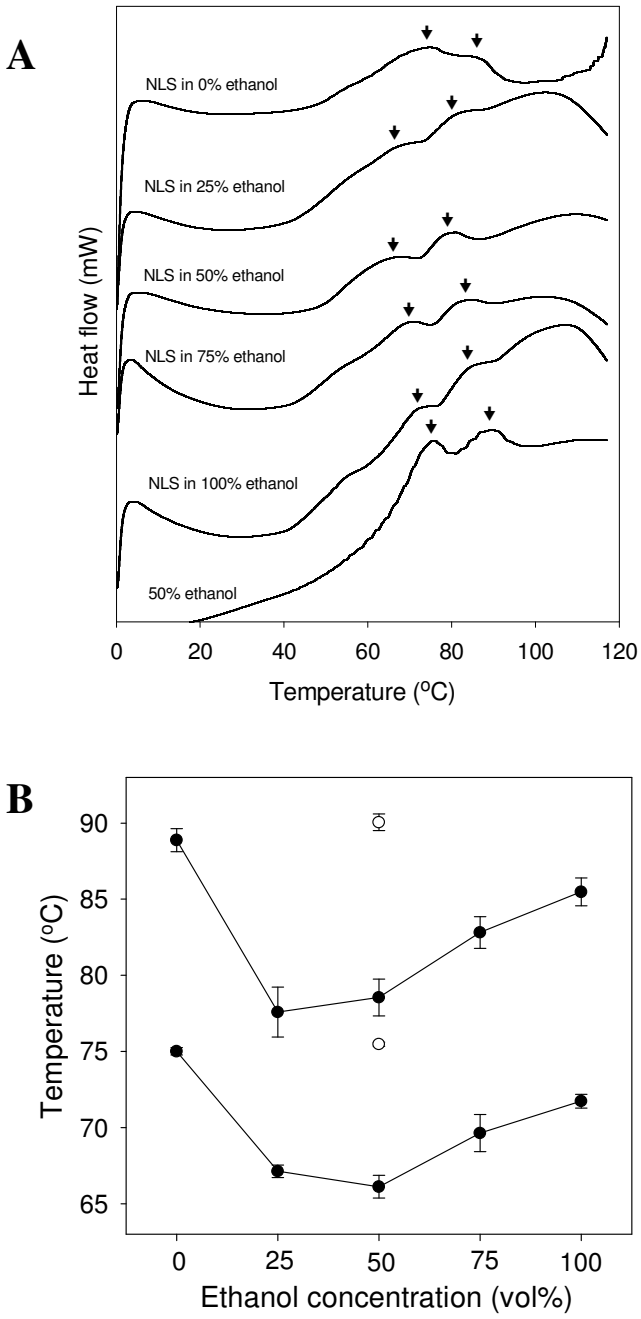

Figure 3. 5 Differential scanning calorimetry (DSC) analysis of human *stratum corneum* as a function of ethanol concentration. (A) DSC thermograms of *stratum corneum* treated with 2% NLS in various concentrations of ethanol and control thermogram for 50% ethanol without NLS. (B) Peak temperature of the two characteristic transitions as function of ethanol concentration (●) with NLS and (○) without NLS. Data points show the average of n≥3 replicates and error bars correspond to the standard error of the mean.

although reductions at 75% and 100% ethanol were also statistically different from the 0% ethanol control (Student's *t* test, $p<0.05$).

In contrast, when *stratum corneum* was treated with a 50% ethanol solution without NLS, neither of the transition temperatures were shifted (Student's *t* test, $p>0.1$). Once again, Figure 3.5A and 3.5B indicate that the lipid transition temperatures are reduced by the addition of ethanol and that the largest reduction is found at 25% and 50% ethanol these increases in lipid fluidization indicated by lower lipid transition temperatures correlate closely with increases in skin permeability (Figure 3.2B) and increases in skin conductivity (Figure 3.3B).

3.3.4 Fourier transform infrared spectroscopy

To further assess changes in molecular conformations within *stratum corneum* after exposure to NLS and ethanol, we employed FTIR spectroscopy. Characteristic peaks are found in FTIR spectra of *stratum corneum* near 2920 cm^{-1}, which corresponds to asymmetric C-H stretching; near 2850 cm^{-1}, which corresponds to symmetric C-H stretching; and near 1650 cm^{-1}, which is the amide I band corresponding to C-O stretching. The frequencies of the two C-H stretching bands are related to lipid order in *stratum corneum* and are significantly influenced by the degree of conformational order, the freedom of alkyl chain motion and possible

incorporation of chemical enhancers, such as NLS. The frequency of the C-O stretching band is related to *stratum corneum* protein conformation [121].

Representative IR absorbance spectra from 3000-2750 and 1850-1300 cm^{-1} of human *stratum corneum* samples are displayed in Figures 3.6A,B and 3.9A,B. In Figure 3.6A and 3.9A, changes in the C-H stretching region and the amide I band, respectively, are shown after treatment of *stratum corneum* with different NLS concentrations. The wave-number position of the three characteristic spectral peaks is shown in Figure 3.6B and 3.9B as a function of NLS concentration. Negative control samples exposed to PBS or to 50% ethanol in the absence of NLS both have C-H asymmetric, C-H symmetric, and C-O stretching peaks at 2918, 2850 and 1648 cm^{-1}, respectively. In contrast, addition of NLS in 50% ethanol increased the wavenumber of each of these three peaks by 1 to 4 cm^{-1} in a dose-dependent manner (Student's *t* test, $p<0.01$). Although these wavenumber shifts are relatively small, they are statistically significant and are consistent in magnitude with previous studies of chemical enhancers [100,122].

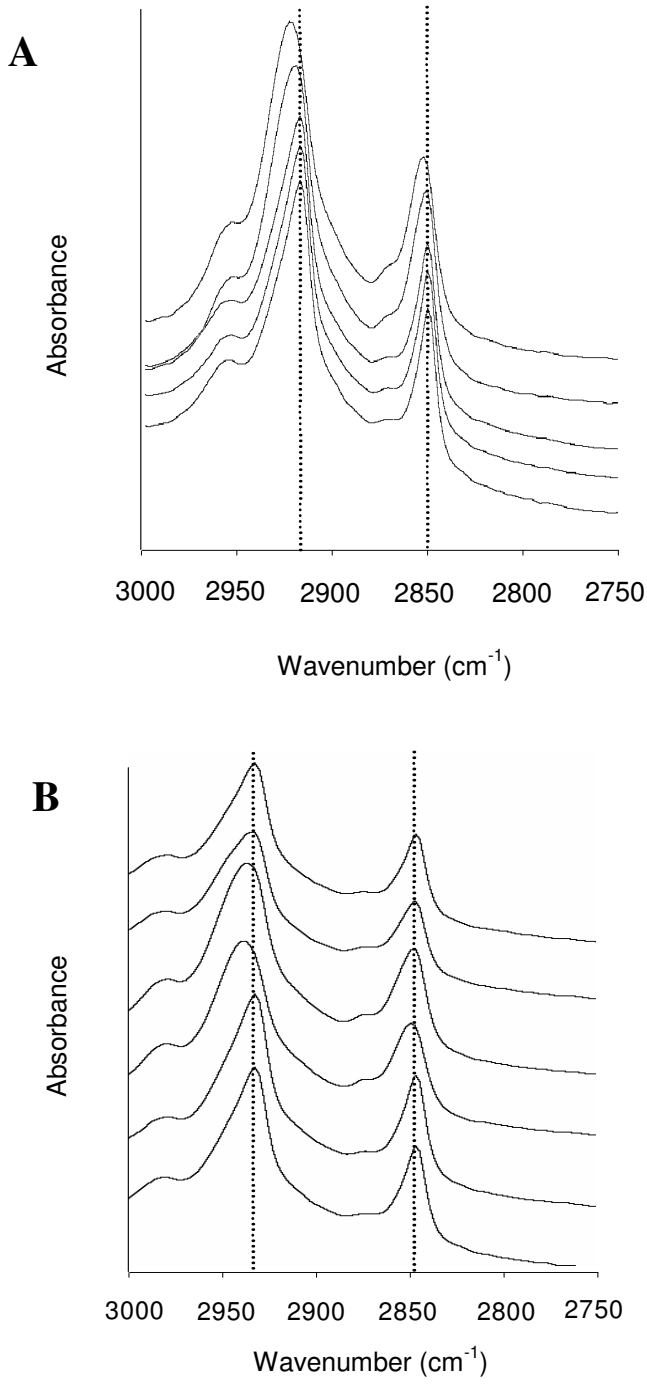

Figure 3. 6 Fourier transform infrared (FTIR) spectral analysis of human *stratum corneum* lipids as a function of NLS and ethanol concentration. (A) FTIR spectra of *stratum corneum* treated with various concentrations of NLS in 50% ethanol. Curves correspond, from top to bottom, to 3% NLS, 2% NLS, 1% NLS, and 0% NLS in 50% ethanol, and untreated skin. (B) FTIR spectra of *stratum corneum* treated with 2% NLS in various concentrations of ethanol. Curves correspond, from top to bottom, to 100% ethanol, 75% ethanol, 50% ethanol, 25% ethanol and 0% ethanol with 2% NLS, and 50% ethanol without NLS.

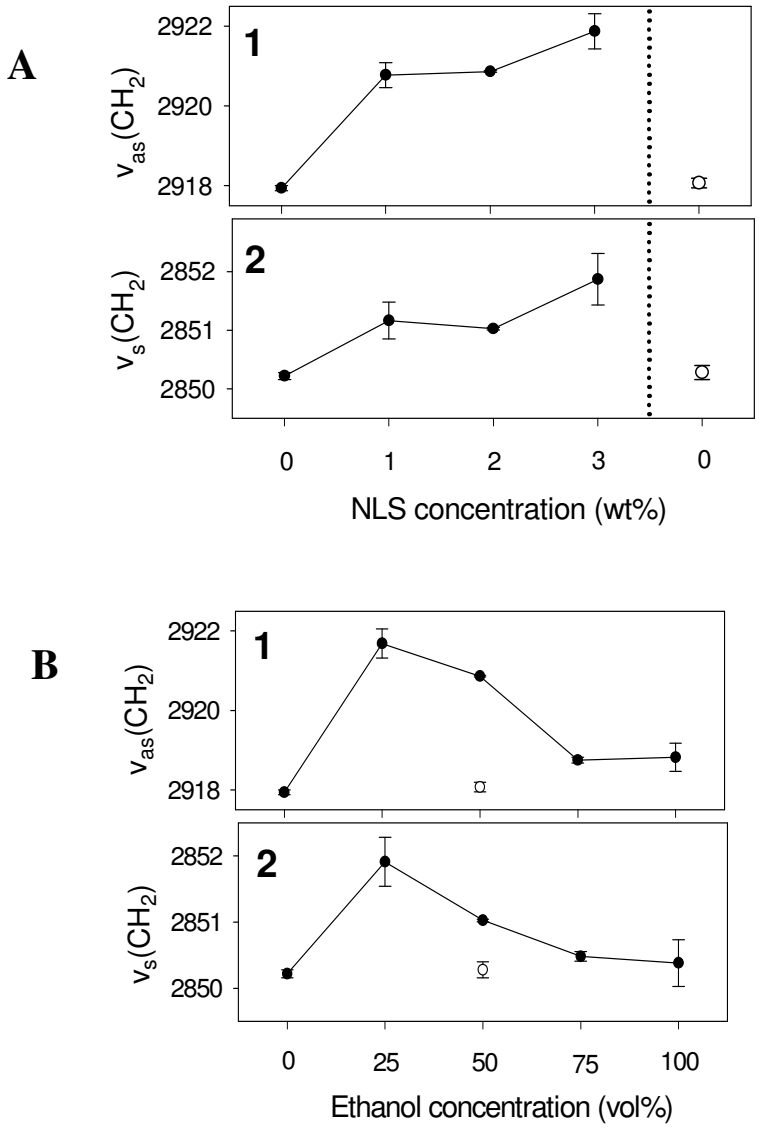

Figure 3. 7 Fourier transform infrared (FTIR) spectral analysis of human *stratum corneum* lipids as a function of NLS and ethanol concentration. Peak wavenumber of characteristic spectral peaks corresponding to (1) asymmetric C-H stretching and (2) symmetric C-H stretching as a function of (C) NLS concentration in (●) 50% ethanol and (○) in PBS and (D) Ethanol concentration (●) with NLS and (○) without NLS. Data points show the average of n≥3 replicates and error bars correspond to the standard error of the mean.

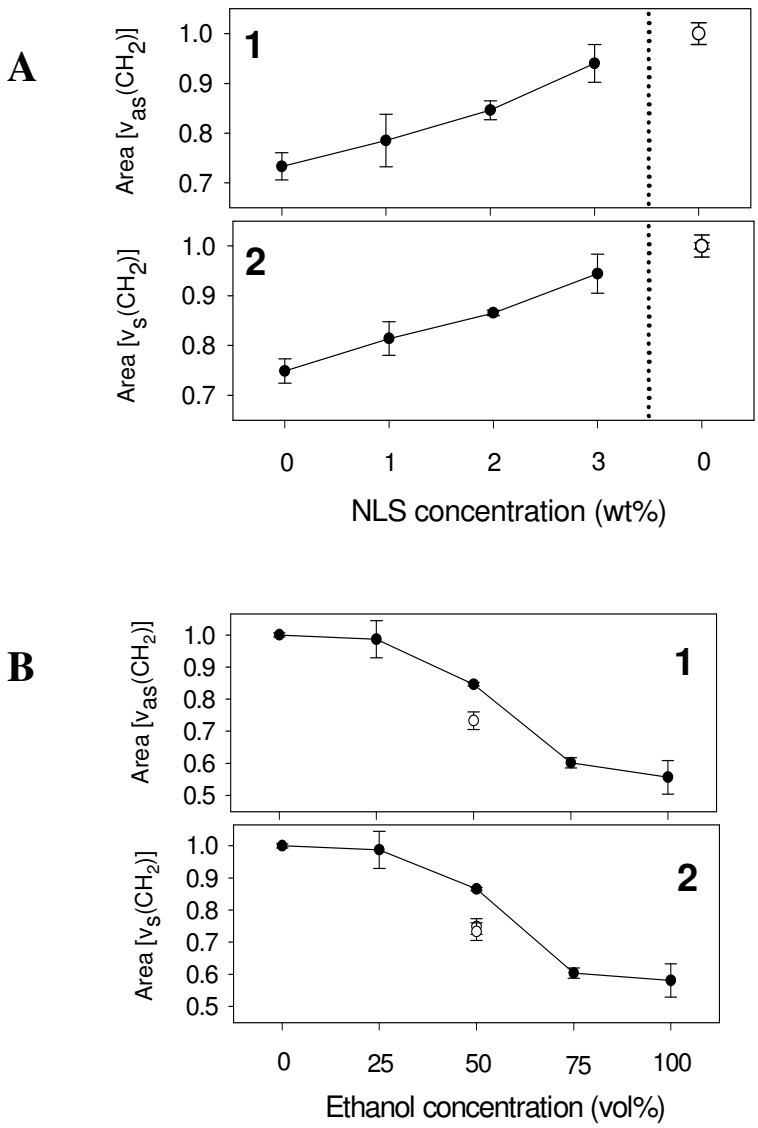

Figure 3. 8 Fourier transform infrared (FTIR) spectral analysis of human *stratum corneum* lipids as a function of NLS and ethanol concentration. Peak area of characteristic spectral peaks corresponding to (1) asymmetric C-H stretching and (2) symmetric C-H stretching as a function of (C) NLS concentration in (●) 50% ethanol and (○) in PBS and (D) Ethanol concentration (●) with NLS and (○) without NLS. Data points show the average of n≥3 replicates and error bars correspond to the standard error of the mean. In (C) and (F), area is normalized to 0% NLS in 0% ethanol.

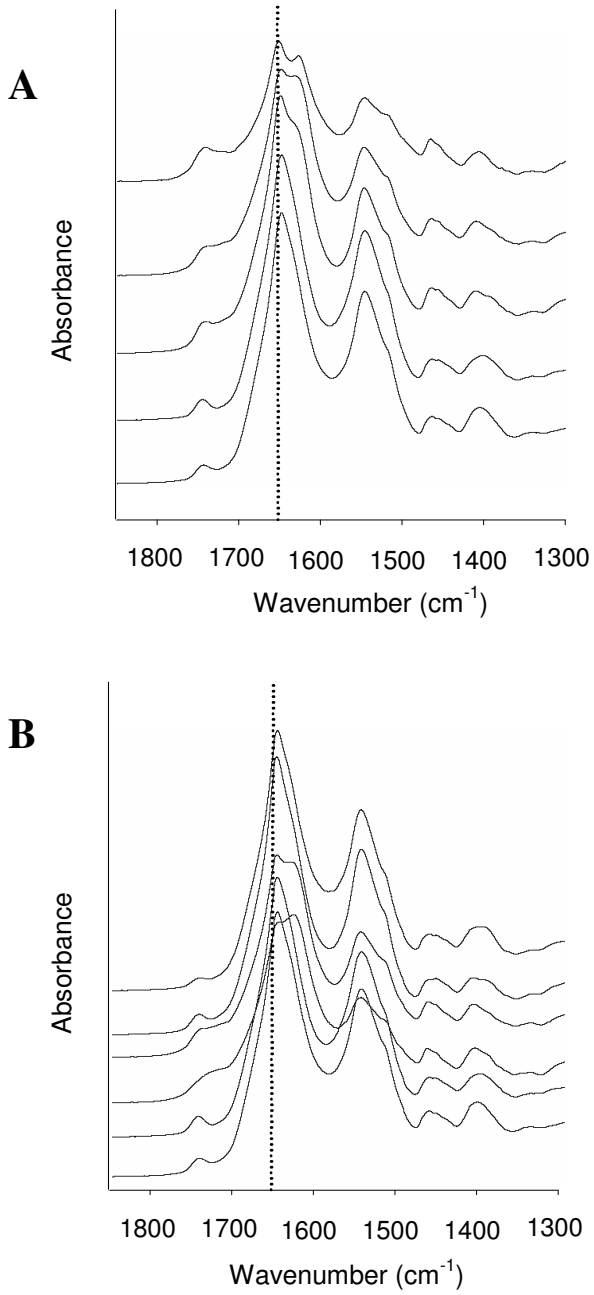

Figure 3. 9 Fourier transform infrared (FTIR) spectral analysis of human *stratum corneum* proteins as a function of NLS and ethanol concentration. (A) FTIR spectra of *stratum corneum* treated with various concentrations of NLS in 50% ethanol. Curves correspond, from top to bottom, to 3% NLS, 2% NLS, 1% NLS, and 0% NLS in 50% ethanol, and untreated skin. (B) FTIR spectra of *stratum corneum* treated with 2% NLS in various concentrations of ethanol. Curves correspond, from top to bottom, to 100% ethanol, 75% ethanol, 50% ethanol, 25% ethanol and 0% ethanol with 2% NLS, and 50% ethanol without NLS.

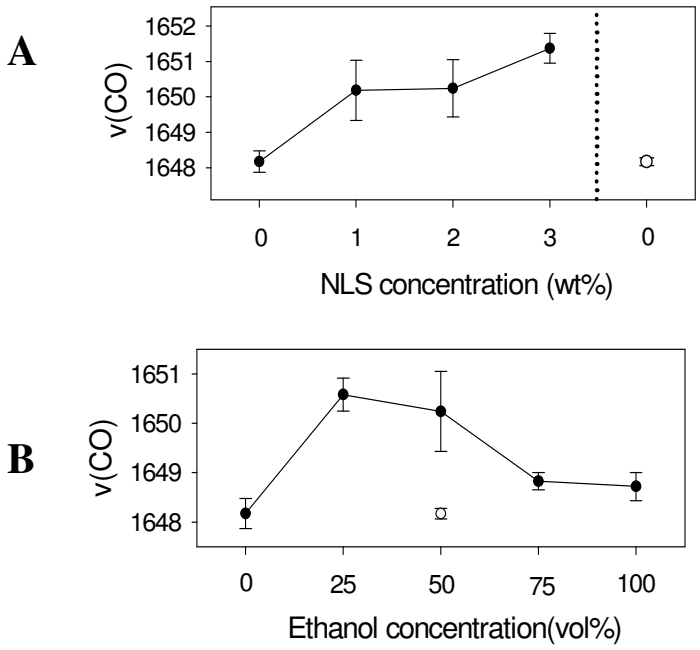

Figure 3. 10 Fourier transform infrared (FTIR) spectral analysis of human *stratum corneum* proteins as a function of NLS and ethanol concentration. Wavenumber of spectral peak corresponding to C-O stretching as a function of (C) NLS concentration in (●) 50% ethanol and (○) in PBS and (D) Ethanol concentration (●) with NLS and (○) without NLS. Data points show the average of n≥3 replicates and error bars correspond to the standard error of the mean.

3.3.4.1 Lipid fluidization

The increased wavenumber of the two C-H stretching peaks (Figure 3.7A) indicates that increasing NLS concentration increased the fluidization of *stratum corneum* lipids, according to established interpretations of FTIR spectra [123]. This fluidization could be from dispersed incorporation of NLS among the *stratum corneum* lipids and, possibly, from pooling of NLS in discrete domains among the

lipids. Comparison with the ethanol-only negative control shows that this was clearly the effect of NLS (in the presence of 50% ethanol) and not the effect of ethanol alone. This is consistent with previous observations that short-chain alcohols have little effect on *stratum corneum* lipid order below 40 ^{o}C [124] and, despite forming localized regions of greater free volume within the lipid alkyl chain regions, exposure to ethanol does not cause overall fluidization of *stratum corneum* lipids [121].

3.3.4.2 Protein conformation

The increased wavenumber of the C=O stretching peak (Figure 3.10A) indicates that increasing NLS concentration also altered *stratum corneum* protein conformation. Closer analysis of Fig. 5B also shows the appearance of an intense new band at 1628 cm^{-1} and increased absorption at 1519 cm^{-1}. Altogether, these changes indicate that increasing NLS concentration caused a shift from the α-helix protein conformation to the β-sheet structure [125]. When considered in the context of skin permeability data (Figure 3.1B), this analysis shows that increased skin permeability correlates with increased *stratum corneum* lipid fluidization and altered *stratum corneum* protein conformation caused by exposure to increasing concentration of NLS in 50% ethanol.

3.3.4.3 Effect of ethanol concentration

We carried out a similar analysis of changes in FTIR spectra for *stratum corneum* samples treated with NLS in different concentrations of ethanol. Changes in the C-H stretching region and the amide I band frequencies are shown in Figure 3.6B and 3.9B, respectively, and summarized in Figure 3.7B and 3.10B. Treatment of *stratum corneum* with NLS in 25% and 50% ethanol significantly increased the wavenumber of all three characteristic spectral peaks relative to the NLS-only and ethanol-only control samples (Student's *t* test, $p<0.05$), whereas treatment with NLS in 75% and 100% ethanol had much less effect (Student's *t* test, $p>0.05$).

3.3.4.4 Lipid extraction

Ethanol and surfactants have been reported to extract lipids from the *stratum corneum* and in that way increase skin permeability [109,126]. To assess the possible role of extraction in this study, the area under the two C-H stretching peaks was measured as a function of NLS and ethanol concentration. Exposure of skin to 50% ethanol significantly decreased the area under both of these peaks (Figure 3.8A,B, Student's t-test, $p<0.01$), which indicated lipid extraction by ethanol, in agreement with previous findings [127]. Addition of NLS in 50% ethanol at progressively larger NLS concentration diminished the effect on peak area (Figure 3.8A, ANOVA,

$p<0.05$), which suggests that addition of NLS either reduced the degree to which 50% ethanol extracted lipids or that NLS possibly replaced the extracted lipids and thereby increased the peak area. At constant NLS concentration, increasing ethanol concentration progressively decreased peak area for both lipid peaks (Figure 3.8B, ANOVA, $p<0.01$), which indicated that higher ethanol concentrations increased lipid extraction.

Notably, the dependence of peak area on NLS and ethanol concentration is different from that of skin permeability. For example, the addition of 50% without NLS caused a large drop in peak area, but had no effect on skin permeability. Moreover, increasing ethanol concentration (in combination with NLS) progressively decreased peak area, but caused skin permeability to go through a maximum at 25 – 50% ethanol. These different functionalities of lipid extraction measured by peak area and skin permeability indicated that although lipid extraction may have occurred, it was not responsible for the observed increases in skin permeability.

Altogether, these observations indicate that NLS in the presence of 25-50% ethanol increases lipid fluidization and alters protein conformation (Figure 3.7B and 3.10B), which correlates with dramatically increased skin permeability (Figure 3.2B). NLS in the presence of 75-100% ethanol had little effect on lipid fluidity and protein

conformation in *stratum corneum*, which similarly correlates with the modest increases in skin permeability seen under those conditions.

3.3.5 Discussion

The results of this study show a remarkably consistent correlation between four different analyses of skin properties as a function of NLS and ethanol concentration. Consistently, treatment using NLS without ethanol or ethanol without NLS had little to no significant effect on skin permeability to fluorescein, skin electrical resistance, DSC thermograms, and FTIR spectra. In contrast, the combination of NLS and ethanol at an optimized concentration of 25-50% uniformly increased skin permeability, decreased skin resistance, decreased DSC transition temperatures, and increased FTIR peak wavenumbers.

Interpretation of these findings demonstrates a correlation, and suggests a causative relationship, between increased skin permeability and increased *stratum corneum* lipid fluidization, as well as changes in protein conformation. We hypothesize that NLS inserts into the *stratum corneum* lipid structures with the aid of ethanol, which disrupts the lipid packing. NLS alone may have difficulty partitioning into the *stratum corneum* lipid domain and ethanol alone is known not to affect lipid fluidity. However, the combination of NLS and ethanol has a synergistic effect, such

that ethanol may facilitate penetration of NLS into the *stratum corneum* lipids, where NLS is then able to fluidize lipid structure.

Although we observed changes in protein conformation as well, we do not expect that these changes are mechanistically responsible for the skin's increased permeability. Skin's barrier properties have been widely established to reside predominantly in the *stratum corneum* lipids, where *stratum corneum* proteins play a secondary role [128,129].

3.4. Conclusion

This study sought to determine the mechanism by which mixtures of NLS and ethanol increase transdermal transport by testing the hypothesis that NLS and ethanol synergistically increase skin permeability by increasing the fluidity of *stratum corneum* lipid structure. When NLS in 50% ethanol was applied to human cadaver skin over a range of NLS concentrations, skin permeability to fluorescein was increased by up to 47 fold in a manner that depended strongly on NLS concentration. Ethanol concentration also strongly affected skin permeability, where formulations containing NLS in 25% and 50% ethanol dramatically enhanced transdermal delivery,

whereas NLS in 0%, 75%, and 100% ethanol had modest or no effect. Ethanol in the absence of NLS had only a small effect on skin permeability.

The degree of skin permeability enhancement correlated with companion measurements of skin electrical resistance, which is a general measurement of skin barrier function associated with an intact *stratum corneum* lipid domain. Increased skin permeability also correlated with altered DSC transition temperatures and FTIR peak shifts that indicate increased fluidity of the *stratum corneum* lipids and changes in protein conformation from the α-helix to the β-sheet structure. These correlations suggest a causative relationship in which increased lipid fluidity is the mechanism by which combinations of NLS and an aqueous ethanol solution increase skin permeability. This formulation also appeared to cause extraction of *stratum corneum* lipids, but the level of extraction did not correlate with skin permeability changes, which suggested it was a secondary effect. Finally, the synergistic effect of this formulation may result from the ability of the ethanol solution to improve the permeation of NLS in the lipid bilayer matrix of the *stratum corneum*, thereby improving the ability of NLS to disrupt the lipid order.

Overall, we conclude that a mixture of NLS in 25-50% ethanol acts synergistically to increase skin permeability. This formulation may be useful for transdermal drug delivery applications.

CHAPTER 4: TRANSDERMAL DELIVERY ENHANCED BY MAGAININ PORE-FORMING PEPTIDE

4.1. Introduction

Transdermal delivery is an attractive method to administer drugs that avoids the pain of injection, reduces the enzymatic degradation associated with oral delivery, and facilitates sustained delivery for up to many days [4]. However, drug delivery into the skin is severely limited by the barrier properties of the *stratum corneum,* which is the outermost layer of skin. The *stratum corneum* is composed of keratin-filled, non-viable cells (corneocytes) embedded in a crystalline intercellular lipid domain. These intercellular lipids compose the continuous domain of the *stratum corneum* and provide its primary barrier properties. *Stratum corneum* lipids consist of an approximately equimolar mixture of free fatty acids, cholesterol and ceramides [21].

Numerous methods have been suggested to overcome the skin barrier for transdermal drug delivery. Chemical penetration enhancement methods have received the most attention, where addition of various chemical agents, such as fatty acids, fatty esters, alcohols, terpenes, pyrrolidones, sulfoxides, and surfactants, has been

tested to increase skin permeability [106]. However, few have succeeded in delivering drugs at therapeutic rates without causing skin irritation or damage. Physical approaches, such as iontophoresis [130], electroporation [131] ultrasound [4], and microneedles [57], have also been evaluated.

In this study, we hypothesize that magainin, a peptide known to form pores in bacterial cell membranes, can increase skin permeability by disrupting stratum corneum lipid structure. A variety of pore-forming peptides are found in nature and have been the subject of intensive research due to their potential application as novel antibiotics [132]. One of the most studied is magainin, which is a 23 amino acid peptide isolated from the skin of the African clawed frog, *Xenopus laevis* [68]. This amphiphilic and non-hemolytic peptide has been shown to kill bacteria by perturbing the membrane function responsible for cellular osmotic balance by self-assembling in the cell membrane to form transmembrane pores [71,133]. Human clinical trials showed that a magainin derivative, Pexiganan, was developed for the intended application to infected diabetic foot ulcers [134]. Other studies have suggested that magainin might be used for contraception [135] and treatment of cancer [136].

To assess the possibility that magainin can increase skin permeability for transdermal drug delivery, our previous work showed that magainin disrupts liposome vesicles made from lipids representative of those found in human *stratum*

corneum [137]. Encouraged by those results, in this study we measured skin permeability after exposure to various magainin formulations and then carried out additional mechanistic analysis using Fourier-transform infrared spectroscopy, X-ray diffraction, and differential scanning calorimetry to characterize the interactions between magainin and *stratum corneum* lipids.

4.2. Materials and Methods

4.2.1 Skin preparation

Same as Chapt 3.

4.2.2 Skin permeability measurement

Same as Chapt 3.

4.2.3 Skin imaging by multi-photon microscopy

To image fluorescein and magainin distribution in the skin, skin was pretreated for 15 h as described above, except that sulphorhodamine-tagged magainin peptide (Microchemical and Proteomics Facility, Emory University) was used. Fluorescein was delivered across the skin, as described above, for 1 h. The skin

sample was then removed from the Franz cell and placed on a glass coverslip. Skin imaging was carried out using a multi-photon microscope (Zeiss LSM/NLO 510, Oberkochen, Germany) with a water immersion lens an oil-immersion lens of 40× magnification to collect "z-stack" optical slices at a series of depths into the epidermis.

4.2.4 Imaging of histological skin sections

To image microscale *stratum corneum* organization, a 2 cm × 2 cm piece of full-thickness skin was pretreated as described above and then cut into 4 mm × 7 mm pieces and placed in a cryoblock with optimal cutting temperature compound (Tissue-Tek, Sakura Finetek, Torrance, CA, USA). After freezing in liquid nitrogen, skin was sectioned on a cryostat (Cryo-star HM 560MV, Microm, Waldorf, Germany) at 40-μm thickness and placed on a glass slide.

To help with imaging the *stratum corneum*, the skin sections were swelled by applying a drop of half-strength Sorensen-Walbum buffer (0.1 N sodium hydroxide solution and 0.1 N glycine solution; Sigma Aldrich) to the tissue for 15 min [138]. Then, a stock solution containing 0.05% (w/v) Nile Red (Molecular Probes, Eugene, OR, USA) in acetone was diluted to 2.5 μg/ml with 75:25 (v/v) glycerol:water and vigorously mixed on a vortexer. A drop of the resulting Nile Red solution was applied on each sample, which was then sealed beneath a cover slip using transparent nail

polish (Revlon, New York, USA) [138] and imaged by a multi-photon microscope (Zeiss LSM/NLO 510).

4.2.5 Fourier-transform infrared spectroscopy

Same as Chapt 3.

4.2.6 X-ray diffraction

Stratum corneum samples were pretreated with enhancer formulations as described above, desiccated under vacuum, and then hydrated for 10 min before examination. The wide-angle X-ray diffraction (PANalytical, Almelo, Netherlands) was carried out at 40 mA and 45 kV and small-angle X-ray diffraction (Rigaku DMAX 2500, Tokyo, Japan) was carried out at 300 mA and 50 kV.

4.2.7 Differential scanning calorimetry

Same as Chapt 3.

4.2.8 Statistical Analysis

Skin permeability to fluorescein, FTIR spectroscopy, and DSC were measured using at least three replicate skin samples at each condition, from which the mean and

standard error of the mean were calculated. A two-tailed Student's t-test was performed when comparing two different conditions. When comparing three or more conditions, a one-way analysis of variance (ANOVA) was performed.

4.3. Results

4.3.1 Effect of magainin formulations on skin permeability

Our previous results showed that incubation with magainin peptide could disrupt vesicles made from lipids representative of those found in human *stratum corneum* [137]. This suggested that magainin could disrupt *stratum corneum* lipids in the skin and thereby increase skin permeability. To test this idea, we exposed human skin to a magainin solution, but there was no change in skin permeability to a model compound, fluorescein (Figure 4.1, Student's *t*-test, p=0.35). To explain this result, we hypothesized that magainin has the ability to insert into a single bilayer, such as that found in a bacterial cell or a liposome vesicle, but may not have a mechanism to cross over additional bilayers, especially given magainin's large size (2494 Da). Because there are close to 100 multilamellar lipid bilayers in a cross section of

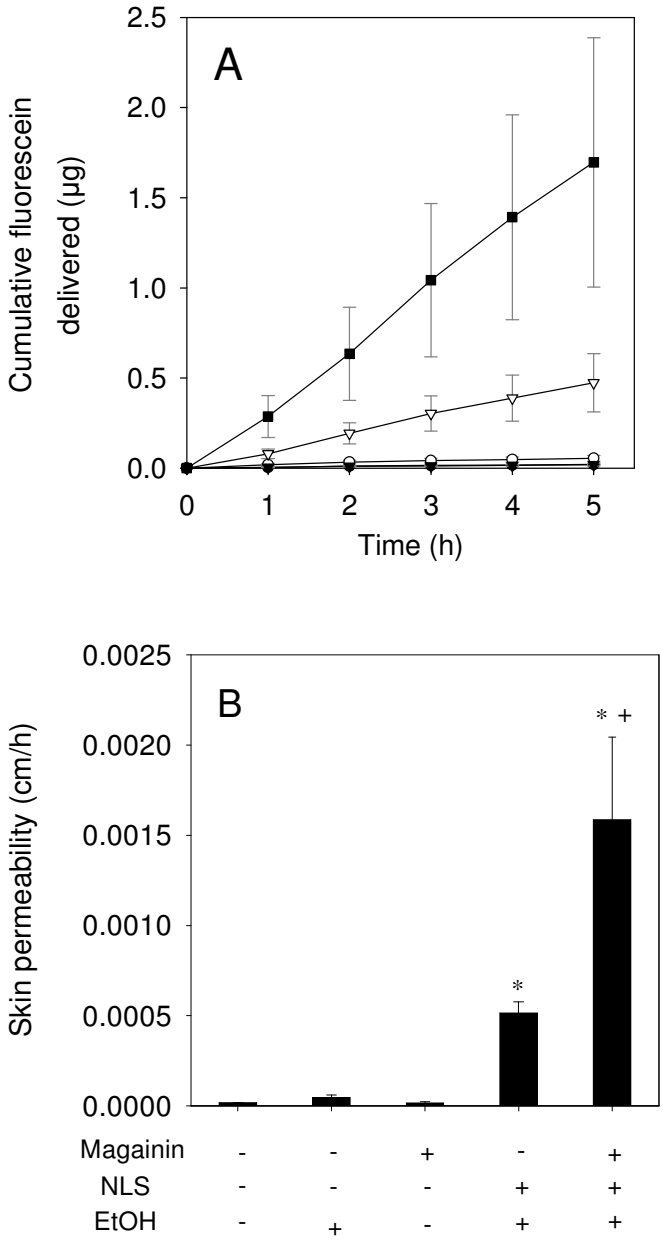

Figure 4. 1 Effect of magainin formulations on skin permeability. (A) Cumulative fluorescein delivered across human cadaver skin pre-treated with (●) no treatment, (▼) magainin peptide in PBS, (○) 50% ethanol, (▽) NLS in 50% ethanol and (■) NLS and magainin peptide in 50% ethanol.(B) Skin permeability values determined from part (A). Data represent averages of n≥3 samples with standard error of the mean. The * symbol identifies permeabilities significantly greater than untreated skin (Student's *t*-test, p<0.05). The + symbol identifies permeabilities after magainin exposure significantly greater than without magainin exposure (Student's *t*-test, p<0.05).

stratum corneum, the ability to cross multiple bilayers is essential to increase skin permeability.

To address this problem, we added a well-known anionic surfactant enhancer – N-lauroyl sarcosine (NLS) – in 50% ethanol solution to facilitate magainin penetration throughout the *stratum corneum*. We used this formulation, because our previous study showed that NLS in 50% ethanol is a good skin permeation enhancer [139]. As shown in Figure 4.1, this magainin-NLS-ethanol combination yielded a 47-fold increase in skin permeability (Student's *t*-test, $p<0.01$), which shows that magainin can increase skin permeability.

Moreover, the enhancement by magainin-NLS-ethanol was significantly greater than the 15-fold increase caused by NLS in ethanol (without magainin) (Student's *t*-test, $p<0.01$) or the 1.3 fold increase caused by ethanol (without magainin or NLS) (Student's *t*-test, $p=0.077$). Because the enhancement of the magainin-NLS-ethanol combination is three-fold greater than the sum of the enhancements by the individual components, this synergy suggests an interaction between magainin and NLS-ethanol and is consistent with the hypothesis that NLS-ethanol increased magainin penetration into skin, which in turn allowed magainin to further disrupt lipid bilayer structures in *stratum corneum*.

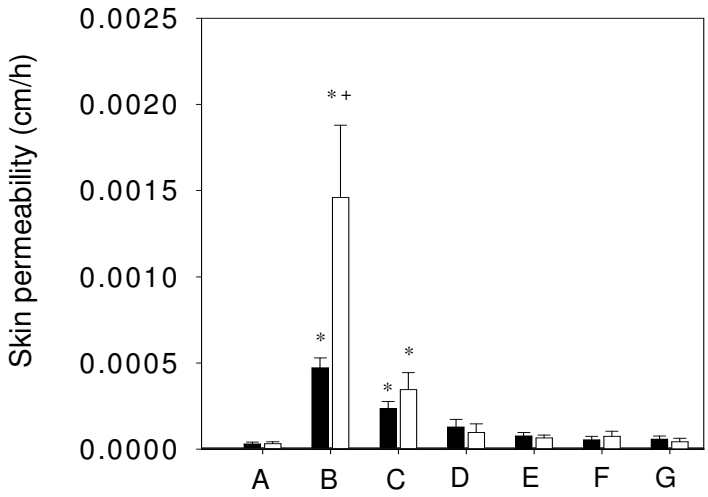

Figure 4. 2 Effect of chemical enhancers on skin permeability and interaction with magainin. Skin permeability to fluorescein after pre-treatment with an enhancer alone (black bars) or in combination with magainin (white bars) for different enhancers: (A) no chemical enhancer, (B) N-lauroyl sarcosine, (C) cetyl trimethyl ammonium bromide, (D) sorbitan monolaurate, (E) oleic acid, (F) isopropyl myristate and (G) phenyl piperazine, all in 50% ethanol. Data represent averages of n≥3 samples with standard error of the mean. The * symbol identifies permeabilities significantly greater than untreated skin (Student's *t*-test, p<0.05). The + symbol identifies permeabilities after magainin exposure significantly greater than without magainin exposure (Student's *t*-test, p<0.05).

To determine if other chemical enhancer formulations might similarly act synergistically with magainin, we compared NLS to five other enhancers from different chemical classes, including a cationic surfactant (cetyl trimethyl ammonium bromide), nonionic surfactant (sorbitan monolaurate), fatty acid (oleic acid), fatty ester (isopropyl myristate), and Azone-like compound (phenyl piperazine). As shown

in Figure 4.2, only NLS and the cationic surfactant directly increased skin permeability to fluorescein (conditions B and C, Student's t-test, $p<0.01$) and only NLS showed a synergistic increase in skin permeability with magainin (condition B, Student's *t*-test, $p=0.046$). The fact that magainin carries a positive charge and NLS carries a negative charge suggests that the ionic attraction between these compounds may be important to their action.

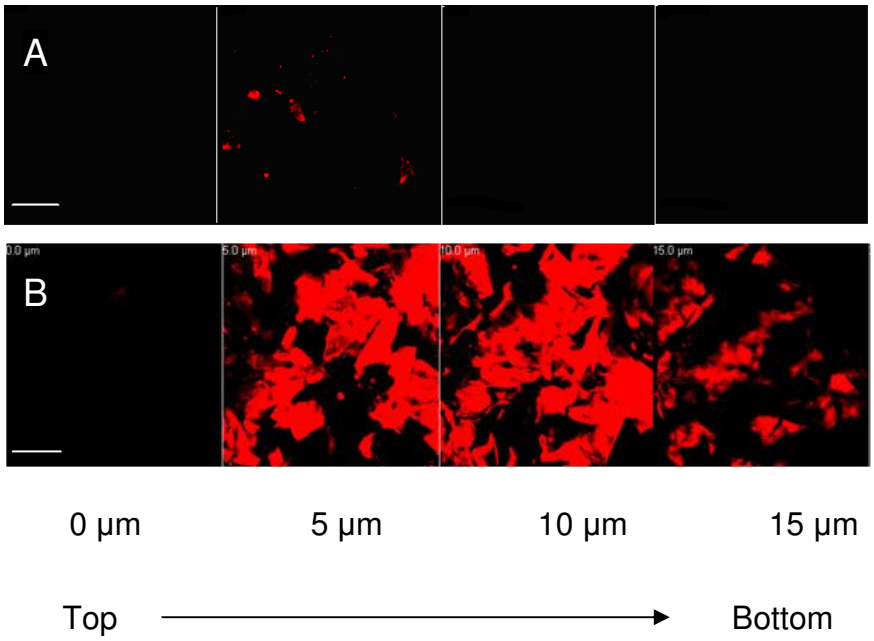

Figure 4. 3 Penetration of sulforhodamine-tagged magainin peptide into human epidermis imaged by multi-photon microscopy. Magainin formulated (A) without NLS and (B) with NLS, both in 50% ethanol. Optical sections taken at 5 µm increments starting at the stratum corneum surface on the left and proceeding deeper on the right. Scale bar is 100 µm.

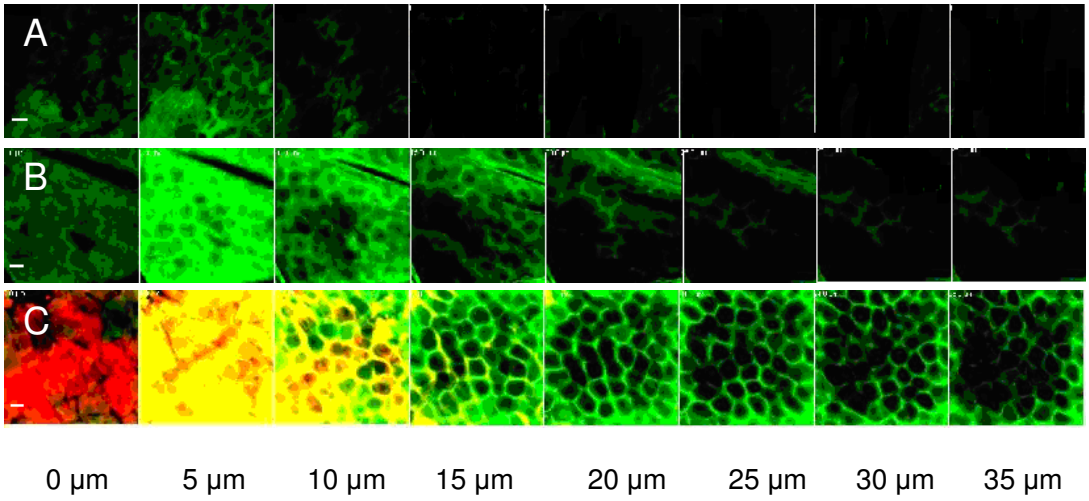

Figure 4. 4 Penetration of fluorescein and sulforhodamine-tagged magainin peptide into human epidermis imaged by multi-photon microscopy. Fluorescein formulated with (A) PBS, (B) with NLS in 50% ethanol and (C) with NLS and magainin in 50% ethanol. Green corresponds to fluorescein, red corresponds to sulforhodamine-tagged magainin and yellow corresponds to co-localization of fluorescein and magainin. Optical sections take at 5 µm increments starting at the stratum corneum surface on the left and proceeding deeper on the right. Scale bar is 100 µm.

4.3.2 Imaging magainin and fluorescein penetration into skin

To more directly test the hypothesis that NLS-ethanol increases magainin penetration into skin, we imaged the skin by multi-photon microscopy after delivery of sulforhodamine-labeled magainin with and without NLS-ethanol enhancement. As shown in Figure 4.3A, very little magainin (red fluorescence) was able to enter the skin without enhancement. In contrast, Figure 4.3B shows that in the presence of

NLS-ethanol, magainin was able to penetrate throughout the 10–15 μm layer of *stratum corneum*.

Figure 4.4 shows complementary data that simultaneously image magainin (red fluorescence) and fluorescein (green fluorescence) transport into the skin. In the absence of NLS-ethanol and magainin, there is little fluorescein delivery into the skin (Figure 4.4A). The addition of NLS-ethanol significantly increased fluorescein delivery (Figure 4.4B), in agreement with skin permeability data in Figure 4.1. Finally, the combination of NLS-ethanol and magainin increased fluorescein delivery even more and was associated with significant magainin penetration into the *stratum corneum* (Figure 4. 4C). It is interesting to note that there is significant co-localization of magainin and fluorescein (indicated by yellow in Figure 4.4C), which is consistent with magainin-mediated disruption of the *stratum corneum* corresponding to pathways for increased fluorescein transport. It is also worth noting that magainin preferentially localized within the *stratum corneum*, which is consistent with its expected mechanism of preferentially inserting into *stratum corneum* lipid bilayers, whereas fluorescein penetrated deeply into the skin.

These observations provide direct evidence that increased magainin penetration into the *stratum corneum* is associated with increased skin permeability and that NLS-ethanol facilitates this increased magainin penetration. This insight not

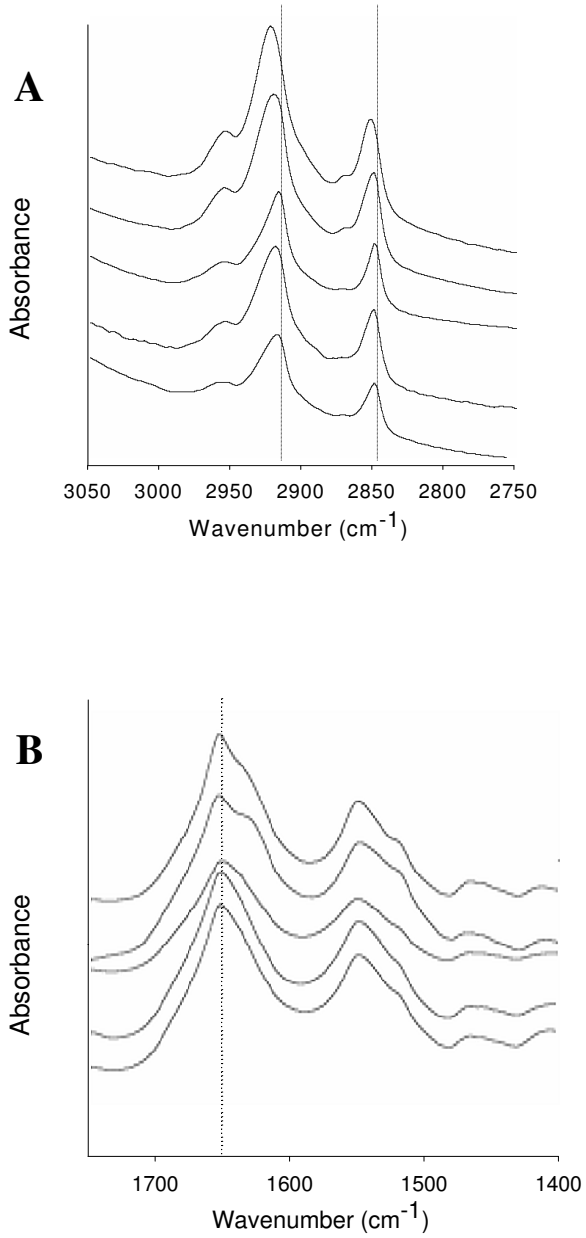

Figure 4. 5 Fourier-transform infrared spectroscopy analysis of human *stratum corneum* treated with different formulations. Spectra of wavenumbers characteristic of (A) C-H stretching in lipids and (B) C-O stretching in proteins treated with (from bottom to top): PBS, magainin in PBS, 50% ethanol, NLS in 50% ethanol, NLS and magainin in 50% ethanol. Dashed lines indicated peaks of interest. Graphs are representative of n≥3 replicate samples.

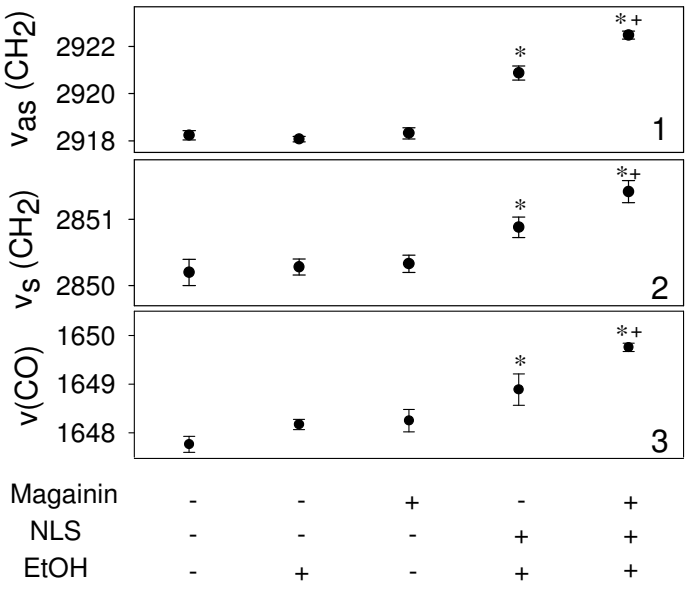

Figure 4. 6 Fourier-transform infrared spectroscopy analysis of human *stratum corneum* treated with different formulations. Change of (1) CH_2 asymmetric stretching frequency, (2) CH_2 symmetric stretching frequency and (3) CO stretching frequency, determined from graphs in Figure 4.5 (A) and (B). Data represent averages of n≥3 samples with standard error of the mean. The * symbol identifies wavenumbers significantly greater than untreated skin (Student's *t*-test, p<0.05). The + symbol identifies wavenumbers after exposure to NLS and magainin that are significantly greater than exposure to just NLS (Student's *t*-test, p<0.05).

not only helps elucidate the mechanism of skin permeability enhancement, but also introduces the novel concept of using a first chemical enhancer to increase delivery of second chemical enhancer into the skin.

4.3.3 Fourier-transform infrared spectroscopy

Because magainin and NLS-ethanol are hypothesized to disrupt *stratum corneum* lipid structure, we characterized *stratum corneum* samples exposed to different formulations using Fourier-transform infrared (FTIR) spectroscopy. To identify alterations in lipid order, we measured changes in carbon-hydrogen stretching frequencies near 2850 and 2920 cm^{-1}, which are due to symmetric [$v_s(CH_2)$] and asymmetric [$v_{as}(CH_2)$] C-H stretching in *stratum corneum* lipid molecules, respectively (Fig. 5A) [123]. To identify alteration in protein structure, we also measured changes in the carbon-oxygen stretching frequency near 1650 cm^{-1} [v(CO)], which is associated with transitions from α-helix to β-sheet structure of *stratum corneum* keratin molecules (Figure 4.5B) [121].

As summarized in Figure 4.6, *stratum corneum* treated with magainin alone or 50% ethanol alone did not cause significant changes in any of the three characteristic stretching frequencies (Student's *t*-test, $p>0.05$). In contrast, treatment with NLS-ethanol caused an increase in $\nu_{as}(CH_2)$ of 2.6 cm^{-1} and $\nu_s(CH_2)$ of 0.85 cm^{-1} relative to untreated skin (Student's *t*-test, $p<0.05$). Addition of magainin peptide raised these stretching frequency values even higher to increases in $\nu_{as}(CH_2)$ of 4.3 cm^{-1} and $\nu_s(CH_2)$ of 1.2 cm^{-1}. These increases in the presence of magainin are significantly different from untreated skin (Student's *t*-test, $p<0.01$) and from skin

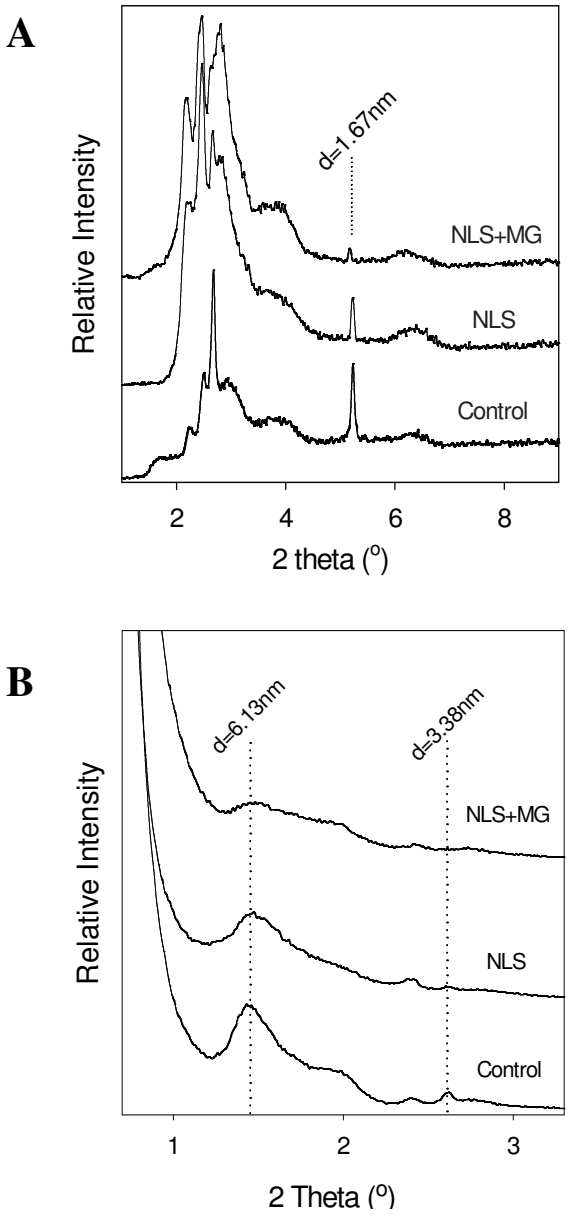

Figure 4. 7 X-ray scattering analysis of human *stratum corneum* treated with different formulations. (A) Wide-angle and (B) small-angle X-ray scattergrams of *stratum corneum* treated with PBS (control), NLS in 50% ethanol or NLS and magainin in 50% ethanol. Dashed lines indicate peaks of interest. Graphs are representative of n≥3 replicate samples.

treated only with NLS-ethanol (Student's *t*-test, $p<0.1$). These data indicate that NLS-ethanol increased *stratum corneum* lipid chain disorder and fluidity and that addition of magainin caused a further increase in this disorder.

Protein structure was also affected by NLS-ethanol and magainin. Treatment with NLS-ethanol caused an increase in ν(CO) of 1.1 cm^{-1} relative to untreated skin (Student's *t*-test, $p=0.028$). Addition of magainin peptide raised ν(CO) even higher to increases of 2 cm^{-1}, which are significantly different from untreated skin (Student's *t*-test, $p=0.002$) and from skin treated only with NLS-ethanol (Student's *t*-test, $p=0.091$). These data indicate that NLS-ethanol and magainin also have effects on *stratum corneum* proteins, possibly promoting a transformation from the α-helix to the β-sheet structure.

4.3.4 X-ray diffraction

To further elucidate effects on *stratum corneum* structure, we used wide-angle and small-angle X-ray diffraction (XRD) to provide a direct measure of changes in lipid bilayer packing. Wide-angle XRD on untreated skin revealed a characteristic peak at 16.7 Å caused by scattering of crystalline cholesterol [102], which is a primary component of *stratum corneum* lipids (Figure 4.7A). Treatment with NLS-ethanol reduced this peak and addition of magainin reduced it still farther. This

suggests that both NLS-ethanol and magainin reduced cholesterol crystallinity, which reduces lipid bilayer order.

Small-angle XRD on untreated skin revealed a number of characteristic peaks, notably corresponding to ceramides (d = 6.13 nm) and crystalline cholesterol (d = 3.38 nm) [140]. Treatment with NLS-ethanol reduced both the ceramide and crystalline cholesterol peaks and addition of magainin reduced them still farther. (Figure 4.7B). This further suggests that both NLS-ethanol and magainin disrupt the order of the dominant components of *stratum corneum* lipid bilayer structures.

4.3.5 Differential scanning calorimetry

Differential scanning calorimetry (DSC) provides another method to probe changes in *stratum corneum* structure, based on its thermal properties. DSC analysis of untreated dry human *stratum corneum* showed two major thermal transitions, T_1 and T_2, at approximately 75 and 90 ^{o}C, respectively (Figure 4.8). T_1 is assigned to lipid structure transformation from lamellar to the disordered, and T_2 is assigned to a protein-associated lipid transition from gel to liquid form [118]. Other previously reported transition peaks at 35-40 ^{o}C and 105-120 ^{o}C were not seen here, in part because the *stratum corneum* samples were desiccated after treatment [119,141].

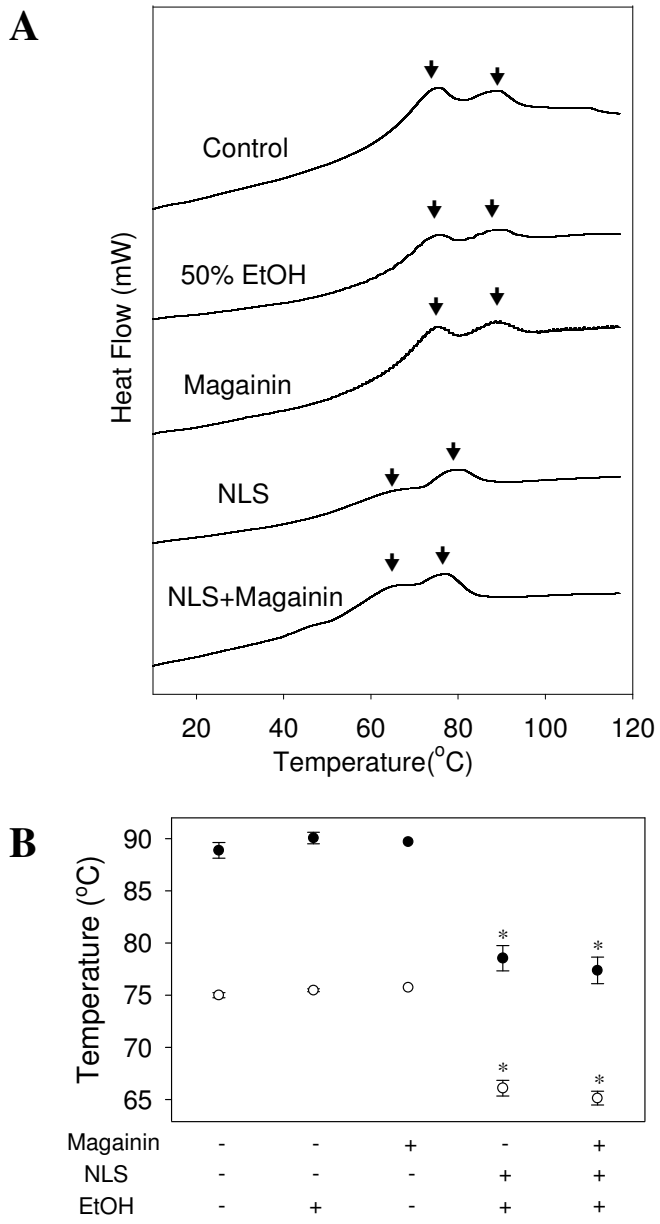

Figure 4. 8 Differential scanning calorimetry (DSC) analysis of human *stratum corneum* treated with different formulations. (A) Thermograms of *stratum corneum* treated with (from top to bottom): PBS (control), magainin in PBS, 50% ethanol, NLS in 50% ethanol, NLS and magainin in 50% ethanol. Arrows indicate peaks of interest. Graphs are representative of n≥3 replicate samples. (B) Changes of two characteristic transition midpoint temperatures (T_1: ●, T_2: ○) determined from graph in (A). Data represent averages of n≥3 samples with standard error of the mean. The * symbol identifies temperatures significantly smaller than untreated skin (Student's *t*-test, p<0.05).

As summarized in Figure 4.8B, *stratum corneum* treated with magainin alone or 50% ethanol alone did not cause significant changes in either of the major thermal transitions (Student's *t*-test, $p>0.1$). In contrast, after treatment with NLS-ethanol, the first and second transition temperatures were decreased by 9 and 10.5 ^{o}C, respectively, relative to untreated skin (Student's *t*-test, $p<0.01$). Addition of magainin further dropped these transition temperatures to decreases of 10 and 11.5 ^{o}C, respectively (Student's *t*-test, $p<0.01$), but these changes were not significantly different from skin treated only with NLS-ethanol (Student's *t*-test, $p>0.1$). Altogether, the decreased lipid transition temperatures indicate that NLS-ethanol disordered *stratum corneum* lipids, but that addition of magainin did not further disorder lipids at detectable levels. The effects of magainin may not have been evident through DSC analysis because DSC measures bulk properties that are relatively insensitive to localized changes. Unlike NLS-ethanol, which can fluidize throughout the *stratum corneum* lipids, magainin's mechanism of action is expected to be in the form of transmembrane pore structures localized on the nanometer scale.

4.3.6 *Stratum corneum* histology

As a final assessment of changes to *stratum corneum* structure, skin was cryo-sectioned, stained and imaged histologically after exposure to different

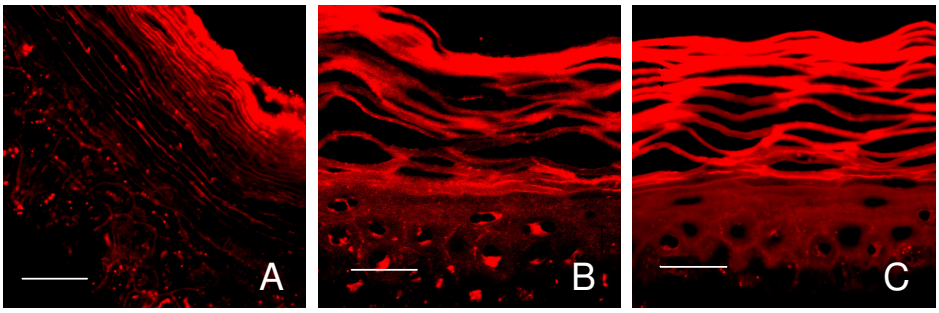

Figure 4. 9 Changes in human *stratum corneum* architecture imaged by multi-photon microscopy of histological cross-sections. *Stratum corneum* was treated with (A) PBS, (B) NLS in 50% ethanol and (C) NLS and magainin in 50% ethanol. To facilitate imaging, stratum corneum was swelled by incubation in Sorensen-Walbum buffer and stained with Nile Red. Scale bar is 20µm.

formulations. As displayed in Figure 4.9A, untreated *stratum corneum* showed intact, densely packed structure. In contrast, *stratum corneum* treated with NLS-ethanol alone (Figure 4.9B) or with magainin peptide (Figure 4.9C) showed disruption and expansion of the *stratum corneum* layers consistent with a loss of lipid structural order. Differences between *stratum corneum* treated with or without magainin peptide were, once again, not evident, perhaps because localized, nanometer-scale pore structures believed to be formed by magainins are not visible by optical microscopy.

4.4. Discussion

4.4.1 Magainin can increase skin permeability by disrupting *stratum corneum* lipid structure

This study investigated the application of a pore-forming peptide, magainin, as a novel transdermal transport enhancer. Toward this end, we tested the hypothesis that magainin, a peptide known to form pores in bacterial cell membranes, can increase skin permeability by disrupting *stratum corneum* lipid structure. In support of this hypothesis, a magainin-based formulation was shown to increase skin permeability to fluorescein by 47 fold (Figure 4.1). The mechanism of disrupting *stratum corneum* lipid structure was supported by multi-photon microscopy imaging, shifted FTIR peak position related to lipid and protein stretching frequencies, and reduced X-ray diffraction peak intensities related to lipid structure.

Multi-photon microscopy showed significant magainin penetration into the *stratum corneum*, but not into the viable epidermis (Figures 4.3 and 4.4). This indicates that the site of action is located in the *stratum corneum*. Although magainin appears to be localized both intracellularly and extracellularly in the *stratum corneum*, fluorescein appears to be located primarily extracellularly (i.e., within the

extracellular lipids). This indicates that the site of magainin action to increase skin permeability was located in the extracellular lipids.

FTIR spectroscopy showed a disruption of *stratum corneum* lipid and protein structure induced by magainin (Figure 4.5 and 4.6). Moreover, for the various formulations used, the degree of structural disruption measured by FTIR correlated with the increase in skin permeability measured by fluorescein delivery, which suggests a mechanistic relationship. Disruption of lipid acyl chain order was indicated by an increase of C-H stretching absorbances to higher wavenumbers [123]. Protein order was also disrupted, as indicated by an increase in C-O stretching consistent with conformational transformation of keratin from the α-helix to the β-sheet structure [121]. This conformational change of keratin may be a secondary effect of the disruption of *stratum corneum* lipid structure [142].

X-ray scattering analysis also indicated a disruption of *stratum corneum* lipid structure induced by magainin (Figure 4.7). Again, there was a dose-response effect, where formulations that caused greater structural disruption corresponded to increased skin permeability. Wide-angle and small-angle XRD showed reduced peak intensity associated with crystalline cholesterol. Cholesterol is the second most abundant lipid in the *stratum corneum* and its role is recognized as providing plasticity in the gel-phase bilayer [143]. On a related note, it has been observed that changes in

cholesterol metabolism in the epidermis leads to a disturbed barrier function of skin [15]. Our formulations containing NLS-ethanol and magainin are hypothesized to increase skin permeability in part by removing or reducing the cholesterol in *stratum corneum*. Previous work has shown that other anionic surfactants, sodium lauryl sulfate and lauroyl isothionate, extract cholesterol from *stratum corneum* cell membranes [144]. Small-angle XRD also showed reduced peak intensity associated with ceramides, which is also one of the most abundant lipids in *stratum corneum*.

DSC analysis showed changes in the thermal profile of *stratum corneum* after treatment with NLS-ethanol that was indicative of increased lipid fluidity. However, further changes in the thermal profile due to addition of magainin were not statistically significant.

4.4.2 Magainin's enhancement requires co-administration with a surfactant chemical enhancer to increase magainin penetration into the skin

Although magainin was previously shown to disrupt liposome vesicles made of lipids representative of stratum corneum [137], magainin without a chemical enhancer had no effect on skin permeability in this study (Figure 4.1). This could be explained by the ability of magainin to inserted into and disrupt an individual lipid bilayer, but an inability to cross over multiple bilayers, such as the multilamellar

stacks of lipids found in *stratum corneum*. Guided by this, we hypothesized that magainin's enhancement requires co-administration with a surfactant chemical enhancer to increase magainin penetration into the skin.

Consistent with this hypothesis, co-administration of magainin and an anionic surfactant, NLS, in a 50% ethanol formulation increased skin permeability 47 fold. In contrast, NLS-ethanol without magainin increase skin permeability just 15 fold (Figure 4.1). This synergistic effect indicated an interaction between NLS and magainin. Multi-photon microscopy supported this, by showing that without NLS-ethanol, little magainin penetration into the skin occurred, but co-administration of magainin and NLS-ethanol led to extensive magainin penetration throughout the *stratum corneum* (Figure 4.3). Comparison to fluorescein transport data (Figures 4.1 and 4.4) showed that increased magainin penetration into stratum corneum correlated with increased skin permeability.

In addition to NLS, five other kinds of chemical enhancers were evaluated, but only the anionic surfactant NLS was found to act synergistically with magainin. This could be because of an ionic attraction between negatively charged NLS and positively charged magainin that facilitates penetration and interaction with the *stratum corneum*. It also might be explained based on an interaction between NLS and skin that makes *stratum corneum* especially permeable and thereby, in a nonspecific

way, increases magainin penetration into *stratum corneum*. This latter argument is supported by the observation that, without magainin, NLS increased skin permeability to fluorescein better than the other five chemical enhancers.

4.5. Conclusions

This study showed that a formulation containing a pore-forming peptide, magainin, and NLS in 50% ethanol synergistically increased skin permeability by 47 fold. Analysis by multi-photon microscopy, FTIR, XRD, and DSC supported the hypothesis that magainin can increase skin permeability by disrupting *stratum corneum* lipid structure, especially ceramides and cholesterol. Additional analysis supported the hypothesis that magainin's enhancement requires co-administration with a surfactant chemical enhancer to increase magainin penetration into the skin

Overall, we conclude that the combination of magainin and NLS-ethanol synergistically increases skin permeability, because NLS-ethanol increased magainin penetration into *stratum corneum*, which further increased *stratum corneum* lipid disruption and skin permeability. We believe this is the first study to use a pore-forming peptide as a skin penetration enhancer and the first study to use one chemical enhancer to increase penetration of another chemical enhancer into the skin.

CHAPTER 5: OPTIMIZATION OF TRANSDERMAL DELIVERY USING MAGAININ PORE-FORMING PEPTIDE

5.1. Introduction

Multilamellar lipid bilayers comprise the continuum portion around the corneocyte cells of *stratum corneum*, which is the primary barrier in skin [145]. Various physical and chemical methods have been tested to increase the permeability of the *stratum corneum* to drugs, which could enable transdermal delivery of more drugs using a transdermal patch. However, few methods have succeeded to deliver relevant agents at the appropriate flux levels without causing skin irritation or damage [4].

This study addresses the use of a naturally occurring pore-forming peptide, magainin, to increase skin permeability. Magainin is a 23-residue helical peptide isolated from the skin of the African frog, which exhibits a broad spectrum of antimicrobial activity properties. It has a net +4 charge and binds to negatively charged phospholipid membranes with the aid of electrostatic interactions, forming an amphiphilic helix and permeabilizing the bilayers [64,68].

Our previous work shows that the use of magainin disrupts vesicles that are made from lipid bilayer components representative of those found in human *stratum*

corneum [137], and that magainin administered in a formulation containing an anionic surfactant, N-lauroyl sarcosine (NLS), in 50% ethanol-in-PBS synergistically increased skin permeability. Mechanistic analysis using differential scanning calorimetry, Fourier-transform infrared spectroscopy, and X-ray diffraction suggested that magainin and NLS can increase skin permeability by disrupting *stratum corneum* lipid structure [146].

Building off the results of our previous work, this study sought to further optimize conditions that increase skin permeability. Because the interaction between magainin and the *stratum corneum* is critical to the enhancement mechanism, we varied the pretreatment time and magainin concentration during exposure to skin. We also tested the effect of molecular weight of delivered molecules on skin permeability.

5.2. Experimental methods

5.2.1 Skin preparation and permeability measurement

Human epidermis (Emory University) was isolated from dermis using the heat separation method [113]. Before measuring skin permeability, skin was pretreated with magainin and other control formulations. Epidermis was placed in a vertical, glass Franz diffusion cell apparatus (PermeGear) with 0.7 cm^2 exposed skin surface area. The receiver chamber was filled with PBS and the donor chamber was filled

with 0.3 ml of a formulation in PBS containing 50% (v/v) ethanol, 2% (w/v) N-lauroyl sarcosine (Fluka) and, sometimes, 1 mM magainin peptide (Emory University). After a 0-12 h exposure to one of these formulations at 4 ^{o}C, the Franz cell was transferred to a heater/stirrer block (PermeGear) maintained at 32 ^{o}C and stirred at 455 rpm for 3 h.

After this pretreatment, the receiver chamber was emptied and filled with fresh PBS and the donor chamber was emptied and filled with 0.3 ml of 1 mM fluorescein, calcein (Sigma Aldrich), or fluorescein-tagged dextran (3000 Da, Molecular Probes) in PBS. Every hour for 5 h, the receiver chamber was sampled. Samples were analyzed by calibrated spectrofluorimetry (Photon Technologies International) to determine transdermal flux and permeability.

5.2.2 Skin imaging by multi-photon microscopy

To image fluorescein and magainin distribution in the skin, skin was pretreated with sulforhodamine-tagged magainin. Fluorescein was then delivered across the skin, as described above, for 1 h. The skin sample was then removed from the Franz cell and placed on a glass cover slip. Skin imaging was carried out using a multi-photon microscope (Zeiss LSM/NLO 510) with an oil-immersion lens of 40× magnification to collect "z-stack" optical slices at a series of depths into the epidermis.

5.3. Results and discussion

To further optimize conditions that enhance skin permeability by magainin, we studied the effect of the duration and concentration of magainin exposure during pretreatment of the skin and the effect of the molecular weight of delivered molecules on skin permeability.

We first hypothesized that increased magainin pretreatment exposure time should increase skin permeability to fluorescein by enabling more magainin to enter the *stratum corneum*. As shown in Figure 5.1A, the amount of fluorescein delivered across the skin increased when we increased the pretreatment time (ANOVA, $p<0.01$). The black bars in Fig. 1-a show the increase in skin permeability caused by incubation with the formulation of NLS in 50% ethanol-in-PBS without magainin. This formulation alone increases skin permeability (ANOVA, $p<0.01$). The white bars show the increase in skin permeability caused by incubation in the same formulation that also contained magainin (ANOVA, $p<0.01$). The addition of magainin further increased skin permeability beyond that of the magainin-free formulation after 12 h (ANOVA, $p<0.05$).

Further examination shows that the permeability increase after 3 h was insignificant (Student's *t*-test, $p>0.05$), whereas the permeability increases after 6 h and longer were significant (Student's *t*-test, $p<0.01$). This led us to conclude

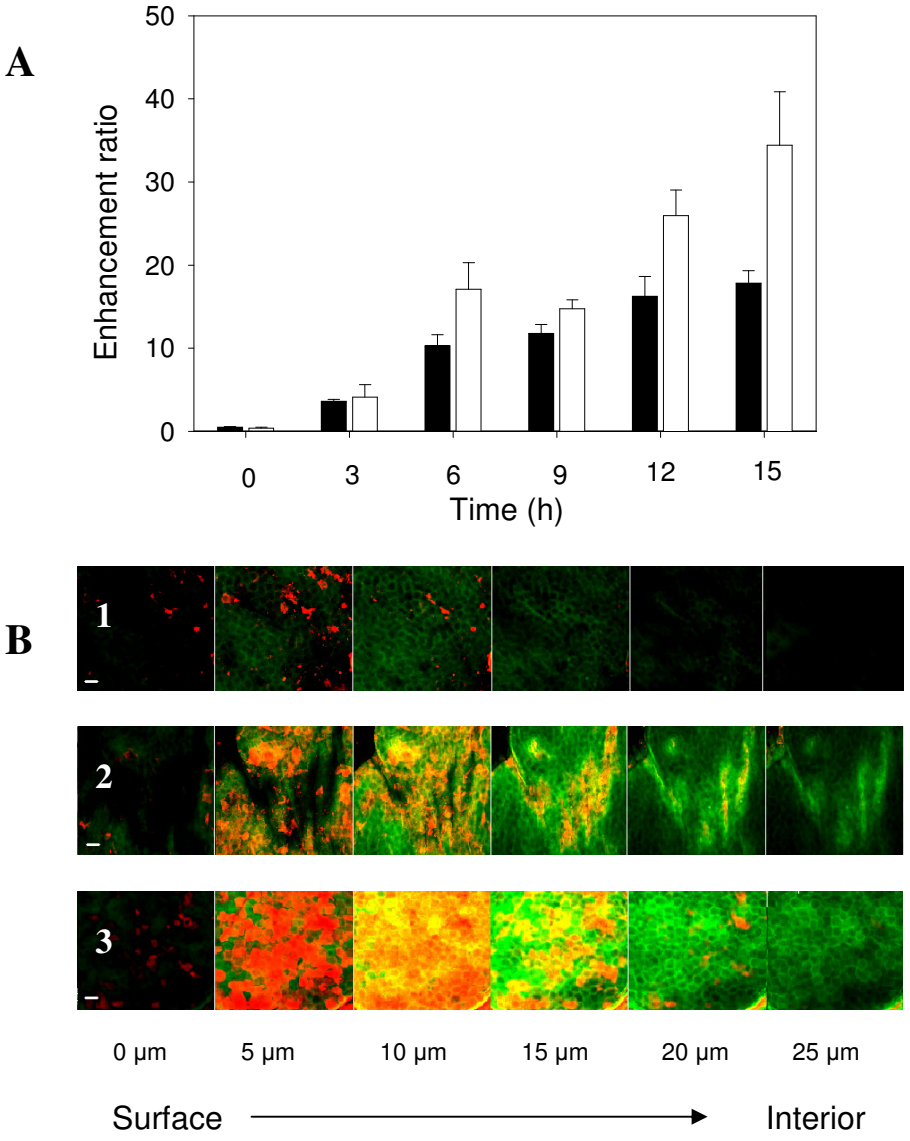

Figure 5. 1 (A) Effect of pretreatment time on the enhancement of skin permeability to fluorescein for skin treated without (■) and with (□) magainin. The enhancement ratio is defined as the skin permeability at the condition tested divided by the permeability of untreated skin. (B) Penetration of fluorescein and sulforhodamine-tagged magainin peptide into human epidermis imaged by multi-photon confocal microscopy. Skin was treated with magainin formulation for (1) 1 h, (2) 4 h, and (3) 12 h. Green corresponds to fluorescein, red corresponds to sulforhodamine-tagged magainin, and yellow corresponds to co-localization of fluorescein and magainin. Optical sections taken at 5 µm increments starting at the *stratum corneum* surface on the left and proceeding deeper on the right. Scale bar is 100 µm.

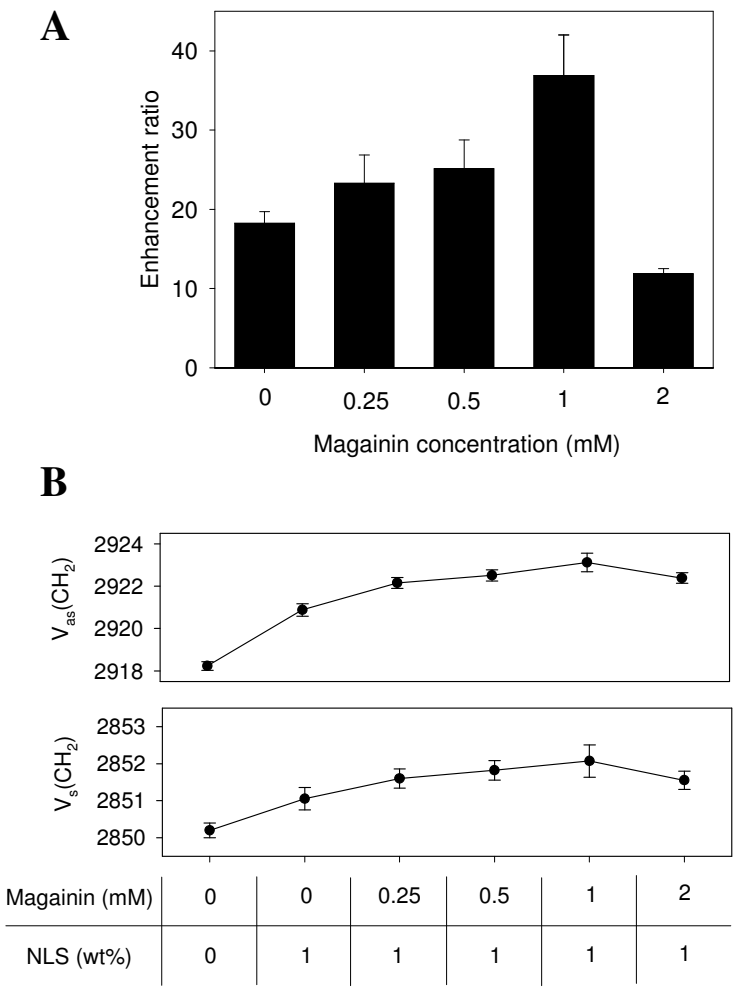

Figure 5.2 Concentration effect of magainin peptide. (A) Transdermal fluorescein skin permeability enhancement ratio (All sample treated with NLS) (B) Fourier transform infrared (FTIR) spectral analysis of human *stratum corneum*. Peak wavenumber of characteristic spectral peaks corresponding to ① asymmetric C-H stretching and ② symmetric C-H stretching as a function of magainin concentration. Data points show the average of n≥3 replicates and error bars correspond to the standard error of the mean.

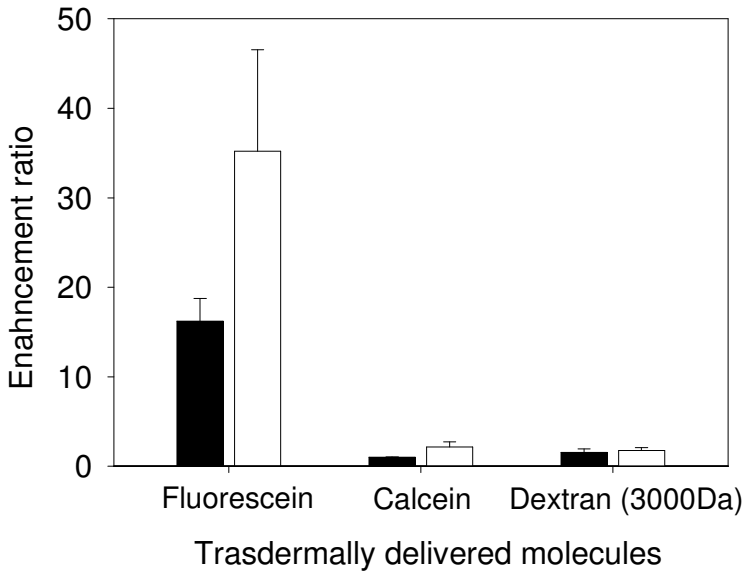

Figure 5.3 Skin permeability to molecules of different sizes: fluorescein (323 Da), calcein (623 Da), and fluorescein-tagged dextran (3,000 Da). Pretreatment solutions were without (■) and with (□) magainin. Data points show the average of n≥3 replicates and error bars correspond to the standard error of the mean.

that a minimum pretreatment time of 6 h is required for significant enhancement.

To better understand the mechanism behind these kinetics, we imaged skin after different pretreatment times using red-fluorescence labeled magainin and green-fluorescent fluorescein. The resulting images, shown in Figure 5.1B, indicate that over time more magainin was able to penetrate into the *stratum corneum* (the upper 10 – 15 μm of skin), which corresponded to more fluorescein transport across the *stratum corneum* and into the deeper skin.

We next hypothesized that increased magainin concentration should increase skin permeability to fluorescein. As shown in Figure 5.2, increasing magainin concentration up to 1 mM increased skin permeability (ANOVA, $p<0.05$). However, further increasing magainin concentration to 2 mM decreased the enhancement ratio by more than a factor of two (Student's *t*-test, $p<0.01$). This effect might be explained by aggregation of high-concentration magainin in the *stratum corneum* lipids, which may disrupt and occlude the expected pore structures formed by lower-concentration magainin [147]. This explanation requires further study.

Finally, we hypothesized that skin permeability increased by magainin should be more effective for lower molecular weight molecules. Figure 5.3 shows skin permeability to molecules of three different sizes: fluorescein (323 Da), calcein (623 Da), fluorescein-tagged dextran (3,000 Da). Skin permeability to fluorescein was significantly increased (Student's *t*-test, $p<0.01$), but permeability to the two larger molecules was not significantly affected by magainin (Student's *t*-test, $p>0.05$). This can be explained because magainin is believed to form Angstrom-scale pores across lipid bilayers that are known to be large enough for transport only of small molecules [148,149].

5.4. Conclusion

This study provided three main conclusions. First, we found that increased magainin pretreatment exposure time increased skin permeability to fluorescein by enabling more magainin to enter the *stratum corneum*. Second, increased magainin concentration up to 1 mM was shown to increase skin permeability to fluorescein, but 2 mM fluorescein reduced this effect, perhaps due to magainin aggregation. Finally, skin permeability increased by magainin was effective for low molecular weight fluorescein (323 Da), but not for higher molecular weight calcein (623 Da) or dextran (3,000 Da). Overall, this study shows that magainin-based formulations can be optimized for increased transdermal delivery of low molecular weight compounds.

CHAPTER 6: TRANSDERMAL DELIVERY ENHANCED BY MODIFIED MAGAININ PEPTIDE

6.1. Introduction

Most animals and plants are constantly exposed to harmful pathogens. Innate defense systems such as gene-encoded antimicrobial peptides (AMPs) help fight off these pathogens and avoid infection [65,150]. More than 750 different antimicrobial peptides, either inducible or constitutive, have been identified and investigated in a wide range of eukaryotic organisms including humans [3]. Pathogenic organisms that are resistant to conventional antibiotics have emerged as a major medical problem; therefore, the pharmacological application of antimicrobial peptides has been considered as a potential novel therapeutic agent, because these peptides act via specific permeabilization of microbial membranes [1,4].

Transdermal delivery using chemical agents have been investigated for more than two decades [106]. However, biochemical molecules such as peptides have not been studied as skin permeation enhancers extensively. Most research has been based on using the conjugation of peptides with target molecules of interest to aid in delivery across biological barriers [73,74]. TD-1 peptide was developed for enhancing

delivery of insulin and achieved efficient delivery of cargo into the skin without linkage or direct conjugation with cargo, but the mechanism was assumed to be different from that of conventional percutaneous enhancers and appeared to involve transport through hair follicles [8]. Our previous work was the first to use a peptide as a percutaneous enhancer with a mechanism similar to a chemical enhancer (i.e. lipid disruption) [146]. The exact mechanism has not been clearly elucidated yet, but the pore-forming peptide, magainin, demonstrated transdermal synergisitic enhancement of delivery.

Numerous magainin peptide derivatives which were modified by changing charge, hydrophobicity, hydrophobic momentum, and helicity have been reported. For example, increasing the magainin charge to +5 resulted in a higher antimicrobial activity due to an increase of ionic peptide–membrane interaction [151,152]. Modifying α-helical structure of magainin by substituting helix promoting residues also increased antimicrobial activity [153]. Hydrophobic peptide-membrane interactions have an effect on hemolytic activity due to the affinity of the peptides to zwitterionic membranes [154,155].

In this study, we hypothesize that a modification of magainin peptide will change the enhancing characteristics of magainin peptide. We would like to investigate which of these characteristics is critical for enhancement properties.

6.2. Materials and Methods

6.2.1 Skin preparation

Same as Chapt 3.

6.2.2 Skin permeability measurement

Same as Chapt 3.

6.2.3 Modified magainin peptides synthesis

All modified magainin peptides were synthesized by Shanghai GL Biochemicals with standard solid-phase FMOC method with an automatic peptide synthesizer (CS Bio). The sequences and characterisitics of magainin-modified peptides are shown in Table 1.

6.2.4 Circular dichroism spectra

Circular dichroism spectra were acquired on a JASCO J-720 CD spectropolarimeter (JASCO, Easton, MD). The spectrum of each sample was obtained by scanning using a capped quartz optical cell (1 mm path length cell; Starna cells, Atascadero, CA, USA) at room temperature, at a wavelength of 250 to 195 nm with continuous scanning mode. Samples were scanned five times at a scan rate of 500 nm/min and a peptide concentration of 5×10^{-5} M in 50% ethanol-PBS solution.

6.2.5 Fourier transform infrared spectroscopy (FT-IR)

Same as Chapt 3.

6.2.6 Statistical Analysis

Skin permeability to fluorescein and FTIR spectroscopy were measured using at least three replicate skin samples at each condition, from which the mean and standard error of the mean were calculated. A two-tailed Student's t-test was performed when comparing two different conditions. When comparing three or more conditions, a one-way analysis of variance (ANOVA) was performed.

6.3. Results and discussion

6.3.1 Effect of magainin-modified peptides on skin permeability

To test our hypothesis that modification of magain peptide will affect skin permeation ability, we applied five different classes of modified magainin peptides for skin permeation enhancer in NLS-ethanol solution. Each modified peptide has a unique characteristic such as charge, hydrophobicity, and hemolytic activity. (Table 6.1)

We first ran a control experiment using a solution containing only NLS

Table 6. 1 Various magainin derivitives

		Modification	Characterisitic	Sequences
B	Magainin [68]	-	Antimicrobial activity	GIGKFLHSAKKFGKAFVGEIMNS
C	Anti-magainin	Charge of magainin modified to negative	Unknown	GIG**E**FLHSA**EE**FG**E**AFVGEIMNS
D	MK5E [152]	Increase chare to +5	Higher antimicrobial activity	GIGKF**I**H**A**VKK**W**GK**T**F**I**GEI**AK**S
E	Magainin H [153]	Replace L-Ala with D-Ala from magainin F	No antimicrobial & hemolytic activity	GIGKFLHS**a**KKF**a**KAFV**a**EIMNS
F	Magainin F [153]	Substitue Gly^{13} & Gly^{18} with Ala	Higher antimicrobial activity	GIGKFLHSAKKF**A**KAFV**A**EIMNS
G	$I^6A^8L^{15}I^{17}$ [154,155]	Increase hydrophobicity	Higher antimicrobial & hemolytic activity	GIGKF**I**H**A**AKKFGK**L**F**I**GEIMNS

surfactant and no peptide. Consistent with previous findings [146], this formulation caused a 16 fold increase in skin permeability. (Figure 6.1 Sample A) Also consistent with our previous work [146], the addition of magainin peptide increased skin permeability 33 fold, (Figure 6.1. Sample B) which was almost twice greater than NLS alone. (Student's *t* test, $p<0.05$)

To asses the role of charge, we modified two different charged peptides.

First, in order to make negative charged-magainin, we replaced all of the positively charged amino acids in magainin (Lysine) with a negatively charged amino acid (Glutamic acid) to form "anti-magainin". This modified peptide (Figure 6.1.

Sample C) had no significant effect on skin permeability and an even lower enhancement ratio than NLS-alone control (Student's *t* test, $p<0.05$).

Second, in order to increase the charge of magainin from +4 to +5, we replaced several amino acids. This high positive charged-magainin peptide (Figure 6.1. Sample D) increased skin permeability 20 fold, but was not statistically different from NLS alone (Student's *t* test, $p>0.5$).

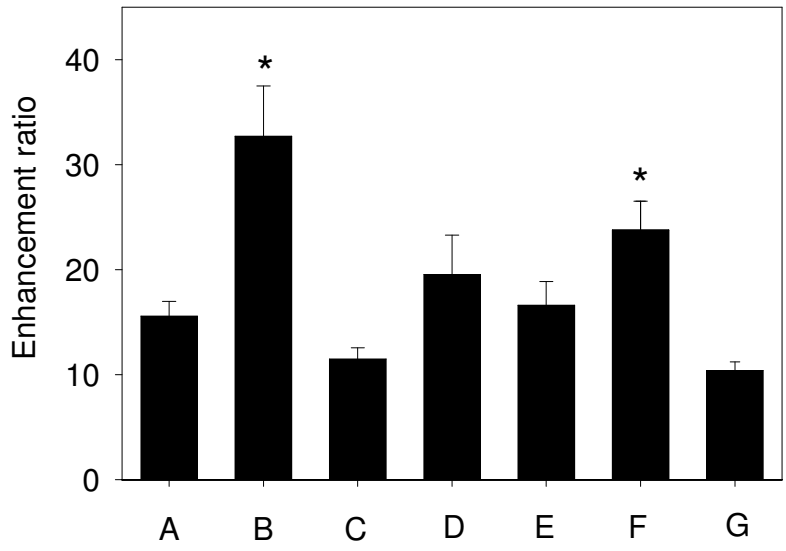

Figure 6. 1 Transdermal fluorescein skin permeability enhancement ratio of skin samples treated with NLS and (A) no peptide, (B) with magainin, (C) with anti magainin, (D) with MK5E, (E) with magainin H, (F) magainin F, and (G) $I^6A^8L^{15}I^{17}$ relative to untreated skin. Data represent averages of n≥3 samples with standard error of the mean. The * symbol identifies skin samples with enhancement statistically higher than the enhancement by NLS alone (Student's *t*-test, $p<0.05$).

We also tested a modified peptide which has no antimicrobial and hemolytic activity at all (Figure 6.1. Sample E). This peptide did not show any enhancement effect (Student's *t* test, $p>0.5$).

Replacing Gly with Ala to increase helix formation (Figure 6.1. Sample F) demonstrated increased skin permeability by 24 fold and it was a statistically significant enhancement (Student's *t* test, $p<0.05$). However, it was not better than enhancement by original magainin peptide.

Finally, in order to test the effect of hydrophobicity (Figure 6.1. Sample G), we increased hydrophobicity by substitution of four amino acids. This modified peptide resulted in no enhancement and rather showed an adverse effect (Student's *t* test, $p<0.05$).

Therefore, we could not find any correlation between antimicrobial activity and the change in skin permeability.

6.3.2 Fourier transform infrared spectroscopy

Fourier transform infrared spectroscopy was used to investigate the *stratum corneum* lipid structural change caused by modification of magainin peptides.

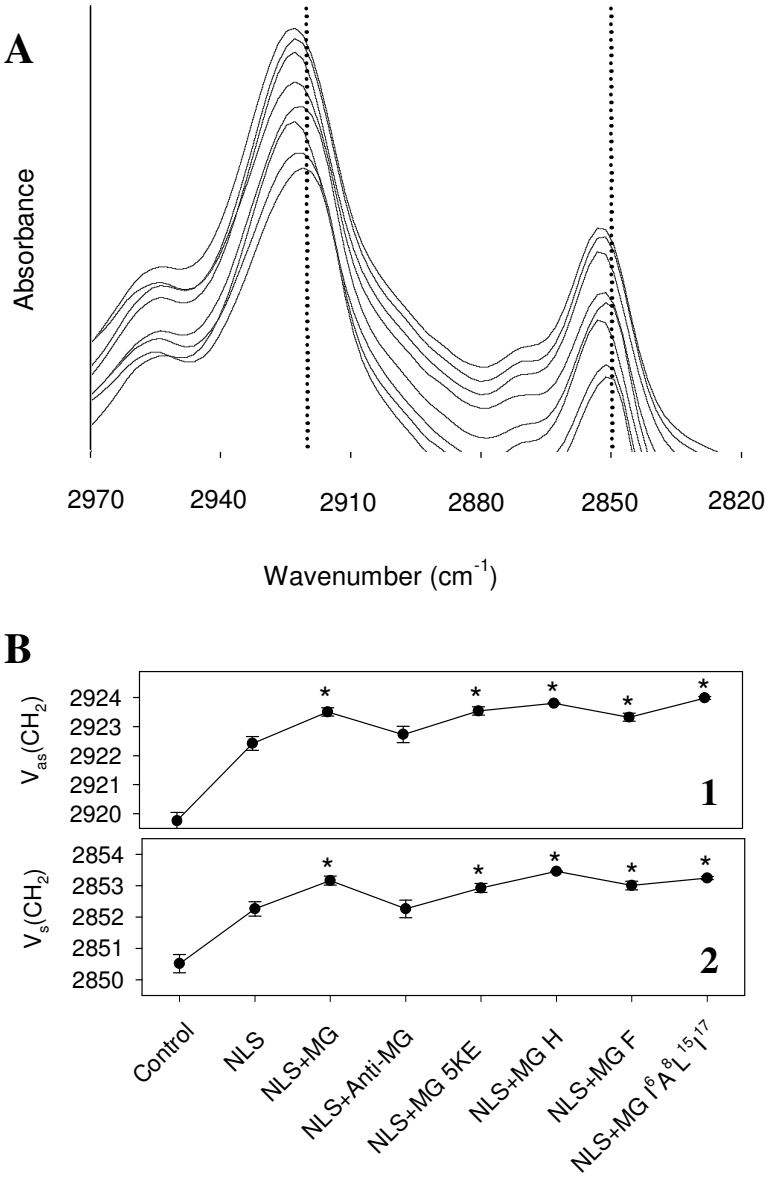

Figure 6. 2 Fourier-transform infrared spectroscopy analysis of human *stratum corneum* treated with different formulations. (A) Spectra of wavenumbers characteristic of C-H stretching in lipids treated with (from bottom to top): PBS, NLS, magainin, anti magainin, magainin 5KE, magainin H, magainin F, magainin I6A8 with NLS in aqueous 50% ethanol Dashed lines indicated peaks of interest. Graphs are representative of n≥3 replicate samples. (B) Change of (1) CH_2 asymmetric stretching frequency, (2) CH_2 symmetric stretching frequency. Data represent averages of n≥3 samples with standard error of the mean. The * symbol identifies wavenumbers significantly greater than skin treated with just NLS (Student's *t*-test, p<0.05).

Representative IR absorbance spectra from 2970-2820 cm^{-1} of human *stratum corneum* samples treated with various formulations are displayed in Figure 6.2A. The wave-number position of the characteristic spectral peaks is shown in Figure 6.2B. As shown in Figure 6.2B, there is a significant difference between control sample treated with PBS and those samples treated with NLS or NLS with modified magainin peptides (ANOVA, $p[\nu_{as}(CH_2)] < 0.01$, $p[\nu_s(CH_2)] < 0.01$). The increased wave-numbers of the two C-H stretching peaks by samples treated with NLS-modified magainin peptides are statistically higher than those treated by NLS alone (Student's *t* test, $p[\nu_{as}(CH_2)] < 0.05$, $p[\nu_s(CH_2)] < 0.05$). However, this does not hold for the sample treated with anti-magainin.

From this result, we observed that magainin and magainin derivatives (except for antimagainin) with NLS fluidized *stratum corneum* lipid further than NLS alone, however, fluidization is not the only cause of skin permeability increase. When we compare Figure 6.1 and 6.2, the wave number increase of CH-stretching of the skin treated with magainin-NLS is similar to that of the skin treated by NLS with magainin MK5E, magainin F, magainin $I^6A^8L^{15}I^{17}$, and magainin H; however, transdermal penetration enhancement was achieved by original magainin and magainin F only. Though the mechanism of transdermal penetration enhancement by magainin-NLS has not been clearly elucidated yet, the skin permeability enhancement may not result

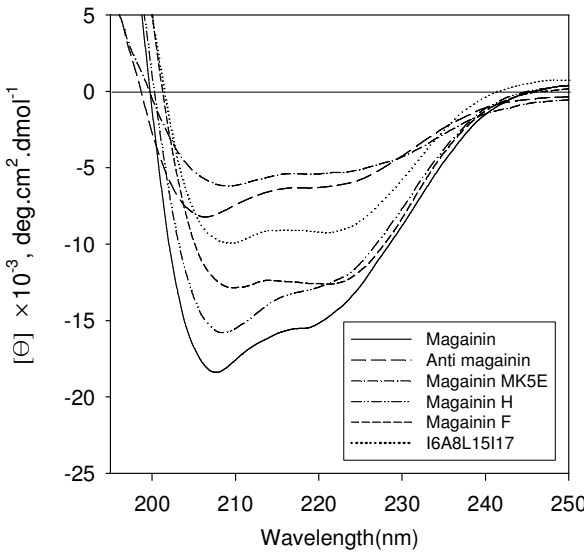

Figure 6. 3 Circular dichroism spectra of various modified magainins in 50% ethanol

merely from skin lipid fluidization. As mentioned in the previous chapter, ionic interactions between peptide and delivered molecules could cause a significant effect.

6.3.3 Circular dichroism (CD) spectra

In order to identify differences between the magainin derivatives that could explain their different behaviors, we used CD spectroscopy. As shown in Figure 6.3, even though alpha helicity is different, all modified magainin peptide maintained alpha helical structure in a hydrophobic environment. Therefore, alpha helical structure may be necessary for skin permeability enhancement, but it is not significant and therefore does not provide an explanation for the different behaviors of the magainin deravitives.

6.4. Conclusions

This study showed that the modification of magainin by sequence replacement has a significant influence on the transdermal enhancement characterisitics of the peptide. By investigating the structure and fluidization ability of each modified magainin peptide, we have concluded that alpha helicity and lipid fluidization ability are not distinguishing factors for percutaneous enhancement. This suggests that lipid fluidization is not a significant factor in additional skin penetration enhancement of magainin-NLS formulation.

CHAPTER 7: TRANSDERMAL DELIVERY ENHANCED BY MAGAININ PEPTIDE - MODIFICATION OF ELECTROSTATIC INTERACTIONS BY CHANGING PH

7.1. Introduction

Traditional approaches to increase transdermal drug delivery [156] have involved synthetic chemical enhancers, such as surfactants, fatty acids, and solvents [106], and physical enhancers, such as electric fields, ultrasound, heat, and microneedles [157]. Recent work has considered the use of biochemical enhancers, such as an 11-amino acid synthetic peptide identified by phage display screening [76], a polyarginine heptamer covaltently bonded to a drug using a prodrug approach [74], and a naturally occurring pore-forming peptide called magainin [146], which is the subject of this study.

Magainin is a 23-residue peptide that is naturally produced on the skin of African clawed frogs and exhibits a broad spectrum of antimicrobial activity properties [68]. It has a net charge up to +4 and binds to negatively charged lipid membranes by way of electrostatic interactions. It is believed to be a random coil in aqueous solution that forms an amphipathic helix when adsorbed onto a negatively charged membrane such as the surface of a bacterium. Magainins can then self-

assemble into transmembrane pores that make the cell membrane leaky and can also lead to cell lysis.

We previously hypothesized that magainin could be used to make lipid bilayers in the skin's *stratum corneum* leaky as well, and showed that magainin can increase skin permeability when delivered from a formulation including an anionic surfactant, N-lauroyl sarcosine,in a 50% ethanol-PBS solution [146]. Initial tests showed that magainin alone had no effect on skin permeability, probably because the relatively large magainin molecule had difficulty penetrating throughout the *stratum corneum* to make continuous transdermal pathways. Addition of the anionic surfactant increased skin permeability and thereby facilitated magainin penetration throughout the *stratum corneum*, which provided a synergistic enhancement. This enhancement was accompanied by increased *stratum corneum* lipid fluidity, as shown through differential scanning calorimetry, infrared spectroscopy and X-ray diffraction measurements. These results were consistent with the hypothesis that magainin makes *stratum corneum* lipid layers leaky.

Building off these observations that magainin, in the presence of surfactant, interacts with *stratum corneum* to increase permeability, this study seeks to investigate the role of interactions between magainin and the drug as it diffuses through magainin-mediated pathways in the *stratum corneum*. We expect that the charge properties of magainin play a role in these interactions, especially with

charged drugs, and have therefore investigated this effect by changing the magainin charge state by changing pH. We hypothesize that electrostatic forces between magainin peptides and drugs mediate drug transport across the skin.

Previous studies have shown that changing pH can alter the structure and properties of antimicrobial peptides in various ways, such as switching between the nematic and isotropic phase of a β-sheet peptide [158], changing the charge of a transmembrane α-helical peptide [159], enhancing antimicrobial activity [160], controlling haemolytic activity [161], and altering pore-formation properties [162].

The effect of pH on transdermal delivery has also been investigated, but has primarily focused on the effects of pH changes on drug properties, such as solubility. For example, indomethacin delivery was enhanced under acidic conditions due to increased drug stability [163] and the dependence of skin permeability to cephalexin on pH was described by a U-shaped curve [164].

7.2. Materials and methods

7.2.1 Skin preparation

Same as Chapt 3.

7.2.2 Skin permeability measurement

Skin permeability measurements were carried out in three steps. As a first step,

skin pretreatment was performed using epidermis (0.7 cm^2 skin surface area) mounted in a vertical, glass Franz diffusion cell (PermeGear, Bethlehem, PA, USA). A solution of 1 mM magainin peptide (Microchemical and Proteomics Facility, Emory University School of Medicine) and 2% (w/v) N-lauroylsarcosine (NLS, 98%, Fluka, Buchs, Switzerland) in 50% (v/v) aqueous ethanol solution was placed in the donor chamber and phosphate-buffered saline (PBS, Sigma Aldrich, St. Louis, MO, USA) was placed in the receiver chamber for 12 h at 4 ^oC to minimize skin degradation. The magainin solution had a pH of 3.5 and the PBS had a pH of 7.4.

As a second step, the Franz cell was removed from refrigeration and placed in a heater/stirrer block (PermeGear) that warmed the receiver chamber at 37 ^oC and maintained stirring at 455 rpm.

As a third step, fresh PBS (pH from 5 to 12) was placed in the receiver chamber and 0.3 mL of 1 mM fluorescein (Sigma Aldrich, St. Louis, MO, USA) solution in PBS (pH from 7.4 to 12) or 1 wt% granisetron hydrochloride (Ultratech SPC PVT Ltd., Mumbai, India) solution in PBS (pH from 5 to 10) was placed in the donor chamber, which replaced the magainin/NLS solution. Every hour for 5 h, the receiver solution was removed for sampling and then replaced with fresh PBS (pH from 5 to 12). The pH of sample solution was adjusted to pH 7.4 by adding 1 N nitric acid to decrease pH and 1 N NaOH solution to increase pH. Samples containing fluorescein were analyzed by spectrofluorimetry (Photon Technologies International,

Birmingham, NJ, USA) to determine fluorescein concentration, from which transdermal fluorescein flux was calculated. Samples containing granisetron were analyzed by HPLC, as described below.

7.2.3 HPLC analysis

HPLC analysis was carried out using an Alliance HPLC system (Waters, Milford, MA, USA) with Empower software, a fluorescence detector (Waters 2475, 305 nm excitation, 350 nm emission gain setting of 1) and a Spherisorb Cyano column (4.6 × 250 mm, Waters). Samples were injected directly into the column and eluted in a 72:28 mixture of acetate buffer (25 mM) and acetonitrile at a flow rate of 1 mL/min. Calibration curves were prepared at a concentration range of 10 – 100 ng/mL granisetron.

7.2.4 Multi-photon excitation microscopy

To image magainin and fluorescein distribution within the skin, epidermis was treated as described above for skin permeability experiments, except that sulphorhodamine-tagged magainin (Microchemical and Proteomics Facility, Emory University School of Medicine) was used instead of the un-labeled magainin used in the first step and the experiment was terminated after 3 h exposure to fluorescein in

the third step, after which the skin sample was removed from the Franz cell and placed on a glass cover-slip.

Imaging was carried out using a Zeiss LSM/NLO 510 Confocal/Multi-Photon Microscope (Zeiss, Oberkochen, Germany) with a 40× oil-immersion objective used in conjunction with an oil having an index of refraction of 1.51, which is similar to that of the *stratum corneum* [165,166].

7.2.5 Circular dichroism spectra

Solutions were prepared containing 50 μM magainin in 50% ethanol. pH was adjusted to a value between 7.4 and 12. Solutions were placed in a capped quartz optical cell (1 mm path length; Starna cells, Atascadero, CA, USA) and circular dichroism spectra were acquired on a JASCO J-720 CD spectropolarimeter (JASCO, Easton, MD). Spectra were obtained at room temperature by scanning five times from 250 nm to 200 nm at a rate of 500 nm/min in continuous scanning mode.

7.2.6 Fourier transform infrared spectroscopy

Stratum corneum was exposed to magainin-NLS solution for 15 h at 4 ^{o}C. Then *stratum corneum* samples were transferred to different pH buffer solutions for 5 h and washed with PBS solution. Fourier-transform infrared spectra were then obtained using a Magma-IR 560 FTIR spectrometer (Nicolet, Thermo Electron Corporation,

Waltham, MA, USA). Reported spectra represent the average of 64 scans over the frequency range of 4000 - 1000 cm^{-1}. OMNIC professional software (Thermo Electron Corporation) was used to measure the peak position. Although the FTIR had a data collection spacing of 4 cm^{-1}, interpolation between points is reliable because the noise level is so low and the reproducibility of FTIR spectra is so high. This permits one to determine the location of a peak, even if it exists between data points that were actually collected. This is well established in the spectroscopy literature [167] and is consistent with many previous studies involving FTIR analysis of skin, where peak shifts much smaller than the data collection spacing are reported [39,125].

7.2.7 Statistical Analysis

Transdermal penetration of fluorescein and granisetron and FTIR spectra were measured using at least three skin specimens, from which the mean and standard error of the mean were calculated. A two-tailed Student's t-test (α=0.05) was performed when comparing two different conditions. When comparing three or more conditions, a one-way analysis of variance (ANOVA; α=0.05) was performed. In all cases, a value $p<0.05$ was considered statistically significant

7.3. Results and discussion

7.3.1 Effect of pH on transdermal flux of fluorescein

We hypothesize that electrostatic forces between magainin peptides and drugs mediate drug transport across the skin. To address this issue, we measured skin permeability to fluorescein over a pH range of 7.4 to 12. Over this range, the charge of the skin [168], NLS surfactant, and fluorescein should all remain strongly negative. However, magainin has an isoelectric point at pH 10.5, such that magainin changes from a +2 positive charge at pH 7.4 to a neutral charge at pH 10.5 and a negative charge at pH 12 [169]. Electrostatic forces between magainin and drugs mediate drug transport across the skin.

We first carried out a control experiment to assess the effect of pH on skin permeability to fluorescein after pretreatment with NLS (without magainin). At pH 7.4, skin permeability was increased 16 fold by the NLS control formulation, as shown in Figure 7.1. Increasing to pH 11 had no additional effect (ANOVA, $p = 0.73$), which is consistent with the expectation that the charge of skin, NLS and fluorescein should be unaffected by increased pH. However, at pH 12, skin permeability approximately doubled relative to pH 7.4 (Student's t-test, $p < 0.05$). This suggested a change in skin properties at high pH, which is consistent with

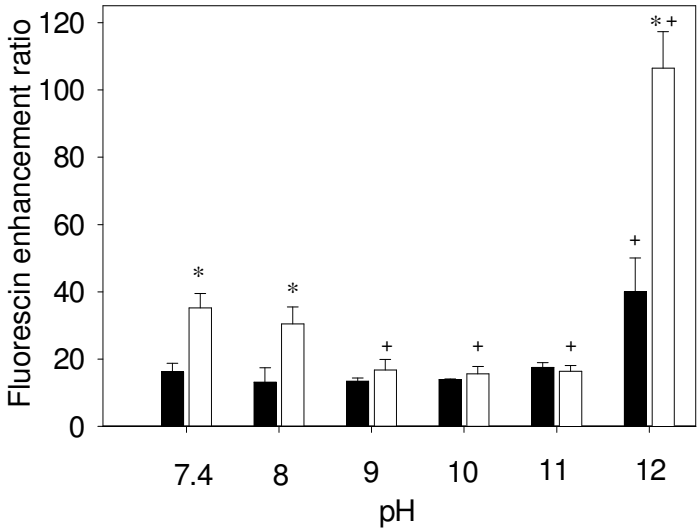

Figure 7. 1 Enhancement of transdermal fluorescein delivery as a function of pH. Skin was pre-treated with NLS (■) or magainin + NLS (□) in 50% ethanol. Enhancement ratio represents the increase in transdermal fluorescein transported across skin over 6 h at various pH values compared to delivery under identical conditions using a formulation of fluorescein in PBS. The * symbol identifies enhancement ratios for magainin + NLS that are significantly different from NLS at the same pH (Student's t-test, $p < 0.05$). The † symbol identifies enhancement ratios at a given pH that are significantly different from the same formulation at pH 7.4 (Student's t-test, $p < 0.05$). Data represent averages of $n \geq 3$ samples ± standard error of the mean.

previous observations that skin permeability is not generally changed at pH values up to 11 [170], but exposure to pH 12 can increase skin permeability [170].

Skin permeability to fluorescein after treatment with magainin and NLS was increased by a factor of 35 at pH 7.4, as shown in Fig. 1. This increase is significantly larger than for NLS without magainin (Student's t-test, $p < 0.01$). However, raising the pH, and thereby reducing magainin charge, progressively removed magainin's enhancement until pH 11 (ANOVA, $p < 0.05$). This suggests that a positively charged

magainin facilitated transdermal transport of negatively charged fluorescein due to electrostatic attraction at pH 7.4, but as the attraction decreased with increasing pH, the skin permeability enhancement decreased as well.

At pH 12, skin permeability was again increased to a 106-fold enhancement, as shown in Fig. 1 (Student's t-test, $p < 0.01$). Although at this pH magainin is negatively charged, which should repel the negatively charged fluorescein, the control experiment suggested that skin itself was altered by the high pH, which complicates any mechanistic interpretation.

7.3.2 Effect of pH on transdermal flux of granisetron

The effect of pH on skin permeability might be mediated by changes in the electrostatic interactions between magainin and fluorescein, but might also be mediated by changes in the interactions between magainin and skin. To address this uncertainty, we measured the effect of pH on skin permeability to granisetron, which differs from fluorescein in that it carries a positive charge, but is similar in that its molecular weight (349 Da) is similar to fluorescein (332 Da).

The control formulation of NLS without magainin at pH 7.4 enhanced transdermal granisetron delivery 59 fold, as shown in Figure 7.2. Neither decreasing to pH 5 nor increasing to pH 10 had any additional effect (ANOVA, $p = 0.84$). Unfortunately, we could not test pH 11 or 12 due to precipitation of granisetron at high pH.

Unlike for fluorescein, the addition of magainin at pH 7.4 had no additional effect on skin permeability to granisetron (Student's t-test, p = 0.167), as shown in Figure 7.2, perhaps because of repulsion between the positively charged magainin and positively charged granisetron. Decreasing the pH to 5, which increased magainin charge to a value of +4, resulted in a reduction of granisetron delivery (Student's t-test , $p < 0.05$)

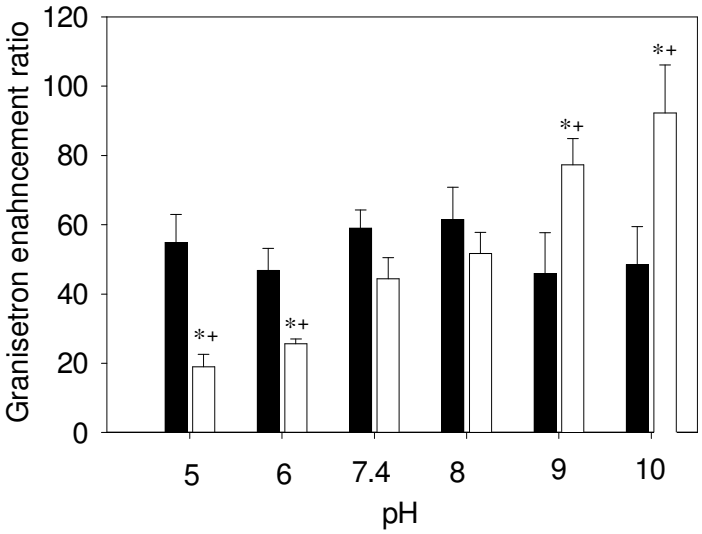

Figure 7. 2 Enhancement of transdermal granisetron delivery as a function of pH. Skin was pre-treated with NLS (■) or magainin + NLS (□) in 50% ethanol. Enhancement ratio represents the increase in transdermal granisetron transported across skin over 6 h at various pH values compared to delivery under identical conditions using a formulation of granisetron in PBS. The * symbol identifies enhancement ratios for magainin + NLS that are significantly different from NLS at the same pH (Student's t-test, $p < 0.05$). The † symbol identifies enhancement ratios at a given pH that are significantly different from the same formulation at pH 7.4 (Student's t-test, $p < 0.05$). Data represent averages of $n \geq 3$ samples ± standard error of the mean.

and raising the pH to 10, which almost eliminated magainin charge, increased granisetron delivery to a peak value of 92–fold enhancement (Student's t-test, $p < 0.05$) due to removal of the electrostatic repulsion.

The opposite effects of pH on skin permeability to fluorescein versus granisetron suggest that the pH changes influenced interactions between magainin and each model drug and did not primarily influence interactions between magainin and skin.

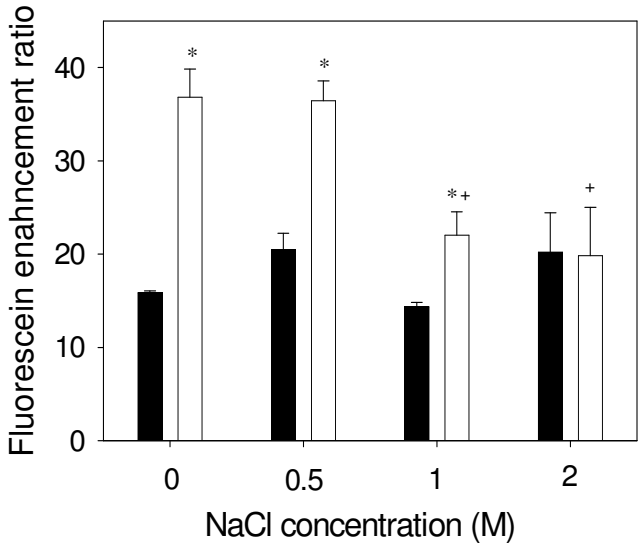

Figure 7. 3 Enhancement of transdermal fluorescein delivery as a function of NaCl concentration. Skin was pre-treated with NLS (■) or magainin + NLS (□) in 50% ethanol at pH 7.4. Enhancement ratio represents the increase in transdermal fluorescein transported across skin over 6 h at various salt concentrations compared to delivery under identical conditions using a formulation of fluorescein in PBS. The * symbol identifies enhancement ratios for magainin + NLS that are significantly different from NLS at the same salt concentration (Student's t-test, $p < 0.05$). The † symbol identifies enhancement ratios at a given pH that are significantly different from the same formulation at 0 M NaCl (Student's t-test, $p < 0.05$). Data represent averages of $n \geq 3$ samples ± standard error of the mean.

7.3.3 Effect of salt concentration on transdermal flux of fluorescein

To further test whether the effect of pH on skin permeability is mediated by electrostatic interactions between magainin and the model drug, we changed salt concentration rather than changing pH to alter electrostatic interactions. An increase of salt concentration screens out electrostatic effects between charged species [171]. Thus, increased salt concentration should effectively neutralize charge-charge interactions in a way similar to increasing pH to the magainin isoelectric point.

For the NLS control formulation, skin permeability to fluorescein was unaffected by salt concentration, as shown in Figure 7.3 (ANOVA, $p = 0.51$). This is consistent with the expectation that skin permeability enhancement by NLS is not mediated by electrostatic interactions. For skin treated with NLS and magainin peptide, skin permeability was increased by magainin at salt concentrations of 0 M and 0.5 M (Student's *t* test, $p < 0.01$). However, increasing the salt concentration to 1 M or 2 M eliminated magainin's enhancement effect, such that skin permeability was indistinguishable from the NLS control (Student's *t* test, $p > 0.05$). This result further confirms the interpretation that magainin increases transdermal transport when there is an attractive electrostatic interaction with a drug and loses its ability to enhance skin permeability if that electrostatic interaction is blocked.

7.3.4 Circular dichroism analysis of magainin structure

Changing the pH could alter magainin structure, which could additionally affect skin permeability enhancement. To assess the effects of pH on magainin secondary structure, we collected circular dichroism spectra of magainin solutions over a range of pH from 7.4 to 12. These spectra showed that magainin retained a α–helix structure over the pH range studied, as shown in Figure 7.4. Although this experiment was done using magainin in solution, rather than within the skin, these results suggest that magainin structure was not altered by pH.

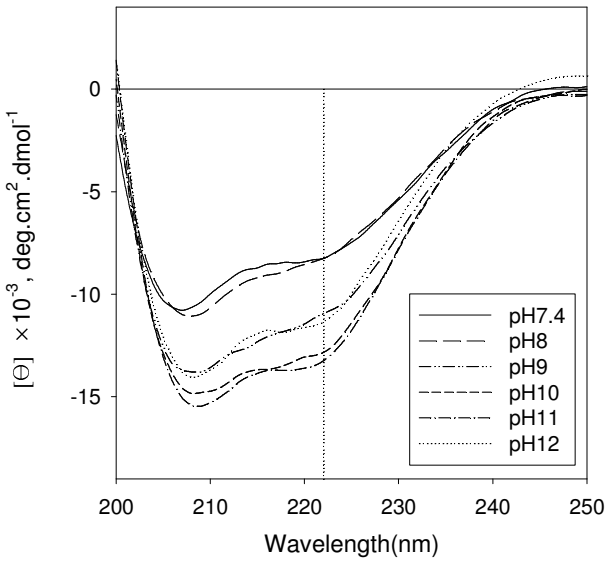

Figure 7. 4 Circular dichroism spectra of magainin as a function of pH. Magainin was dissolved in 50 % ethanol at various pH values.

7.3.5 Microscopy analysis of magainin and fluorescein delivery into *stratum corneum*

Changing pH could alter the amount of magainin in the *stratum corneum*, which could thereby alter skin permeability. To assess the effects of pH on magainin content in the stratum corneum, we imaged the amount of sulforhodamine-labelled magainin inside *stratum corneum* using multi-photon excitation microscopy at various pH values. Magainin delivered to skin in the absence of NLS surfactant had limited penetration into the skin and showed no dependence on pH, as shown in Figures 7.5A – 5D. Magainin formulated with NLS was delivered to a much greater extent than in the absence of NLS, but also did not show any dependence on pH, as shown in Figures 7.5E – 5H. These data indicate that the effects of pH on skin permeability cannot be explained by changes in the amount of magainin peptide present in the *stratum corneum*.

To provide additional insight into the flux data presented in Figure 7.1, we imaged the amount of fluorescein delivered into the skin using multi-photon excitation microscopy at various pH values. Consistent with the flux data, optical sections through the epidermis show that the smallest amount of fluorescein was seen in the skin at pH 10, when magainin charge was almost neutralized (Figure 7.6B); a greater amount was seen at pH 7.4, when magainin carried a +2 charge that attracted negatively charged fluorescein (Figure 7.6A); and the greatest amount was seen at pH 12, when the high pH directly affected skin properties (Figure 7.6C). Z-stack images

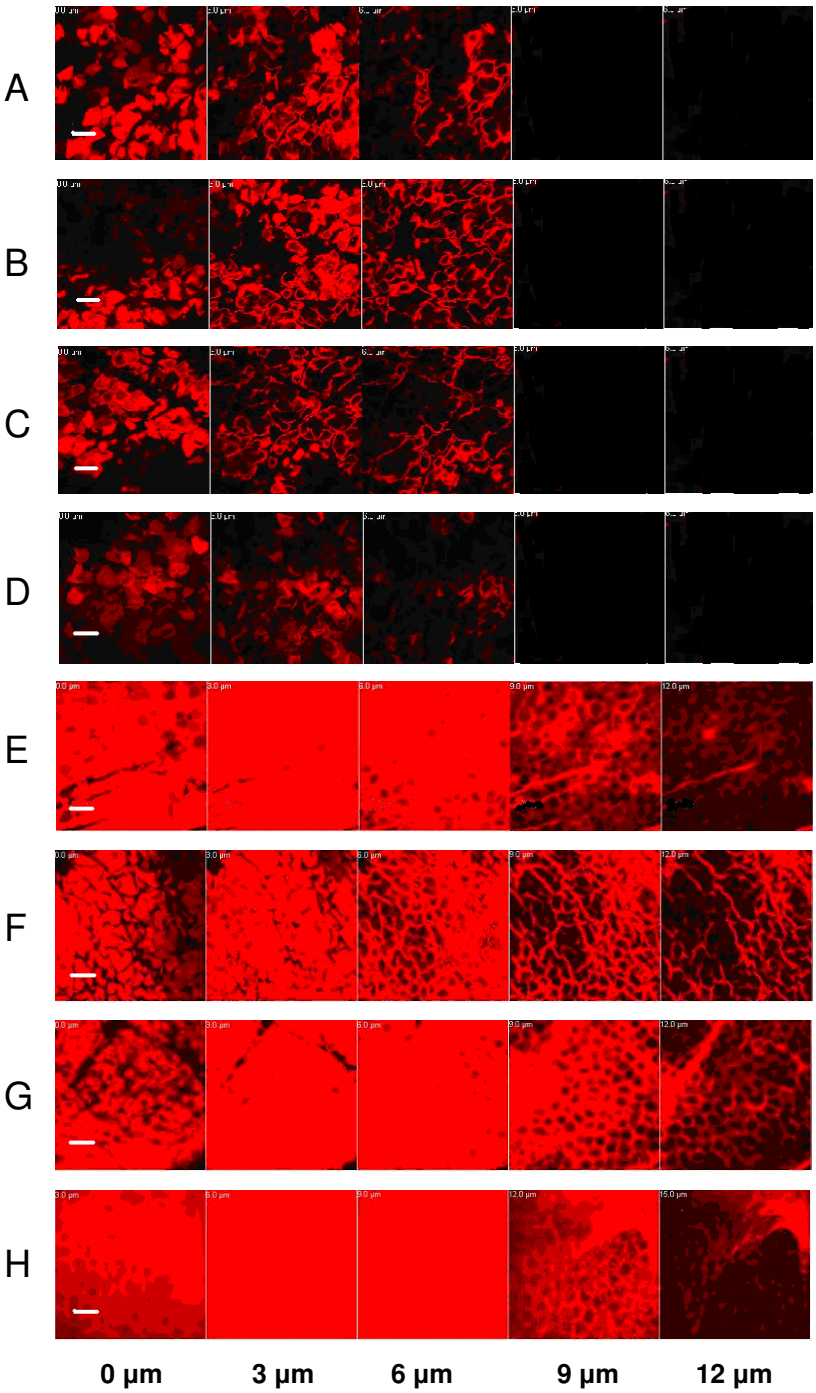

Figure 7. 5 Penetration of sulforhodamine-tagged magainin peptide into human epidermis imaged by multi-photon microscopy. Skin was pre-treated with magainin formulated (A-D) without NLS and (E-H) with NLS for 15 h. Skin was exposed PBS solution for 5 h at pH (A, E) 5, (B, F) 7.4, (C, G) 10, and (D, H) 12. Optical sections were taken at 5 µm increments starting at the stratum corneum surface on the left and proceeding deeper on the right. Scale bar is 50 µm.

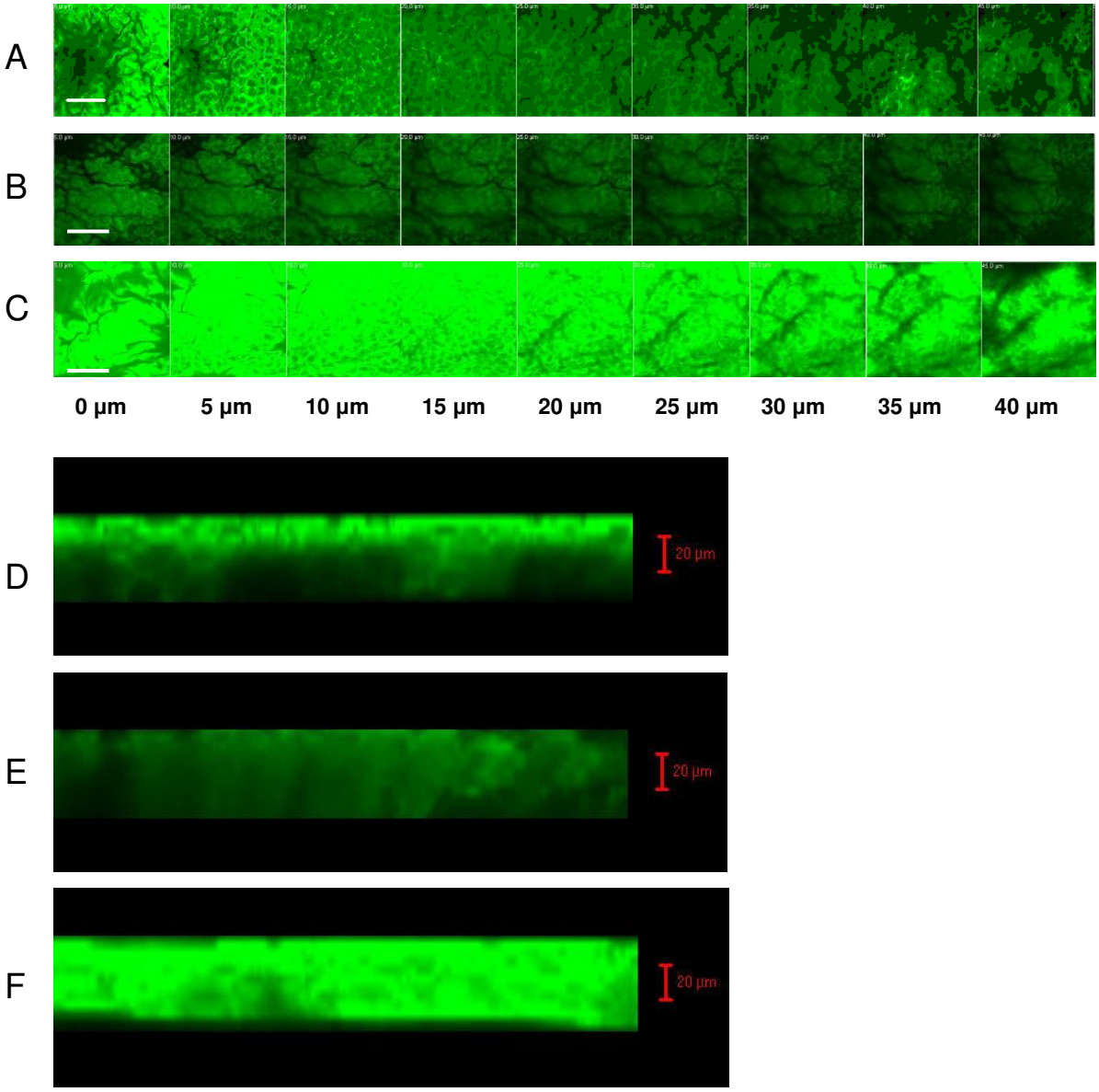

Figure 7. 6 Penetration of fluorescein into human epidermis imaged by multi-photon microscopy. Skin was treated with magainin + NLS. Fluorescein was delivered to skin for 5 h at (A, D) pH 7.4, (B, E) pH 10, and (C, F) pH 12. (A-C) Optical sections were taken at 5 µm increments starting at the *stratum corneum* surface on the left and proceeding deeper on the right. Scale bar is 100 µm. (D-F) Cross-sectional images were reconstructed as z-stacks with the *stratum corneum* surface on top and deeper tissue below. Scale bar is 20 µm.

showing cross-sectional views of the epidermis in Figures 7.6D – 6F provide similar, complimentary results. Transdermal transport was not imaged at lower pH values (e.g., pH 5) due to extensive fluorescein bleaching at acidic pH [172].

7.3.6 Fourier transform infrared spectroscopy

Changing pH could directly alter *stratum corneum* lipid structure or could change the way that magainin alters *stratum corneum* lipid structure. To assess these effects, we used Fourier-transform infrared spectroscopy to measure the degree of *stratum corneum* lipid disruption. Representative spectra are shown for untreated skin (Figure 7.7A), skin treated with NLS (Figure 7.7B) and skin treated with magainin and NLS (Figure 7.7C) as a function of pH. Characteristic peaks can be seen in these spectra near 2920 cm^{-1}, which corresponds to asymmetric C-H stretching, and near 2850 cm^{-1}, which corresponds to symmetric C-H stretching. The frequencies of these C-H stretching bands are related to lipid order in *stratum corneum* and are significantly influenced by the degree of conformational order, the freedom of alkyl chain motion, and possible incorporation of chemical enhancers, such as NLS [97].

To address the effect of pH alone on skin, the frequency of the two characteristic peaks showed no dependence on pH (ANOVA; Figure 7.7D, black circles, $p = 0.26$; Figure 7.7E, black circles, $p = 0.89$). This indicates that pH itself did not affect *stratum corneum* lipid order. Thus, the increased skin permeability

observed at pH 12 in Figure 7.1 cannot be explained by increased lipid disorder. This finding is consistent with a previous study which reported that exposure to pH 12 for 24 h did not shift the position of these characteristic peaks [173].

After treatment with formulations containing NLS or magainin + NLS, there was no statistically significant effect on lipid order over the pH range of 7.4 to 12 for skin treated with NLS (ANOVA; Figure 7.7D, gray squares, $p = 0.54$; Figure 7.7E, gray squares, $p = 0.12$) and with magainin + NLS (ANOVA; Figure 7.7D, white triangles. $p = 0.29$; Figure 7.7E, white triangles, $p = 0.09$). However, exposure at pH 5 significantly decreased the peak frequency (i.e., increased lipid order) for skin treated with NLS (ANOVA; Figure 7.7D, gray squares, $p < 0.01$; Figure 7.7E, gray squares, $p < 0.01$) and with magainin + NLS (ANOVA; Figure 7.7D, white triangles, $p < 0.05$; Figure 7.7E, white triangles, $p < 0.05$), when considered over the full range of pH 5 to 12.

Although the lowest pH had an effect of lipid order, there was no effect over the pH range of 7.4 to 12, which is the range over which pH was shown to have a dramatic effect on skin permeability to fluorescein in Figure 7.1. These data suggest that the effects of pH on skin permeability cannot be explained by changes in *stratum corneum* lipid order.

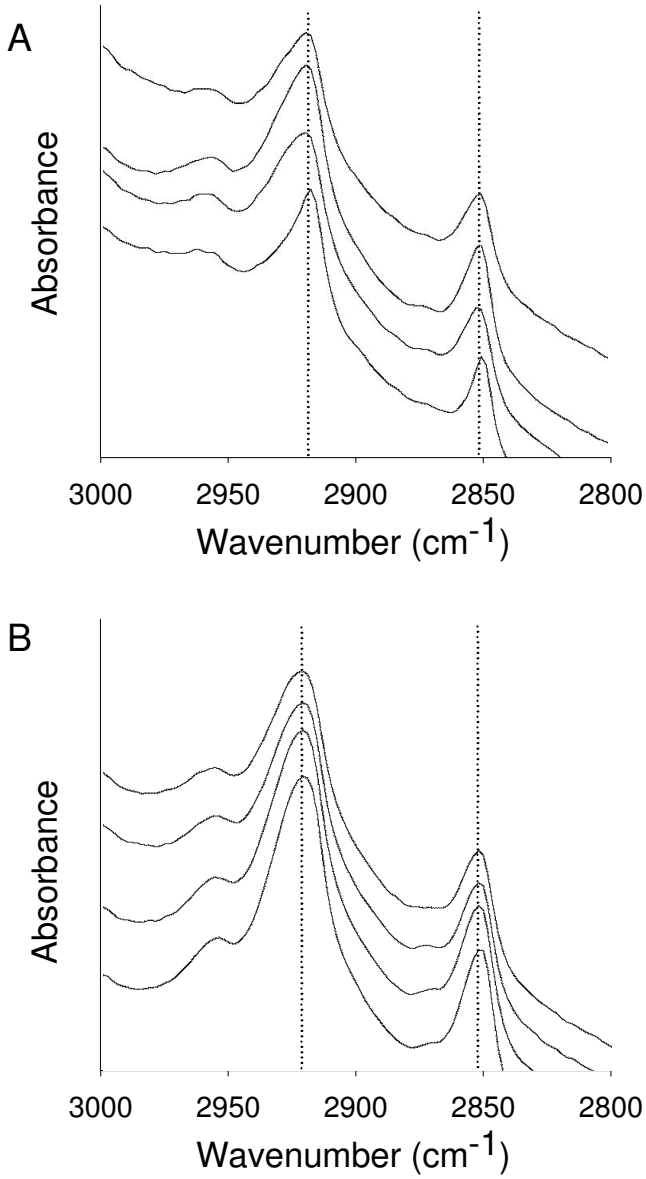

Figure 7. 7 Fourier-transform infrared spectroscopy analysis of human *stratum corneum* treated with different formulations as a function of pH. Representative spectra highlighting wavenumbers characteristic of C-H stretching in *stratum corneum* lipids after pre-treatment with (A) PBS, (B) NLS, and (C) magainin + NLS for 15 H and soaked in PBS at pH 5, 7.4, 10 and 12 (shown from top to bottom). Dashed lines identify peaks of interest. Change of (D) CH_2 asymmetric stretching frequency and (E) CH_2 symmetric stretching frequency for stratum corneum pre-treated with PBS (●), NLS (■), and magainin + NLS (Δ) determined from graphs like (A), (B) and (C), respectively. Data represent averages of n ≥ 3 samples ± standard error of the mean. The * symbol identifies wavenumbers significantly different from the corresponding wavenumber at pH 7.4 (Student's *t*-test, p<0.05).

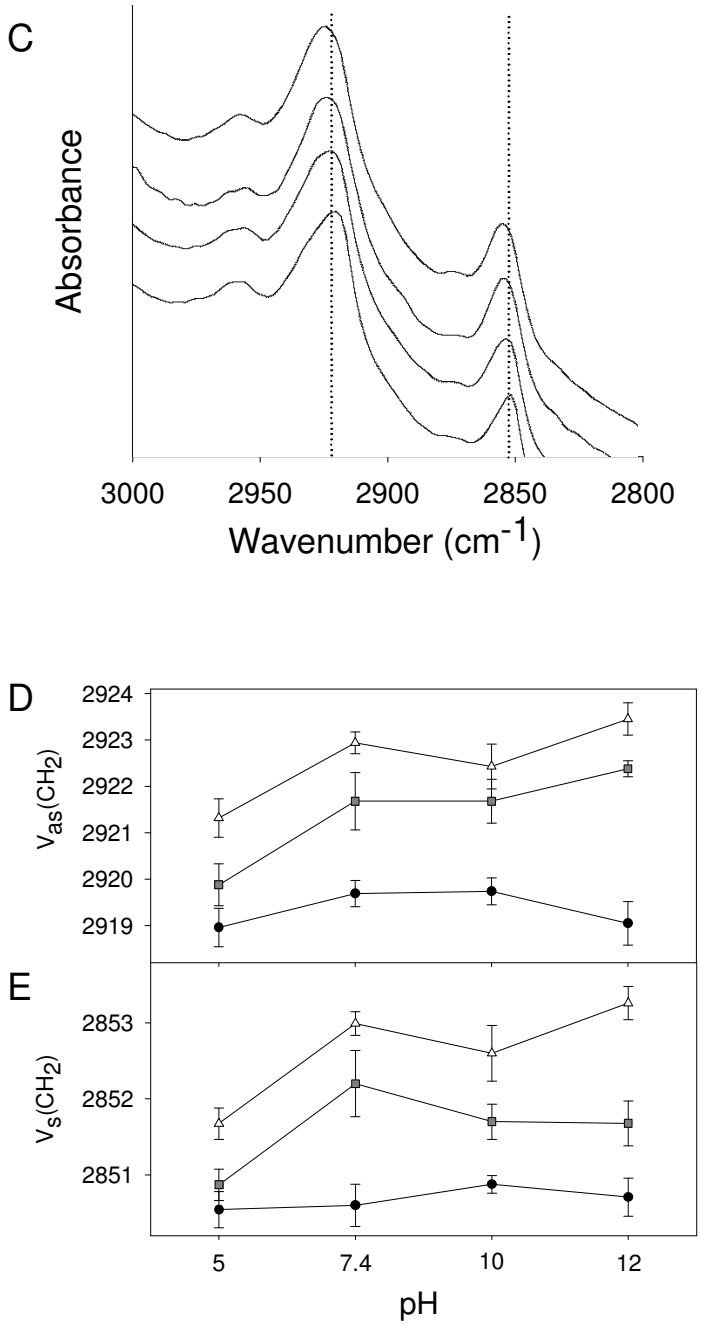

Figure 7.7. Continued

7.3.7 Interpretation of the data

Our previous studies showed that NLS surfactant is needed to drive magainin into the skin. This finding was confirmed by Figure 7.5, which showed little magainin

penetration into the *stratum corneum* in the absence of NLS and extensive magainin penetration with NLS. Our previous studies also showed that the presence of magainin increased skin permeability, which is consistent with Figures 7. 1 and 2, and the increased skin permeability was associated with increased *stratum corneum* lipid disorder, which is consistent with Figure 7.7.

For the first time, this study examined the effects of pH on skin permeability and other properties. Our data support the hypothesis that electrostatic forces between magainin peptides and drugs mediate drug transport across the skin. We found that transdermal transport of negatively charged fluorescein decreased as the positive charge of magainin was reduced by increasing pH. We also found that transdermal transport of positively charge granisetron increased as the positive charge of magainin was reduced by increasing pH. Finally, we found that transdermal transport of fluorescein also decreased as the screening of electrostatic interactions with magainin increased by increasing salt concentration.

These three observations are all consistent with the proposed hypothesis and are not consistent with changes in magainin conformation, magainin content in the skin or magainin interaction with the skin being directly responsible for increased transdermal transport. This is because these effects should not depend on the charge of the molecule being delivered across the skin and should not be effected by changing the pH and by increasing salt concentration.

In addition, CD measurements demonstrated that pH did not change the secondary structure of magainin in ethanol solution, microscopy indicated that pH did not affect the magainin content in the stratum corneum, and FTIR showed that pH did not affect lipid order, except at the lowest pH. Altogether, these data suggest that electrostatic interactions between magainin peptides and drugs provide the most plausible explanation for the observed effects.

7.3.8 Debye length calculations

The effect of salt concentration on skin permeability provides an opportunity to further evaluate the transport pathways created by magainin peptides. As salt concentration increases, the Debye length decreases. The Debye length is a measure of the distance over which the electric field of a charge is felt. As greater numbers of salt ions in solution surround the charge on a magainin peptide, they shield its electric field.

Debye length, λ_D, can be calculated at the conditions used in this study [174].

$$\lambda_d = \sqrt{\frac{\varepsilon_0 \varepsilon_R RT}{2F^2 C}} \qquad (1)$$

where ε_0 is the permittivity of an electrical field in free space (8.8542×10^{-12} F m^{-1}), ε_r is the dielectric constant (66.89 for 0.5 M saline and 59.89 for 1.0 M saline at 32ºC and 1 atm [175-177], R is the gas constant (8.314 N m K^{-1} mol^{-1}), T is the absolute

temperature (310.15 K), F is the Faraday constant (96,485.34 C mol^{-1}), and C is the salt concentration (0.5 M or 1.0 M).

At a salt concentration of 0.5 M, the Debye length is 4.02 Å. At this salt concentration, the electrostatic interactions between magainin peptides and fluorescein molecules were still effective. At a salt concentration of 1 M, the Debye length is 2.69 Å. At this salt concentration, the electrostatic interactions between magainin peptides and fluorescein molecules were blocked.

Fluorescein molecules have a radius of approximately 5 Å [178]. The fact that the Debye length at which magainin – fluorescein interactions are shielded is smaller than the radius of the fluorescein molecule indicates that the pathways created by magainins in the skin are just slightly larger than a fluorescein molecule. The screening of the attractive electrostatic interaction by such a small change in the Debye length implies that the fluorescein molecule must be close to the edge of this pathway. This is consistent with our previous finding that magainin did not enhance transdermal transport of molecules larger than fluorescein [179], such as calcein (623 Da, r = 6 Å [180] and dextran (3,000 Da, r = 16 Å [181]. This is also consistent with previous studies of magainin in simpler lipid bilayer systems, in which the pores are believed to be of Angstrom dimensions [148,149].

7.3.9 Implications for drug delivery

Biochemical enhancers are a novel approach to increasing skin permeability for transdermal drug delivery. However, the use of peptides to increase transdermal transport has been addressed in just a small number of studies. This study provides insight into the mechanism by which magainin peptides increases skin permeability, which may have broader relevance to other peptide-based enhancement strategies.

The use of magainin peptide in combination with NLS surfactant increased transdermal transport of fluorescein 35 fold at pH 7.4 and up to 106 fold at pH 12. Magainin with NLS also increased transdermal transport of granisetron 59 fold at pH 7.4 and up to 92 fold at pH 10. These large increases in skin permeability may be useful for transdermal drug delivery. Although fluorescein is a model compound, granistron is a drug in clinical use to prevent nausea and is in late-stage development as a transdermal patch (ProStrakan announces filing of MAA for Sancuso, ProStrakan Group plc, Galashiels, Scotland, July 16, 2007).

The dependence of transdermal transport on pH, as well as on salt concentration, presents the opportunity to modulate or trigger transdermal delivery rates by increasing or decreasing pH or salt. Although we do not yet know the speed with which changing pH or salt concentration can alter transdermal transport, novel approaches to initiate, terminate or otherwise modulate transdermal delivery rates could be achieved by changing pH or salt concentration.

7.4. Conclusion

This study supported the hypothesis that electrostatic forces between magainin peptides and drugs mediate drug transport across the skin. Mechanisms of transport were studied by measuring rates of transdermal transport, fluorescence microscopy, and CD and FTIR spectroscopy,

Transdermal delivery of negatively charged fluorescein was shown to be increased 35 fold using a formulation containing magainin peptide that carried a +2 charge at pH 7.4 and thereby provided an attractive electrostatic interaction with fluorescein. Increasing pH to 10 or 11, which neutralized the charge on magainin and thereby removed the electrostatic attraction, eliminated the enhancement due to magainin. Blocking electrostatic interactions at high salt concentration similarly eliminated the enhancement due to magainin. Finally, increasing pH to 12 increased transdermal fluorescein delivery 106 fold by a mechanism that appeared to involve effects of the pH on both the skin and magainin.

Transdermal delivery of positively granisetron was shown to be increased 92 fold using the same formulation containing magainin peptide that was neutralized at pH 10. Decreasing pH to 7.4, which gave magainin a +2 charge and thereby provided a repulsive electrostatic interaction with granisetron, eliminated the enhancement due to

magainin. Decreasing pH further to 5, which gave magainin a +4 charge, inhibited granisetron flux.

These observations are consistent with the stated hypothesis and are not consistent with changes in magainin conformation, magainin content in the skin, or magainin interaction with the skin being directly responsible for increased transdermal transport. CD analysis, fluorescence microscopy and FTIR spectroscopy, respectively, provided further evidence to rule out these alternative mechanisms.

Overall, magainin peptides represent a novel class of biochemical enhancers of transdermal transport. Their ability to increase skin permeability and to be modulated by pH and salt concentration suggest applications for transdermal drug delivery.

CHAPTER 8: CONCLUSIONS

In order to deliver drugs across the skin efficiently, various percutaneous enhancers have been investigated. However, few enhancers can deliver drugs at therapeutic dosages while avoiding skin irritation or damage.

In this study, we found that an anionic surfactant – NLS - and ethanol solvent showed synergistic skin permeability enhancement. NLS penetrated into the skin lipid domain with the aid of ethanol, whereupon NLS could fluidize the lipid domain of the *stratum corneum*. When magainin was applied with the NLS-ethanol formulation, additional synergy was found. After NLS and ethanol disrupted the skin, the magainin peptide was able to penetrate into the *stratum corneum*. Although, the skin was more fluidized by the addition of the magainin peptide, flux increased by an amount disproportionately higher than the fluidization increase. Modified magainin derivitives were able to fluidize the *stratum corneum* lipid, but they did not demonstrate skin permeability enhancement to fluoresceinn. We found that skin permeability enhancement is not solely caused by skin lipid disruption. The enhancement appears to result from a charge interaction between the magainin peptide and the transporting molecule.

The first part of this thesis investigated the mechanism of transdermal drug delivery enhancement using mixtures of NLS and ethanol. Skin permeability to fluorescein depended strongly on NLS concentration. The ethanol concentration also strongly affected skin permeability, where formulations containing NLS in 25% and 50% ethanol dramatically enhanced transdermal delivery. Increased skin permeability strongly correlated with the skin's electrical resistance, decreased lipid transition temperatures by DSC, and increased wavenumber of CH stretching by FTIR, which indicated increased fluidity of the *stratum corneum*. The synergistic effect of this formulation may result from the ability of the ethanol solution to improve the permeation of NLS in the lipid bilayer matrix of the *stratum corneum*, thereby improving the ability of NLS to disrupt the lipid order.

The second part of this thesis showed that a formulation containing a pore-forming peptide, magainin, and NLS in 50% ethanol synergistically increased skin permeability. Increased skin permeability was strongly correlated with decreased lipid transition temperatures by DSC and increased wavenumber of CH stretching by FTIR. In addition, reduction of lipid component was confirmed by wide and small-angled X-ray diffraction methods. Analysis by multi-photon microscopy demonstrated that NLS-ethanol increased magainin penetration into the *stratum corneum*, which further increased *stratum corneum* lipid disruption and skin permeability.

The optimization study lead us to conclude that increased magainin pretreatment time increased transport of fluorescein owing to the increasing penentration of magainin into the skin. We found the optimum magainin peptide concentration to be 1 mM with inhibition occurring above this concentration. This concentration dependence was confirmed by FTIR study which investigated lipid peak change: lipid fluidization was maximized at 1mM magainin peptide. Moreover, the percutaneous penetration enhancement by magainin-NLS formulation was only effective for small molecules such as fluorescein.

The modification of magainin peptide sequence did not have a significant influence on the transdermal enhancement characterisitics of the peptide. By investigating the structure and fluidization ability of each modified magainin peptide, we have concluded that alpha helicity and fluidization ability are not distinguishing factors for percutaneous enhancement.

The final part of this thesis showed that a greater increase in skin permeability can be realized by manipulating the charge properties of magainin peptide by changing pH. Skin permeability is increased when magainin and the drug have attractive electrostatic interactions and decreased when those interactions are repulsive. Addition of salt ions interfered with the electrostatic interaction, which resulted in decreased enhancement of transdermal flux.

Overall, this thesis presents not only the first study to use a pore-forming peptide as a skin penetration enhancer, but also the novel approach to use one percutaneous enhancer to increase the penetration of another percutaneous enhancer into the skin. From this thesis, it is suggested that antimicrobial peptides can be used as efficient skin permeability enhancers in conjunction with other enhancers. By changing the pH of the drug solution, we can also control the drug delivery amount. Furthermore, magainin peptide has been certified as a safe agent for human use by the FDA, and since the peptide did not penetrate deeply into the epidermis or dermis, this material could be a great clinical tool for chemical permeation enhancement. Finally, this thesis work may shed light on exploring the mechanism of skin permeability increased by a combination of antimicrobial peptide and chemical enhancers.

CHAPTER 9: RECOMMENDATIONS

This thesis showed that pore-forming peptides can be used as percutaneous drug delivery enhancers with co-application of a chemical enhancer. The mechanism behind this phenomenon has not yet been completely elucidated, but important factors have been uncovered. Lipid disruption or fluidization by chemical enhancer and the molecular ionic interaction between delivered molecules and magainin peptide result in synergistic transdermal drug delivery enhancement. However, the transport pathway, creation of pores, and changes in the magainin structure inside of *stratum corneum* are not clearly understood. Therefore, these should be further investigated.

In this thesis, only magainin and magainin derivatives were studied in detail; however, more antimicrobial peptides could be applied as percutaneous drug delivery enhancers. Also, more chemical enhancer-peptide combinations should be explored using a number of screening experiments. For the purpose of elucidating the mechanism, we could use molecular modeling between the lipid layer and the antimicrobial peptide to validate a proposed mechanism.

Future studies should also evaluate the effects of skin irritation by various formulations; finding an optimum formulation of chemical enhancer, peptide enhancer, and solvent that has the minimum level of skin irritation will be an

important subject to study. Skin irritation potential could be measured using Epiderm (MatTek, Ashland, MA) which consists of cell cultures of normal epidermal keratinocytes from humans.

In this thesis, the effects of combining an antimicrobial peptide with a chemical enhancer were tested, but antimicrobial peptides could be combined with physical transdermal enhancement methods such as electroporation, sonophoresis, iontophoresis, laser, and even microneedles. With the aid of physical methods, magainin may be delivered into the *stratum corenum*, then magainin could disrupt the lipid domain of the *stratum corenum*. Application of physical methods can avoid any side effects resulting from interaction between peptide and chemical enhancer. Also physical methods would be able to shorten treatment times compared to treatment times of chemical enhancers.

For actual medical application, we need to do an intense *in vivo* study. After the conclusion of *in vitro* experiments using hairless rat epidermis, we could perform *in vivo* experiments using hairless rats which would be a good model for mimicking human skin.

From an economical point of view, the price of magainin synthesis may make this approach infeasible. We should find a cheaper method of obtaining the magainin peptide. Removal of the purification step could reduce the price of peptide synthesis.

(There are no significant differences in skin permeation between magainin with purity above 90% and above 50%, data not shown)

In our studies, we showed that hydrophilic drugs with molecular weight below 400 Da demonstrated good penetration in our system; however, we need to test hydrophobic drugs, which have a transport pathway different from hydrophilic drugs.

In order to improve patient compliance, we need to minimize the time and number of steps required for the application process. Current technology requires two separate processes: pretreatment with a chemical enhancer and delivery of the drug for transport. If we use two compartments (enhancer and drug) separated by a memebrane, after a built-in preatment time, the membrane could be dissolved so that drug would be in contact with the skin.

Finally, the following are some additional advantages of our drug delivery system: Permeation by magainin is changed according to the pH change, so we can control the permeation of drugs by pH control. In addition, the magainin peptide has natural antimicrobial activity; therefore, microbial infection, which is a main concern in traditional transdermal delivery systems can be addressed simultaneously by this system.

APPENDIX A.1: TRANSDERMAL DELIVERY ENHANCED BY MAGAININ PEPTIDE: ADDITIONAL STUDY

A.1.1. Results

From chapter 3 Figure 3.2, we observed that skin permeability enhancement was strongly dependent on ethanol concentration. And from chapter 4 Figure 4.1, there is synergisitic skin permeability enhancement by magainin peptide and NLS.

Therefore, we tested the effect of the combination of these two results on skin

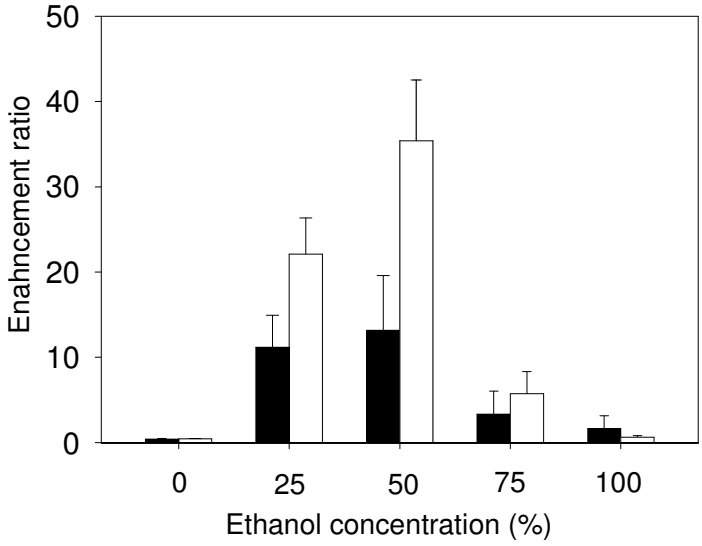

Figure A.1.1 Effect of ethanol concentration on the enhancement of skin permeability to fluorescein for skin treated without (■) and with (□) magainin after 5h. Data points show the average of n≥3 replicates and error bars correspond to the standard error of the mean.

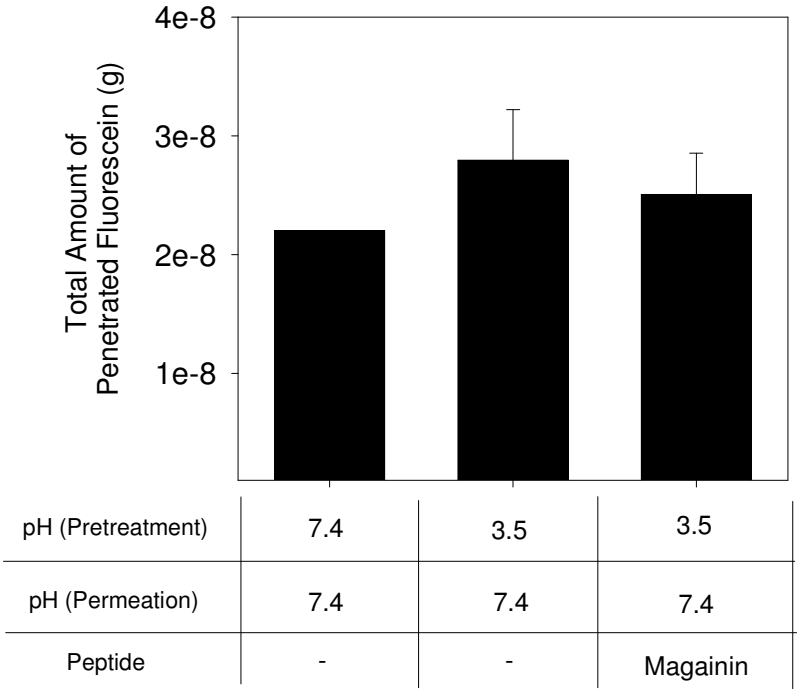

Figure A.1.2 Effect of acidic pH on the enhancement of skin permeability to fluorescein for skin treated without (■) and with (□) magainin after 15h. Data points show the average of n≥3 replicates and error bars correspond to the standard error of the mean.

permeability enhancement. As shown in Figure A1.1, the combination of ethanol with magainin peptide produces a trend similar to the previous ethanol study. The enhancement by magainin-NLS formulation at 50% ethanol solution is significantly larger than other ethanol concentration samples.

Because the pH of NLS solution was 3.5, we tested the acidic effect on skin permeability enhancement. Instead of using an NLS-ethanol solution, we put pH 3.5 PBS solution in during pretreatment. As shown in Figure A1.2, acidic pH alone has no effect on skin permeability. Additionally, when we put magainin in acidic solution in pretreatment we did not observe any enhancement of skin permeability.

Finally, from chapter 4 Figure 4.3, we took the image of the skin using multi-photon microscopy after delivery of sulforhodamine-labeled magainin with and without NLS-ethanol treatment. This study used NLS as an enhancer to increase penetration of another chemical enhancer, magainin peptide, into the skin. We also applied a physical delivery method in order to deliver magainin peptide into the skin instead of using a chemical enhancer. We used iontophoresis in pretreatment to deliver magainin into the skin for 15 h; however, the skin penetration enhancement for fluorescein molecule was not increased. (Figure A1.3)

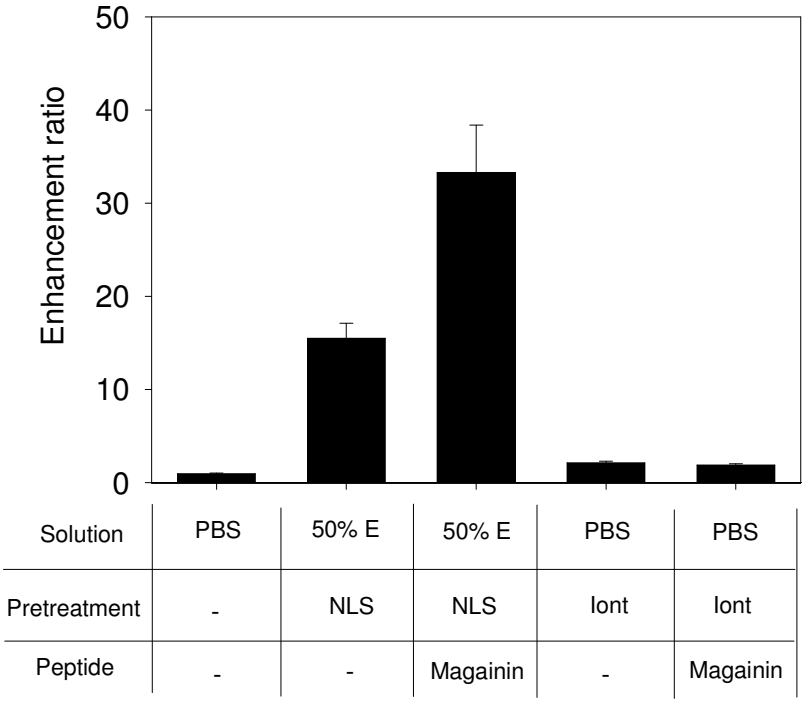

Figure A1.3 Effect of delivery of magainin into the skin by iontophoresis on skin permeability to fluorescein (Iont: Iontophoresis)

APPENDIX A.2: TRANSDERMAL DELIVERY ENHANCED BY VARIOUS ANTIMICROBIAL AND CELL-PENETRATING PEPTIDES

A.2.1. Results

We screened various different antimicrobial peptides as percutaneous enhancers in

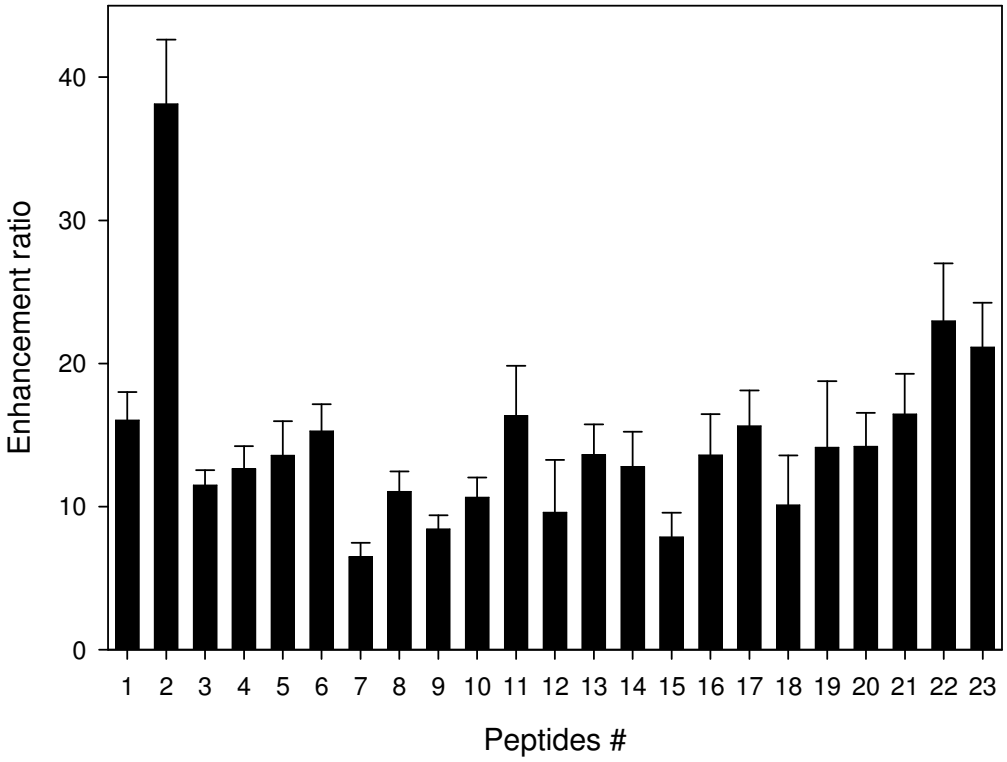

Figure A.2.1 Transdermal fluorescein skin permeability enhancement ratio of skin samples treated with NLS and various peptides: 1. NLS only, 2. Magainin, 3. Anti-magainin, 4. TD-1, 5. Maximin H5, 6. Pin2, 7. Oxkil, 8. Androctonin, 9. Hexapeptide, 10. Thanatin, 11. LL-37, 12. Polyphemusin1, 13. Misugurin, 14. Penetratin, 15. Tachyplesin, 16. Protegrin, 17. P5, 18. Fall-39, 19. Clavanin A, 20. Indolicidin, 21. Dermcidin, 22. Lys-Leu Peptide, 23. Melittin. Data represent averages of n≥3 samples with standard error of the mean.

Table A.2.1 Characteristics and sequences of various antimicrobial and cell-penetrating peptides.

	Peptides	Character	Sequences
2	Magainin [68]	Antimicrobial peptide	GIGKFLHSAKKFGKAFVGEIMNS
3	Anti-magainin	Charge of magainin modified to negative	GIGEFLHSAEEFGEAFVGEIMNS
4	TD-1 [76]	Insulun delivery peptide	ACSSSPSKHCG
5	Maximin H5 [182]	Anionic antimicrobial peptide	ILGPVLGLVSDTLDDVLGIL-NH_2
6	Pandinin 2 [183]	Pore-forming antimicrobial peptide	FWGALAKGALKLIPSLFSSFSKKD
7	Oxyopinin 1 [183]	Pore-forming antimicrobial peptide	FRGLAKLLKIGLKSFARVLKKVLPKAAKAGKALAKSM ADENAIRQQNQ
8	Androctonin [184]	Cysteine-rich antimicrobial peptide	RSVCRQIKICRRRGGCYYKCTNRPY
9	Hexapeptide [185]	Short antimicrobial peptide	Ac-RRWWCF-NH_2
10	Thanatin [186]	Antimicrobial without pore-forming	GSKKPVPIIYCNRRTGKCQRM
11	LL-37 [187]	Human antibiotic peptide	LLGDFFRKSKEKIGKEFKRIVQRIKDFLRNLVPRTES
12	Polyphemusin1 [188]	Antiparallel β–hairpin peptide	RRWCFRVCYRGFCYRKCR-$CONH_2$
13	Misgurin [189]	Pore-forming antimicrobial peptide	RQRVEELSKFSKKGAAARRRK
14	Penetratin [190]	Cell-penetrating peptides	RQIKIWFQNRRMKWKK
15	Tachyplesin [191]	Disulfide bond	KWCFRVCYRGICYRRCR-$CONH_2$
16	Protegrin [192]	β-sheet antimicrobial peptide	NH_2-RGGRLCYCRRRFCVCVGR-$CONH_2$
17	P5 [193]	Excellent antimicrobial peptide	KWKKLLKKPLLKKLLKKL-NH_2
18	Fall-39 [194]	Human antibiotic peptide	FALLGDFFRKSKEKIGKEFKRIVORIKDFLRNLVPRTS
19	Clavanin A [195]	α-helical antimicrobial peptide	VFQFLGKIIHHVGNFVHGFSHVF-$CONH_2$
20	Indolicidin [196]	Bovine antibiotic peptide	ILPWKWPWWPWRR-NH_2
21	Dermcidin [197]	Human antibiotic peptide	SSLLEKGLDGAKKAVGGLGKLGKDAVEDL ESVGKGAVHDVKDVLDSV
22	Lys-Leu Peptide [198]	High positive charge peptide	NH_2-KLLLKLLLKLLKLWLKLLKLLLK-COOH
23	Melittin [199]	Antimicrobial and hemolytic peptide	GIGAVLKVLTTGLPALISWIKRKRQQ

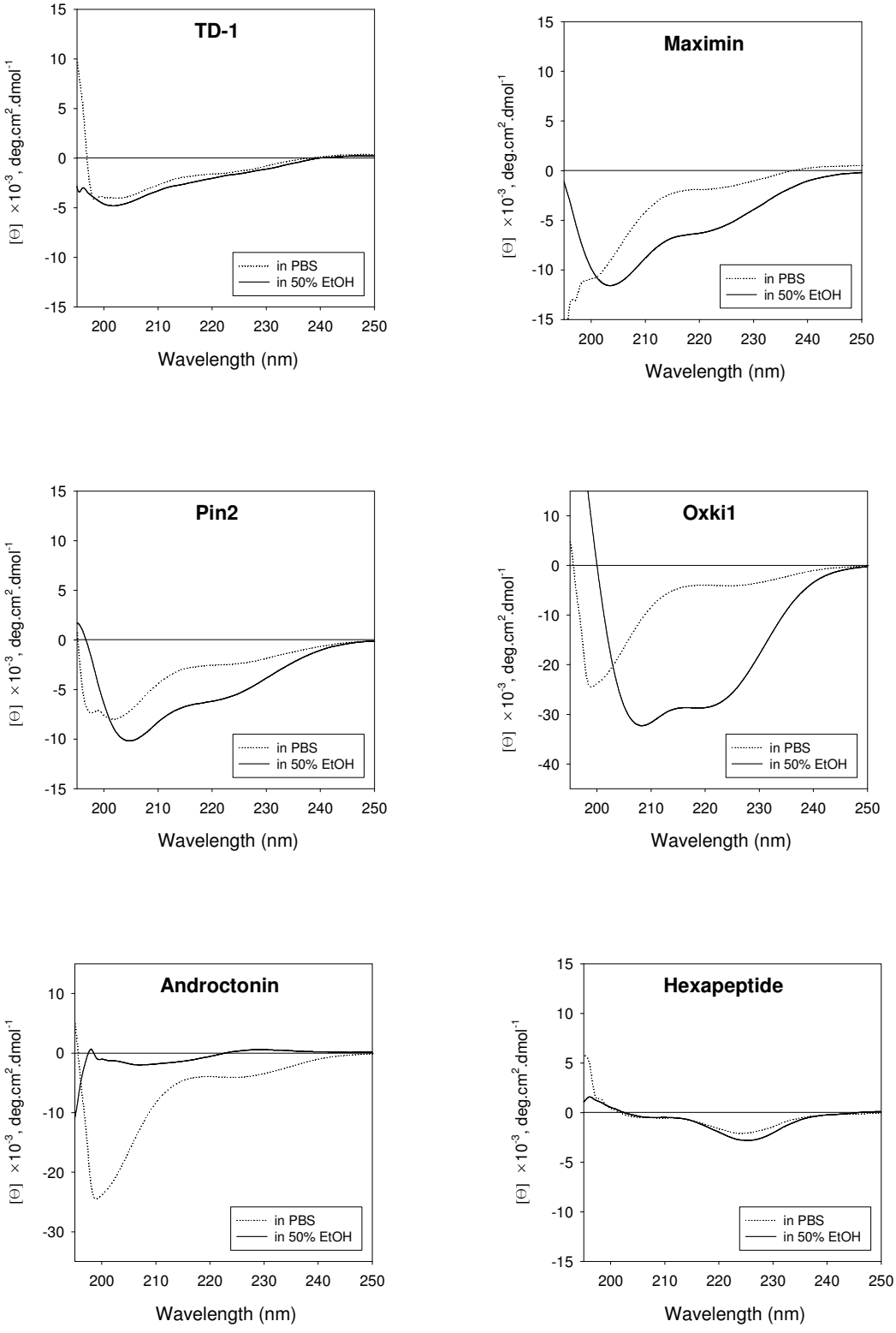

Figure A.2.2 Circular dichroism spectra of various antimircrobial or cell-penetrating peptides in PBS solution and 50% ethanol solution.

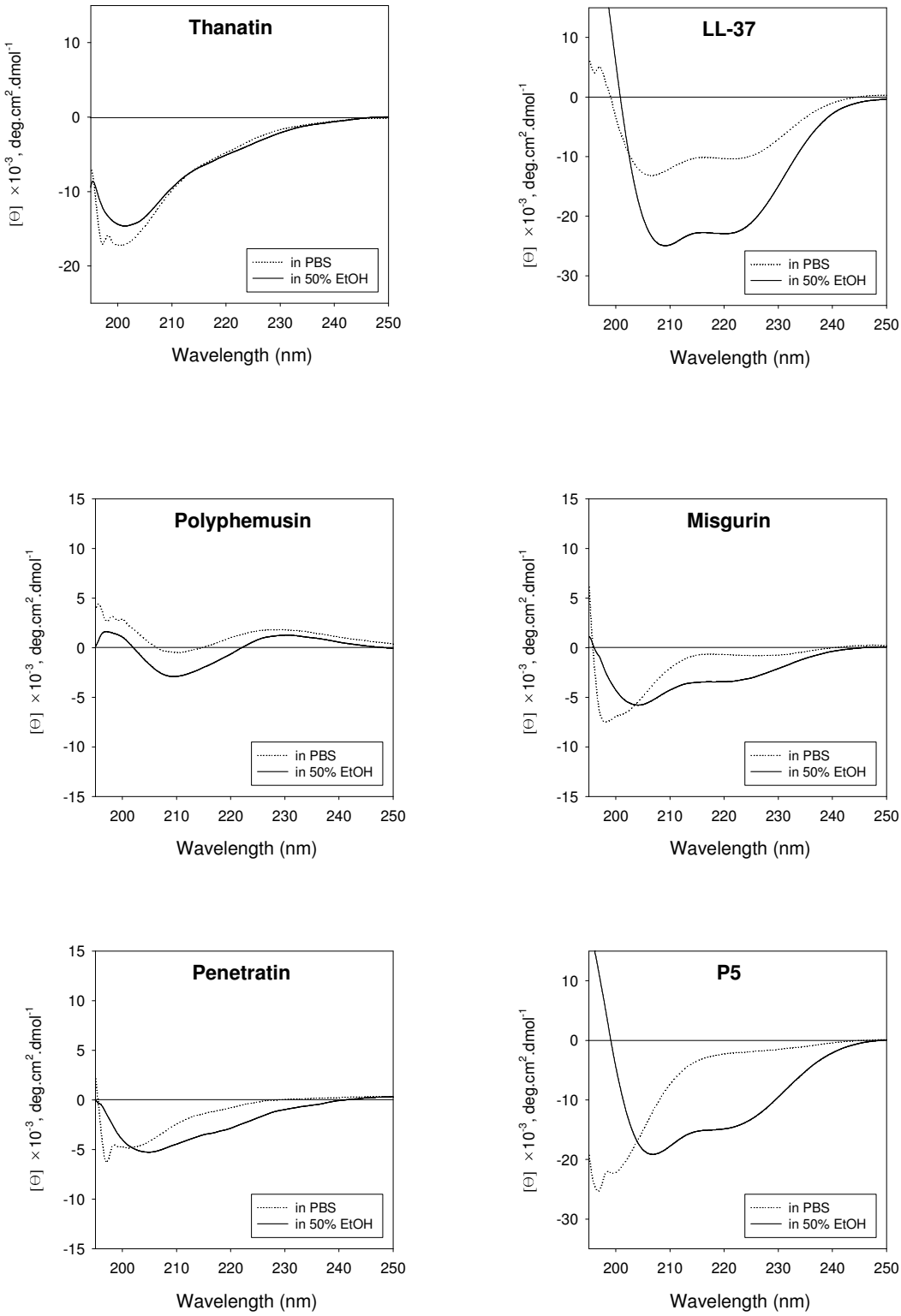

Figure A.2.2 Continued

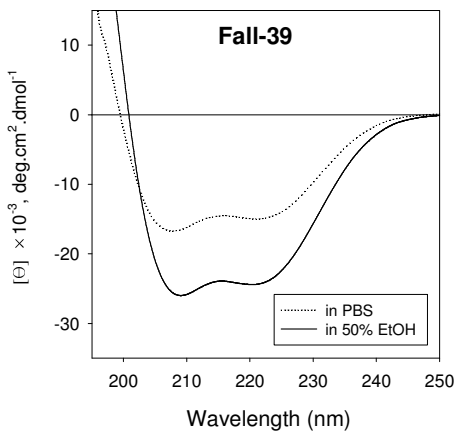

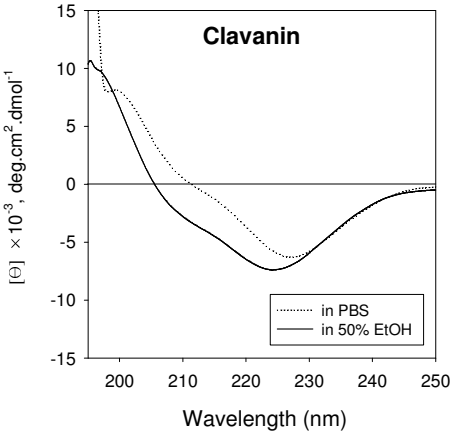

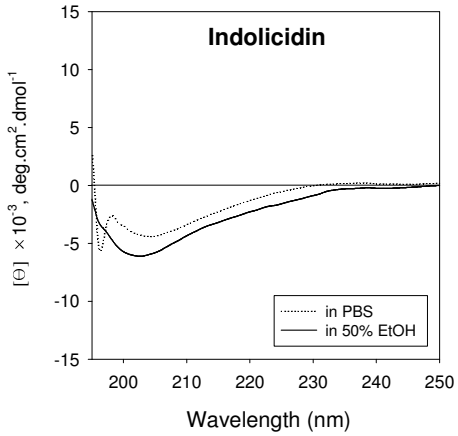

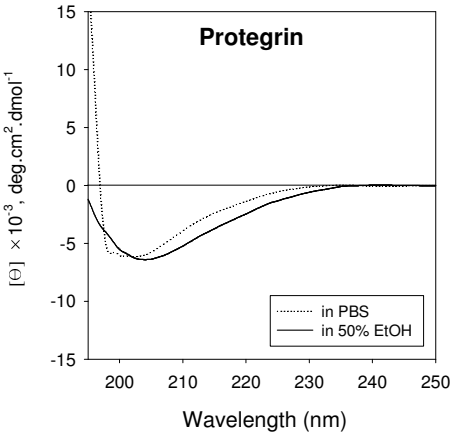

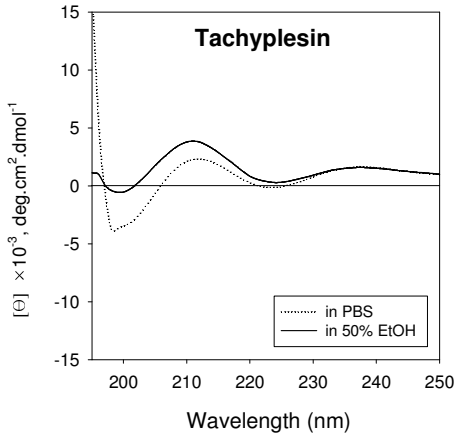

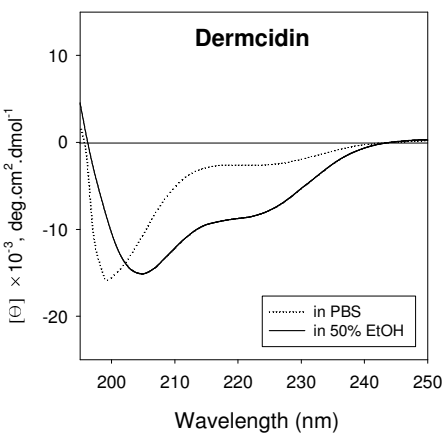

Figure A.2.2 Continued

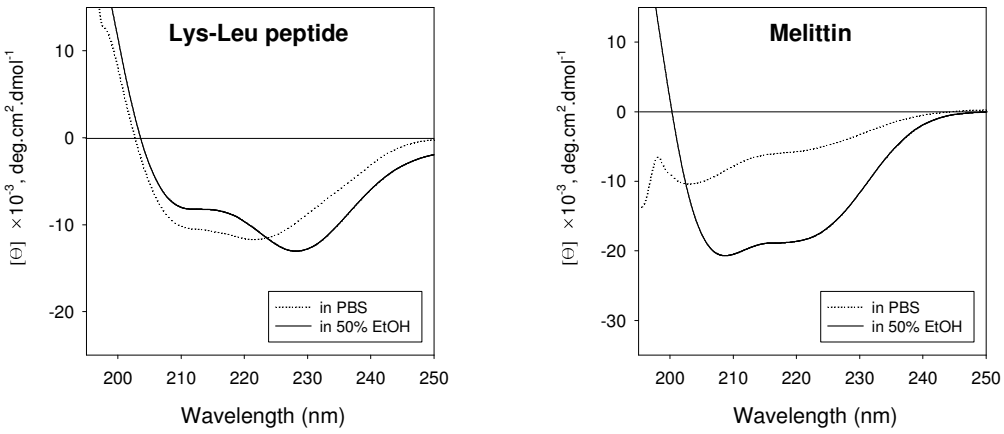

Figure A.2.2 Continued

an attempt to find alternative antimicrobial peptides that provided enhancement. As shown in Figure A2.1, none of antimicrobial peptides demonstrate similar skin penetration as magianin peptide. Characteristics and sequences of the various antimicrobial and cell-penetrating peptides are shown in Table A2.1.

In Figure A2.2, the structures of peptides were measured using CD-spectroscopy. Maximin H5, Pin2, Oxkil, LL-37, Misugurin, P5, Fall-39, Clavanin A, Dermcidin, Lys-Leu Peptide, and Melittin show alpha helicity in 50% ethanol. However, compared with Figure A 2-1, there are no correlations between alpha-helicity and skin permeability enhancement. From chapter 5 Figure 5.2, skin permeability was strongly dependent on magainin peptide concentration. As shown in Figure A2.3, we tested three other antimicrobial peptides and we found that these three peptides also show a concentration-dependent effect on skin permeability for

fluorescein. Based on these results, we found the optimum concentration of each peptide needed to see an increase in skin permeability.

We compared the skin permeability enhancement of four different peptides at their optimum concentration. As shown in Figure Az2.4, 0.25 mM Pin 2 and 1 mM Lys-Leu peptide show significantly higher enhancement than NLS only, but this enhancement is lower than 1mM magainin peptide.

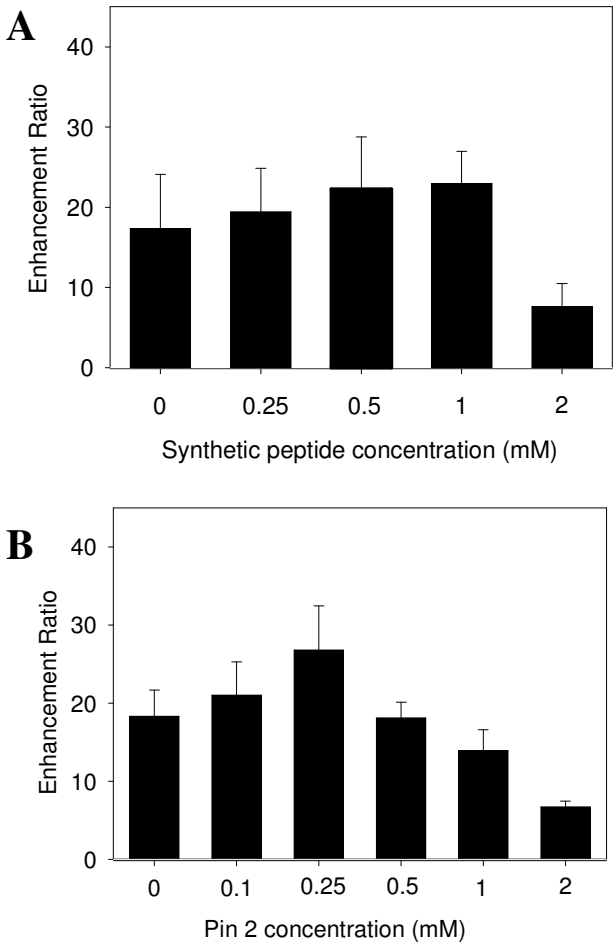

Figure A.2.3 Concentration effect of (A) Lys-Leu (B) Pin2 (C) Oxki1 peptide on the transdermal fluorescein skin permeability enhancement ratio (All sample treated with NLS). Data points show the average of n≥3 replicates and error bars correspond to the standard error of the mean.

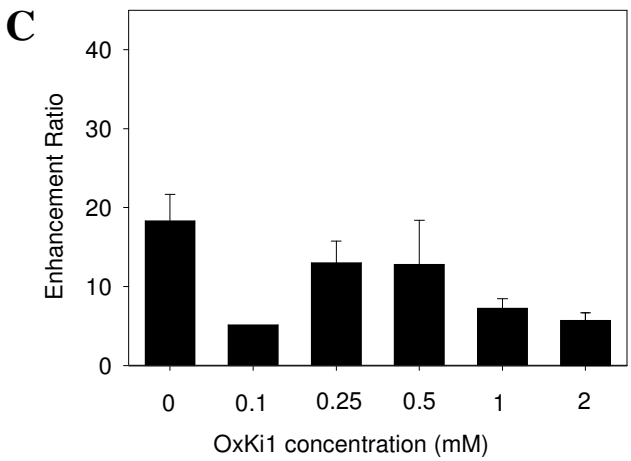

Figure A.2.3 Continued

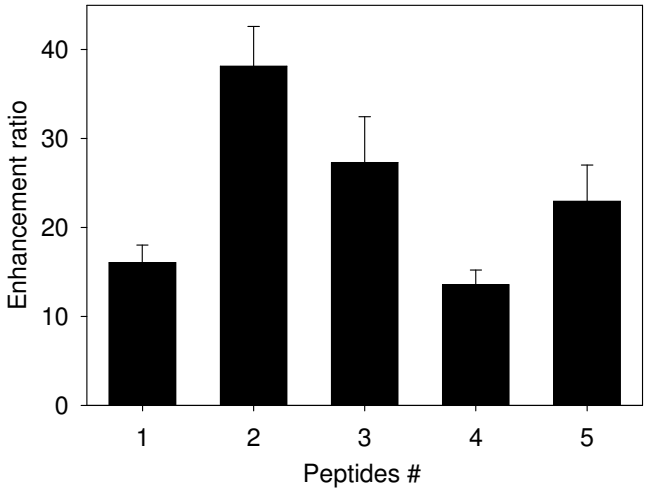

Figure A.2.4 Comparison of transdermal fluorescein skin permeability enhancement ratio of skin samples treated with NLS and selective peptides with optimized concentration. 1. NLS only, 2. 1mM Magainin, 3. 0.25mM Pin 2, 4. 0.5 mM Oxki1, 5. 1mM Lys-Leu Peptide. Data represent averages of n≥3 samples with standard error of the mean.

REFERENCES

[1] B.W. Barry, Novel mechanisms and devices to enable successful transdermal drug delivery, European Journal of Pharmaceutical Sciences 14(2) (2001) 101-114.

[2] S. Scheindlin, Transdermal drug delivery: Past, present, future, Molecular Interventions 4(6) (2004) 308-312.

[3] A. Naik, Y.N. Kalia, R.H. Guy, Transdermal drug delivery: overcoming the skin's barrier function Pharmaceutical science & technology today 3(9) (2000) 318-326.

[4] M.R. Prausnitz, S. Mitragotri, R. Langer, Current status and future potential of transdermal drug delivery, Nature Reviews Drug Discovery 3(2) (2004) 115-124.

[5] R. Langer, Transdermal drug delivery: past progress, current status, and future prospects, Advanced Drug Delivery Reviews 56(5) (2004) 557-558.

[6] A.F. Kydonieus, J.J. Wille, G.F. Murphy, Fundamental concepts in transdermal delivery of drugs, In : Kydonieus, A.F., Wille, J.J. (Eds.), Biochemical modulation of skin reactions, CRC Press, New York 2000.

[7] B.J. Thomas, B.C. Finnin, The transdermal revolution, Drug Discovery Today 9(16) (2004) 697-703.

[8] J.L. Zatz, B. Lee, Skin penetration enhancement by surfactants, Marcel Dekker, New York, 1997.

[9] T.J. Franz, P.A. Lehman, The skin as a barrier: structure and function, CRC Press, New York 2000.

[10] K.A. Holbrook, The structure and development of skin, McGraw Hill, New York, 1993.

[11] K.A. Holbrook, G.F. Odland, Regional differences in thickness (cell layers) of human *stratum-corneum* - Ultrastructural analysis, Journal of Investigative Dermatology 62(4) (1974) 415-422.

[12] R.J. Scheuple, L.J. Morgan, Bound water in keratin membranes measured by a microbalance technique, Nature 214(5087) (1967) 456-458.

[13] A.G. Matoltsy, C.A. Balsamo, A study of the components of the cornified epithelium of human skin, Journal of Biophysical and Biochemical Cytology 1(4) (1955) 339-360.

[14] J.A. Bouwstra, F.E.R. Dubbelaar, G.S. Gooris, M. Ponec, The lipid organisation in the skin barrier, Acta Dermato-Venereologica Suppl. 208 (2000) 23-30.

[15] J. Brod, Characterization and physiological-role of epidermal lipids, International Journal of Dermatology 30(2) (1991) 84-90.

[16] P.W. Wertz, B. van den Bergh, The physical, chemical and functional properties of lipids in the skin and other biological barriers, Chemistry and Physics of Lipids 91(2) (1998) 85-96.

[17] L. Coderch, O. Lopez, A. de la Maza, J.L. Parra, Ceramides and skin function, American Journal of Clinical Dermatology 4(2) (2003) 107-129.

[18] S. Engstrom, K. Ekelund, J. Engblom, L. Eriksson, E. Sparr, H. Wennerstrom, The skin barrier from a lipid perspective, Acta Dermato-Venereologica Suppl. 208 (2000) 31-35.

[19] A.P.M. Lavrijsen, J.A. Bouwstra, G.S. Gooris, A. Weerheim, H.E. Bodde, M. Ponec, Reduced skin barrier function parallels abnormal *stratum-corneum* lipid organization in patients with lamellar ichthyosis, Journal of Investigative Dermatology 105(4) (1995) 619-624.

[20] K.J. Robson, M.E. Stewart, S. Michelsen, N.D. Lazo, D.T. Downing, 6-Hydroxy-4-sphingenine in human epidermal ceramides, Journal of Lipid Research 35(11) (1994) 2060-2068.

[21] P.W. Wertz, Lipids and barrier function of the skin, Acta Dermato-Venereologica Suppl. 208 (2000) 7-11.

[22] H. Schaefer, T.E. Redelmeier, Skin barrier : principles of percutaneous absorption, Karger, Basel, 1996.

[23] M.A. Lampe, M.L. Williams, P.M. Elias, Human epidermal lipids - Characterization and modulations during differentiation, Journal of Lipid Research 24(2) (1983) 131-140.

[24] J.A. Bouwstra, G.S. Gooris, F.E.R. Dubbelaar, A. Weerheim, M. Ponec, pH, cholesterol sulfate and fatty acids affect stratum corneum lipid organization, Journal of Investigative Dermatology Symposium Proceedings 3 (1998) 69-74.

[25] P.M. Elias, Epidermal lipids, barrier function, and desquamation, Journal of Investigative Dermatology 80 (1983) S44-S49.

[26] A.S. Michaels, S.K. Chandrasekaran, J.E. Shaw, Drug permeation through human skin - Theory and invitro experimental measurement, Aiche Journal 21(5) (1975) 985-996.

[27] B. Yu, C.Y. Dong, P.T.C. So, D. Blankschtein, R. Langer, In vitro visualization and quantification of oleic acid induced changes in transdermal

transport using two-photon fluorescence microscopy, Journal of Investigative Dermatology 117(1) (2001) 16-25.

[28] B. Forslind, A domain mosaic model of the skin barrier, Acta Dermato-Venereologica 74(1) (1994) 1-6.

[29] B. Forslind, S. Engstrom, J. Engblom, L. Norlen, A novel approach to the understanding of human skin barrier function, Journal of Dermatological Science 14(2) (1997) 115-125.

[30] L. Norlen, Skin barrier structure and function: The single gel phase model, Journal of Investigative Dermatology 117(4) (2001) 830-836.

[31] J.A. Bouwstra, P.L. Honeywell-Nguyen, G.S. Gooris, M. Ponec, Structure of the skin barrier and its modulation by vesicular formulations, Progress in Lipid Research 42(1) (2003) 1-36.

[32] H.C. Ansel, L.V. Allen, N.G. Popovich, Pharmaceutical dosage forms and drug delivery sustems, Lippincott Williams & Wilkins, Baltimore, 1999.

[33] B.C. Finnin, T.M. Morgan, Transdermal penetration enhancers: Applications, limitations, and potential, Journal of Pharmaceutical Sciences 88(10) (1999) 955-958.

[34] S.C. Chattaraj, R.B. Walker, Penetration enhancer classification, CRC Pres, Boca Raton, FL, 1995.

[35] J. Hadgraft, D.G. Williams, G. Allan Azone: Mechanism of action and clinical effect, Dekker, New York, 1993.

[36] F.R. Bezema, E. Marttin, P.E.H. Roemele, J. Brussee, H.E. Bodde, H.J.M. deGroot, H-2 NMR Evidence for dynamic disorder in human skin induced by the penetration enhancer Azone, Spectrochimica Acta Part A-Molecular and Biomolecular Spectroscopy 52(7) (1996) 785-791.

[37] J. Hadgraft, J. Peck, D.G. Williams, W.J. Pugh, G. Allan, Mechanisms of action of skin penetration enhancers retarders: Azone and analogues, International Journal of Pharmaceutics 141(1-2) (1996) 17-25.

[38] B.J. Aungst, Fatty acids as skin permeation enhancers, CRC Pres, Boca Raton, FL, 1995.

[39] A. Naik, L. Pechtold, R.O. Potts, R.H. Guy, Mechanism of oleic acid-induced skin penetration enhancement in vivo in humans, Journal of Controlled Release 37(3) (1995) 299-306.

[40] M.L. Francoeur, G.M. Golden, R.O. Potts, Oleic-acid - Its effects on *stratum-corneum* in relation to (trans)dermal drug delivery, Pharmaceutical Research 7(6) (1990) 621-627.

[41] B.W. Barry, A.C. Williams, Terpenes as skin pentration enhancers, Dekker, New York, 1993.

[42] D.A. Godwin, B.B. Michniak, Influence of drug lipophilicity on terpenes as transdermal penetration enhancers, Drug Development and Industrial Pharmacy 25(8) (1999) 905-915.

[43] H.K. Vaddi, P.C. Ho, Y.W. Chan, S.Y. Chan, Terpenes in ethanol: haloperidol permeation and partition through human skin and stratum corneum changes, Journal of Controlled Release 81(1-2) (2002) 121-133.

[44] H.K. Vaddi, P.C. Ho, S.Y. Chan, Terpenes in propylene glycol as skin-penetration enhancers: Permeation and partition of haloperidol, fourier transform infrared spectroscopy, and differential scanning calorimetry, Journal of Pharmaceutical Sciences 91(7) (2002) 1639-1651.

[45] B. Berner, P. Liu, Alcohols, CRC Press, Boca Raton, 1995.

[46] T. Kuriharabergstrom, K. Knutson, L.J. Denoble, C.Y. Goates, Percutaneous-absorption enhancement of an ionic molecule by ethanol water-systems in human skin, Pharmaceutical Research 7(7) (1990) 762-766.

[47] M. Sznitowska, The influence of ethanol on permeation behaviour of the porous pathway in the stratum corneum, International Journal of Pharmaceutics 137(1) (1996) 137-140.

[48] T. Akimoto, Y. Nagase, Novel transdermal drug penetration enhancer: synthesis and enhancing effect of alkyldisiloxane compounds containing glucopyranosyl group, Journal of Controlled Release 88(2) (2003) 243-252.

[49] S.B. Ruddy, Surfactants, CRC Press, Boca Raton, 1995.

[50] R.J. Scheuplein, L. Ross, Effects of surfactants and solvents on the permeability of epidermis, Journal of the Society of Cosmetic Chemists 21(13) (1970) 853-873.

[51] B.W. Barry, Action of skin penetration enhancers - the lipid protein partitioning theory, International Journal of Cosmetic Science 10(6) (1988) 281-293.

[52] A.K. Banga, Y.W. Chien, Iontophoretic delivery of drugs - Fundamentals, developments and biomedical applications, Journal of Controlled Release 7(1) (1988) 1-24.

[53] M.R. Prausnitz, V.G. Bose, R. Langer, J.C. Weaver, Electroporation of mammalian skin - a mechanism to enhance transdermal drug-delivery, Proceedings of the National Academy of Sciences of the United States of America 90(22) (1993) 10504-10508.

[54] S. Mitragotri, J. Kost, Low-frequency sonophoresis: A review, Advanced Drug Delivery Reviews 56(5) (2004) 589-601.

[55] J.A. Friedland, E.W. Buchel, Skin care and the topical treatment of aging skin, Clinics in Plastic Surgery 27(4) (2000) 501-506.

[56] J.S. Dover, G.J. Hruza, K.A. Arndt, Lasers in skin resurfacing, Seminars in Cutaneous Medicine and Surgery 19(4) (2000) 207-220.

[57] M.R. Prausnitz, Microneedles for transdermal drug delivery, Advanced Drug Delivery Reviews 56(5) (2004) 581-587.

[58] S.N. Murthy, Magnetophoresis: an approach to enhance transdermal drug diffusion, Pharmazie 54(5) (1999) 377-379.

[59] S. Lee, N. Kollias, D.J. McAuliffe, T.J. Flotte, A.G. Doukas, Topical drug delivery in humans with a single photomechanical wave, Pharmaceutical Research 16(11) (1999) 1717-1721.

[60] P.M. Elias, J. Tsai, G.K. Menon, W.M. Holleran, K.R. Feingold, The potential of metabolic interventions to enhance transdermal drug delivery, Journal of Investigative Dermatology Symposium Proceedings 7(1) (2002) 79-85.

[61] J.C. Tsai, R.H. Guy, C.R. Thornfeldt, W.N. Gao, K.R. Feingold, P.M. Elias, Metabolic approaches to enhance transdermal drug delivery. 1. Effect of lipid synthesis inhibitors, Journal of Pharmaceutical Sciences 85(6) (1996) 643-648.

[62] Babita, S. Gupta, A.K. Tiwary, Role of sphingosine synthesis inhibition in transcutaneous delivery of levodopa, International Journal of Pharmaceutics 238(1-2) (2002) 43-50.

[63] K.R. Gunatatna, M. Anderson, L. Good, Microbial membrane-permeating peptides and their applications, CRC Press, Boca Raton, 2002.

[64] K. Matsuzaki, Magainins as paradigm for the mode of action of pore forming polypeptides, Biochimica Et Biophysica Acta-Reviews on Biomembranes 1376(3) (1998) 391-400.

[65] M. Zasloff, Antimicrobial peptides of multicellular organisms, Nature 415(6870) (2002) 389-395.

[66] Z. Oren, Y. Shai, Mode of action of linear amphipathic alpha-helical antimicrobial peptides, Biopolymers 47(6) (1998) 451-463.

[67] Y. Shai, Mechanism of the binding, insertion and destabilization of phospholipid bilayer membranes by alpha-helical antimicrobial and cell non-selective membrane-lytic peptides, Biochimica Et Biophysica Acta-Biomembranes 1462(1-2) (1999) 55-70.

[68] M. Zasloff, Magainins, a class of antimicrobial peptides from *Xenopus* skin - Isolation, characterization of 2 active forms, and partial cDNA sequence of a precursor, Proceedings of the National Academy of Sciences of the United States of America 84(15) (1987) 5449-5453.

[69] K. Matsuzaki, O. Murase, N. Fujii, K. Miyajima, Translocation of a channel-forming antimicrobial peptide, magainin-2, across lipid bilayers by forming a pore, Biochemistry 34(19) (1995) 6521-6526.

[70] K. Matsuzaki, A. Nakamura, O. Murase, K. Sugishita, N. Fujii, K. Miyajima, Modulation of magainin 2-lipid bilayer interactions by peptide charge, Biochemistry 36(8) (1997) 2104-2111.

[71] K. Matsuzaki, K. Sugishita, M. Harada, N. Fujii, K. Miyajima, Interactions of an antimicrobial peptide, magainin 2, with outer and inner membranes of Gram-negative bacteria, Biochimica Et Biophysica Acta-Biomembranes 1327(1) (1997) 119-130.

[72] S.J. Ludtke, K. He, W.T. Heller, T.A. Harroun, L. Yang, H.W. Huang, Membrane pores induced by magainin, Biochemistry 35(43) (1996) 13723-13728.

[73] L.B. Lopes, C.M. Brophy, E. Furnish, C.R. Flynn, O. Sparks, P. Komalavilas, L. Joshi, A. Panitch, M.V.L.B. Bentley, Comparative study of the skin penetration of protein transduction domains and a conjugated peptide, Pharmaceutical Research 22(5) (2005) 750-757.

[74] J.B. Rothbard, S. Garlington, Q. Lin, T. Kirschberg, E. Kreider, P.L. McGrane, P.A. Wender, P.A. Khavari, Conjugation of arginine oligomers to cyclosporin A facilitates topical delivery and inhibition of inflammation, Nature Medicine 6(11) (2000) 1253-1257.

[75] M.P.M. Schutze-Redelmeier, S. Kong, M.B. Bally, J.P. Dutz, Antennapedia transduction sequence promotes anti tumour immunity to epicutaneously administered CTL epitopes, Vaccine 22(15-16) (2004) 1985-1991.

[76] Y.P. Chen, Y.Y. Shen, X. Guo, C.S. Zhang, W.J. Yang, M.L. Ma, S. Liu, M.B. Zhang, L.P. Wen, Transdermal protein delivery by a coadministered peptide identified via phage display, Nature Biotechnology 24(4) (2006) 455-460.

[77] S. Mitragotri, Synergistic effect of enhancers for transdermal drug delivery, Pharmaceutical Research 17(11) (2000) 1354-1359.

[78] Y.N. Kalia, R.H. Guy, Interaction between penetration enhancers and iontophoresis: Effect on human skin impedance in vivo, Journal of Controlled Release 44(1) (1997) 33-42.

[79] L. Wearley, Y.W. Chien, Enhancement of the invitro skin permeability of Azidothymidine (AZT) via iontophoresis and chemical enhancer, Pharmaceutical Research 7(1) (1990) 34-40.

[80] K.S. Bhatia, S. Gao, T.P. Freeman, J. Singh, Effect of penetration enhancers and iontophoresis on the ultrastructure and cholecystokinin-8 permeability through porcine skin, Journal of Pharmaceutical Sciences 86(9) (1997) 1011-1015.

[81] M. Artusi, S. Nicoli, P. Colombo, R. Bettini, A. Sacchi, P. Santi, Effect of chemical enhancers and iontophoresis on thiocolchicoside permeation across

rabbit and human skin in vitro, Journal of Pharmaceutical Sciences 93(10) (2004) 2431-2438.

[82] O. Pillai, R. Panchagnula, Transdermal delivery of insulin from poloxamer gel: ex vivo and in vivo skin permeation studies in rat using iontophoresis and chemical enhancers, Journal of Controlled Release 89(1) (2003) 127-140.

[83] A.M. de Graaff, G.L. Li, A.C. van Aelst, J.A. Bouwstra, Combined chemical and electrical enhancement modulates stratum corneum structure, Journal of Controlled Release 90(1) (2003) 49-58.

[84] A. Sen, Y.L. Zhao, L. Zhang, S.W. Hui, Enhanced transdermal transport by electroporation using anionic lipids, Journal of Controlled Release 82(2-3) (2002) 399-405.

[85] J.C. Weaver, R. Vanbever, T.E. Vaughan, M.R. Prausnitz, Heparin alters transdermal transport associated with electroporation, Biochemical and Biophysical Research Communications 234(3) (1997) 637-640.

[86] L. Ilic, T.R. Gowrishankar, T.E. Vaughan, T.O. Herndon, J.C. Weaver, Spatially constrained skin electroporation with sodium thiosulfate and urea creates transdermal microconduits, Journal of Controlled Release 61(1-2) (1999) 185-202.

[87] S.N. Murthy, A. Sen, S.W. Hui, Surfactant-enhanced transdermal delivery by electroporation, Journal of Controlled Release 98(2) (2004) 307-315.

[88] M.E. Johnson, S. Mitragotri, A. Patel, D. Blankschtein, R. Langer, Synergistic effects of chemical enhancers and therapeutic ultrasound on transdermal drug delivery, Journal of Pharmaceutical Sciences 85(7) (1996) 670-679.

[89] S. Mitragotri, D. Ray, J. Farrell, H. Tang, B. Yu, J. Kost, D. Blankschtein, R. Langer, Synergistic effect of low-frequency ultrasound and sodium lauryl sulfate on transdermal transport, Journal of Pharmaceutical Sciences 89(7) (2000) 892-900.

[90] P. Karande, A. Jain, A. Arora, M.J. Ho, S. Mitragotri, Synergistic effects of chemical enhancers on skin permeability: A case study of sodium lauroylsarcosinate and sorbitan monolaurate, European Journal of Pharmaceutical Sciences 31(1) (2007) 1-7.

[91] P. Karande, A. Jain, S. Mitragotri, Discovery of transdermal penetration enhancers by high-throughput screening, Nature Biotechnology 22(2) (2004) 192-197.

[92] J.A. Nicolazzo, T.M. Morgan, B.L. Reed, B.C. Finnin, Synergistic enhancement of testosterone transdermal delivery, Journal of Controlled Release 103(3) (2005) 577-585.

[93] C. Buehler, K.H. Kim, C.Y. Dong, B.R. Masters, P.T.C. So, Innovations in two-photon deep tissue microscopy, Ieee Engineering in Medicine and Biology Magazine 18(5) (1999) 23-30.

[94] B. Yu, K.H. Kim, P.T.C. So, D. Blankschtein, R. Langer, Visualization of oleic acid-induced transdermal diffusion pathways using two-photon fluorescence microscopy, Journal of Investigative Dermatology 120(3) (2003) 448-455.

[95] R.O. Potts, M.L. Francoeur, Infrared spectroscopy of *stratum corneum* lipids, Marcel Dekker, New York, 1993.

[96] A.K. Levang, K. Zhao, J. Singh, Effect of ethanol propylene glycol on the in vitro percutaneous absorption of aspirin, biophysical changes and macroscopic barrier properties of the skin, International Journal of Pharmaceutics 181(2) (1999) 255-263.

[97] A. Naik, R.H. Guy, Infrared spectroscopic and differential scanning calorimetric investigations of stratum corneum barrier function, Marcel Dekker, New York, 1997.

[98] P. Karande, A. Jain, K. Ergun, V. Kispersky, S. Mitragotri, Design principles of chemical penetration enhancers for transdermal drug delivery, Proceedings of the National Academy of Sciences of the United States of America 102(13) (2005) 4688-4693.

[99] R.P. Oertel, Protein conformational-changes induced in human *stratum-corneum* by organic sulfoxides - IR spectroscopic investigation, Biopolymers 16(10) (1977) 2329-2345.

[100] R.O. Potts, G.M. Golden, M.L. Francoeur, V.H.W. Mak, R.H. Guy, Mechanism and enhancement of solute transport across the *stratum-corneum*, Journal of Controlled Release 15(3) (1991) 249-260.

[101] J.A. Bouwstra, G.S. Gooris, S.H. White, X-ray analysis of the *stratum corneum* and its lipids, Marcel Dekker, New York, 1997.

[102] O. Lopez, M. Cocera, L. Campos, A. de la Maza, L. Coderch, J.L. Parra, Use of wide and small angle X-ray diffraction to study the modifications in the stratum corneum induced by otyl glucoside, Colloids and Surfaces A-Physicochemical and Engineering Aspects 162(1-3) (2000) 123-130.

[103] S.H. White, D. Mirejovsky, G.I. King, Structure of lamellar lipid domains and corneocyte envelopes of murine *stratum-corneum* - an X-ray-diffraction study, Biochemistry 27(10) (1988) 3725-3732.

[104] I. Hatta, N. Ohta, S. Ban, H. Tanaka, S. Nakata, X-Ray diffraction study on ordered, disordered and reconstituted intercellular lipid lamellar structure in stratum corneum, Biophysical Chemistry 89(2-3) (2001) 239-242.

[105] P.M. Elias, Epidermal barrier function: Intercellular lamellar lipid structures, origin, composition and metabolism, Journal of Controlled Release 15(3) (1991) 199-208.

[106] A.C. Williams, B.W. Barry, Penetration enhancers, Advanced Drug Delivery Reviews 56(5) (2004) 603-618.

[107] M. Malmsten, Surfactants and polymers in drug delivery, Marcel Dekker, New York, 2002.

[108] J.L. Zatz, B. Lee, Skin penetration enhancement by surfactants. In : Rieger, M.M., Rhein, L.D. (Eds.), Surfactants in Cosmetics., Marcel Dekker, New York, 1997.

[109] G. Imokawa, S. Akasaki, Y. Minematsu, M. Kawai, Importance of intercellular lipids in water-retention properties of the *stratum-corneum*: Induction and recovery study of surfactant dry skin, Archives of Dermatological Research 281(1) (1989) 45-51.

[110] A. Aioi, K. Kuriyama, T. Shimizu, M. Yoshioka, S. Uenoyama, Effects of vitamin-E and squalene on skin irritation of a transdermal absorption enhancer, lauroylsarcosine, International Journal of Pharmaceutics 93(1-3) (1993) 1-6.

[111] A. Nokhodchi, J. Shokri, A. Dashbolaghi, D. Hassan-Zadeh, T. Ghafourian, M. Barzegar-Jalali, The enhancement effect of surfactants on the penetration of lorazepam through rat skin, International Journal of Pharmaceutics 250(2) (2003) 359-369.

[112] B. Berner, P. Liu, Alcohols. In: Smith, E.W., Maibach, H.I.(Eds), Percutaneous Penetration Enhancers., CRC Press, Boca Raton, FL, pp. 45, 1995.

[113] R. Scheuplein, Mechanism of percutaneous adsorption. I. Routes of penetration and influence of solubility, Journal of Investigative Dermatology 45(5) (1965) 334-346.

[114] B. Berner, G.C. Mazzenga, J.H. Otte, R.J. Steffens, R.H. Juang, C.D. Ebert, Ethanol water mutually enhanced transdermal therapeutic system. 2. Skin permeation of ethanol and nitroglycerin, Journal of Pharmaceutical Sciences 78(5) (1989) 402-407.

[115] P. Karande, A. Jain, S. Mitragotri, Relationships between skin's electrical impedance and permeability in the presence of chemical enhancers, Journal of Controlled Release 110(2) (2006) 307-313.

[116] A.H. Lackermeier, E.T. McAdams, G.P. Moss, A.D. Woolfson, In vivo AC impedance spectroscopy of human skin - Theory and problems in monitoring of passive percutaneous drug delivery, Electrical Bioimpedance Methods: Applications to Medicine and Biotechnology 873 (1999) 197-213.

[117] K. Kontturi, L. Murtomaki, J. Hirvonen, P. Paronen, A. Urtti, Electrochemical characterization of human skin by impedance spectroscopy - the effect of penetration enhancers, Pharmaceutical Research 10(3) (1993) 381-385.

[118] H. Tanojo, J.A. Bouwstra, H.E. Junginger, H.E. Bodde, Thermal analysis studies on human skin and skin barrier modulation by fatty acids and propylene glycol, Journal of Thermal Analysis and Calorimetry 57(1) (1999) 313-322.

[119] C.S. Leopold, B.C. Lippold, An attempt to clarify the mechanism of the penetration enhancing effects of lipophilic vehicles with differential scanning calorimetry (DSC), Journal of Pharmacy and Pharmacology 47(4) (1995) 276-281.

[120] G.M. Golden, J.E. Mckie, R.O. Potts, Role of *stratum-corneum* lipid fluidity in transdermal drug flux, Journal of Pharmaceutical Sciences 76(1) (1987) 25-28.

[121] C.Y. Goates, K. Knutson, Enhanced permeation of polar compounds through human epidermis. 1. Permeability and membrane structural-changes in the presence of short-chain alcohols, Biochimica Et Biophysica Acta-Biomembranes 1195(1) (1994) 169-179.

[122] K.S. Bhatia, S. Gao, J. Singh, Effect of penetration enhancers and iontophoresis on the FT-IR spectroscopy and LHRH permeability through porcine skin, Journal of Controlled Release 47(1) (1997) 81-89.

[123] H.L. Casal, H.H. Mantsch, Polymorphic phase-behavior of phospholipid-membranes studied by infrared-spectroscopy, Biochimica Et Biophysica Acta 779(4) (1984) 381-401.

[124] K. Knutson, S.L. Krill, J. Zhang, Solvent-mediated alterations of the *stratum-corneum*, Journal of Controlled Release 11(1-3) (1990) 93-103.

[125] A.N.C. Anigbogu, A.C. Williams, B.W. Barry, H.G.M. Edwards, Fourier-transform raman-spectroscopy of interactions between the penetration enhancer dimethyl-sulfoxide and human *stratum-corneum*, International Journal of Pharmaceutics 125(2) (1995) 265-282.

[126] D. Bommannan, R.O. Potts, R.H. Guy, Examination of the effect of ethanol on human s*tratum-corneum* in vivo using infrared-spectroscopy, Journal of Controlled Release 16(3) (1991) 299-304.

[127] K.S. Bhatia, J. Singh, Mechanism of transport enhancement of LHRH through porcine epidermis by terpenes and iontophoresis: Permeability and lipid extraction studies, Pharmaceutical Research 15(12) (1998) 1857-1862.

[128] G. Grubauer, K.R. Feingold, R.M. Harris, P.M. Elias, Lipid-content and lipid type as determinants of the epidermal permeability barrier, Journal of Lipid Research 30(1) (1989) 89-96.

[129] G. Imokawa, H. Kuno, M. Kawai, *Stratum-corneum* lipids serve as a bound-water modulator, Journal of Investigative Dermatology 96(6) (1991) 845-851.

[130] Y.N. Kalia, A. Naik, J. Garrison, R.H. Guy, Iontophoretic drug delivery, Advanced Drug Delivery Reviews 56(5) (2004) 619-658.

[131] A.R. Denet, R. Vanbever, V. Preat, Skin electroporation for transdermal and topical delivery, Advanced Drug Delivery Reviews 56(5) (2004) 659-674.

[132] R.M. Epand, H.J. Vogel, Diversity of antimicrobial peptides and their mechanisms of action, Biochimica Et Biophysica Acta-Biomembranes 1462(1-2) (1999) 11-28.

[133] H.W. Huang, F.Y. Chen, M.T. Lee, Molecular mechanism of peptide-induced pores in membranes, Physical Review Letters 92(19) (2004) -.

[134] D.W. Paquette, D.M. Simpson, P. Friden, V. Braman, R.C. Williams, Safety and clinical effects of topical histatin gels in humans with experimental gingivitis, Journal of Clinical Periodontology 29(12) (2002) 1051-1058.

[135] A. Clara, D.D. Manjramkar, V.K. Reddy, Preclinical evaluation of magainin-A as a contraceptive antimicrobial agent, Fertility and Sterility 81(5) (2004) 1357-1365.

[136] Y. Ohsaki, A.F. Gazdar, H.C. Chen, B.E. Johnson, Antitumor-activity of magainin analogs against human lung-cancer cell-lines, Cancer Research 52(13) (1992) 3534-3538.

[137] S. Kaushik, A. Krishnan, M.R. Prausnitz, P.J. Ludovice, Magainin-mediated disruption of stratum corneum lipid vesicles, Pharmaceutical Research 18(6) (2001) 894-896.

[138] P.S. Talreja, N.K. Kleene, W.L. Pickens, T.F. Wang, G.B. Kasting, Visualization of the lipid barrier and measurement of lipid pathlength in human stratum corneum, AAPS Pharmsci 3(2) (2001) 1-9.

[139] Y. Kim, P.J. Ludovice, M.R. Prausnitz, Synergistic enhancement of skin permeability by N-lauroylsarcosine and ethanol, International Journal of Pharmaceutics, *in press.*

[140] V. Schreiner, G.S. Gooris, S. Pfeiffer, G. Lanzendorfer, H. Wenck, W. Diembeck, E. Proksch, J. Bouwstra, Barrier characteristics of different human skin types investigated with X-ray diffraction, lipid analysis, and electron microscopy imaging, Journal of Investigative Dermatology 114(4) (2000) 654-660.

[141] G.M. Golden, D.B. Guzek, R.R. Harris, J.E. Mckie, R.O. Potts, Lipid yhermotropic transitions in human *stratum-corneum*, Journal of Investigative Dermatology 86(3) (1986) 255-259.

[142] Y. Takeuchi, H. Yasukawa, Y. Yamaoka, Y. Kato, Y. Morimoto, Y. Fukumori, T. Fukuda, Effects of fatty-acids, fatty amines and propylene-glycol on rat *stratum-corneum* lipids and proteins in vitro measured by Fourier-transform infrared attenuated total reflection (FT-IR/ATR) spectroscopy, Chemical & Pharmaceutical Bulletin 40(7) (1992) 1887-1892.

[143] P.L. Yeagle, Cholesterol and the cell-membrane, Biochimica Et Biophysica Acta 822(3-4) (1985) 267-287.

[144] J.D. Middleton, Mechanism of Action of Surfactants on Water Binding Properties of Isolated Stratum Corneum, Journal of the Society of Cosmetic Chemists 20(7) (1969) 399-412.

[145] T.J. Franz, P.A. Lehman, The skin as a barrier: structure and function, CRC Press, New York, 2000.

[146] Y. Kim, P.J. Ludovice, M.R. Prausnitz, Transdermal delivery enhanced by magainin pore-forming peptide, Journal of Controlled Release 122 (2007) 375-383.

[147] T. Tachi, R.F. Epand, R.M. Epand, K. Matsuzaki, Position-dependent hydrophobicity of the antimicrobial magainin peptide affects the mode of peptide-lipid interactions and selective toxicity, Biochemistry 41(34) (2002) 10723-10731.

[148] S. Ludtke, K. He, H. Huang, Membrane thinning caused by magainin 2, Biochemistry 34(51) (1995) 16764-16769.

[149] K. Matsuzaki, O. Murase, N. Fujii, K. Miyajima, An antimicrobial peptide, magainin 2, induced rapid flip-flop of phospholipids coupled with pore formation and peptide translocation, Biochemistry 35(35) (1996) 11361-11368.

[150] A. Tossi, L. Sandri, A. Giangaspero, Amphipathic, alpha-helical antimicrobial peptides, Biopolymers 55(1) (2000) 4-30.

[151] R. Bessalle, H. Haas, A. Goria, I. Shalit, M. Fridkin, Augmentation of the antibacterial activity of magainin by positive-charge chain extension, Antimicrobial Agents and Chemotherapy 36(2) (1992) 313-317.

[152] M. Dathe, H. Nikolenko, J. Meyer, M. Beyermann, M. Bienert, Optimization of the antimicrobial activity of magainin peptides by modification of charge, Febs Letters 501(2-3) (2001) 146-150.

[153] H.C. Chen, J.H. Brown, J.L. Morell, C.M. Huang, Synthetic magainin analogs with improved antimicrobial activity, Febs Letters 236(2) (1988) 462-466.

[154] M. Dathe, T. Wieprecht, H. Nikolenko, L. Handel, W.L. Maloy, D.L. MacDonald, M. Beyermann, M. Bienert, Hydrophobicity, hydrophobic moment and angle subtended by charged residues modulate antibacterial and haemolytic activity of amphipathic helical peptides, Febs Letters 403(2) (1997) 208-212.

[155] T. Wieprecht, M. Dathe, M. Beyermann, E. Krause, W.L. Maloy, D.L. MacDonald, M. Bienert, Peptide hydrophobicity controls the activity and selectivity of magainin 2 amide in interaction with membranes, Biochemistry 36(20) (1997) 6124-6132.

[156] M.R. Prausnitz, R. Langer, Transdermal Drug Delivery, Nature Biotechnology, *Submitted*.

[157] S.E. Cross, M.S. Roberts, Physical enhancement of transdermal drug application: Is delivery technology keeping up with pharmaceutical development?, Current Drug Delivery 1(1) (2004) 81-92.

[158] A. Aggeli, M. Bell, L.M. Carrick, C.W.G. Fishwick, R. Harding, P.J. Mawer, S.E. Radford, A.E. Strong, N. Boden, pH as a trigger of peptide beta-sheet self-assembly and reversible switching between nematic and isotropic phases, Journal of the American Chemical Society 125(32) (2003) 9619-9628.

[159] W.K. Subczynski, A. Wisniewska, A. Kusumi, R.N. McElhaney, Effects of pH-induced variations of the charge of the transmembrane alpha-helical peptide Ac-K-2(LA)(12)K-2-amide on the organization and dynamics of the host dimyristoylphosphatidylcholine bilayer membrane, Biochimica Et Biophysica Acta-Biomembranes 1720(1-2) (2005) 99-109.

[160] I.H. Lee, Y. Cho, R.I. Lehrer, Effects of pH and salinity on the antimicrobial properties of clavanins, Infection and Immunity 65(7) (1997) 2898-2903.

[161] R. Moser, Design, Synthesis and structure of an amphipathic peptide with pH-inducible hemolytic-activity, Protein Engineering 5(4) (1992) 323-331.

[162] Y. Shai, Y.R. Hadari, A. Finkels, pH-dependent pore formation properties of pardaxin analogs, Journal of Biological Chemistry 266(33) (1991) 22346-22354.

[163] C.H. Chiang, J.S. Lai, K.H. Yang, The Effects of pH and chemical enhancers on the percutaneous-absorption of indomethacin, Drug Development and Industrial Pharmacy 17(1) (1991) 91-111.

[164] T. Hatanaka, S. Morigaki, T. Aiba, K. Katayama, T. Koizumi, Effect of pH on the skin permeability of a zwitterionic drug, cephalexin, International Journal of Pharmaceutics 125(2) (1995) 195-203.

[165] P. Corcuff, C. Bertrand, J.L. Leveque, Morphometry of human epidermis in-vivo by real-time confocal microscopy, Archives of Dermatological Research 285(8) (1993) 475-481.

[166] A. Knuttel, M. Boehlau-Godau, Spatially confined and temporally resolved refractive index and scattering evaluation in human skin performed with optical coherence tomography, Journal of Biomedical Optics 5(1) (2000) 83-92.

[167] D.G. Cameron, J.K. Kauppinen, D.J. Moffatt, H.H. Mantsch, Precision in condensed phase vibrational spectroscopy, Applied Spectroscopy 36(3) (1982) 245-250.

[168] D. Marro, R.H. Guy, M.B. Delgado-Charro, Characterization of the iontophoretic permselectivity properties of human and pig skin, Journal of Controlled Release 70(1-2) (2001) 213-217.

[169] B. Skoog, A. Wichman, Calculation of the isoelectric points of polypeptides from the amino-acid-composition, Trac-Trends in Analytical Chemistry 5(4) (1986) 82-83.

[170] M. Sznitowska, S. Janicki, A. Baczek, Studies on the effect of pH on the lipoidal route of penetration across *stratum corneum*, Journal of Controlled Release 76(3) (2001) 327-335.

[171] S.K. Kandasamy, R.G. Larson, Effect of salt on the interactions of antimicrobial peptides with zwitterionic lipid bilayers, Biochimica Et Biophysica Acta-Biomembranes 1758(9) (2006) 1274-1284.

[172] N. Yoshida, M. Tamura, M. Kinjo, Fluorescence correlation spectroscopy: A new tool for probing the microenvironment of the internal space of organelles, Single Molecules 1(4) (2000) 279-283.

[173] M. Sznitowska, S. Janicki, A. Williams, S. Lau, A. Stolyhwo, pH-induced investigated modifications to stratum corneum lipids using thermal, spectroscopic, and chromatographic techniques, Journal of Pharmaceutical Sciences 92(1) (2003) 173-179.

[174] R.J. Goldston, P.H. Rutherford, Introduction to plasma physics, Institute of Physics Publishing, Philadelphia, 1995.

[175] J.A. Lane, J.A. Saxton, Dielectric dispersion in pure polar liquids at very high radio frequencies. 3. The effect of electrolytes in solution, Proceedings of the Royal Society of London Series A - Mathematical and Physical Sciences 214(1119) (1952) 531-545.

[176] C.G. Malmberg, A.A. Maryott, Dielectric constant of water from 0-degrees-C to 100-degrees-C, Journal of Research of the National Bureau of Standards 56(1) (1956) 1-8.

[177] A. Stogryn, Equations for Calculating Dielectric Constant of Saline Water, IEEE Transactions on Microwave Theory and Techniques 19(8) (1971) 733-736.

[178] M.R. Prausnitz, J.S. Noonan, Permeability of cornea, sclera, and conjunctiva: A literature analysis for drug delivery to the eye, Journal of Pharmaceutical Sciences 87(12) (1998) 1479-1488.

[179] Y. Kim, P.J. Ludovice, M.R. Prausnitz, Optimization of transdermal delivery using magainin pore-forming peptide, Journal of Physics and Chemistry of Solids, *in press.*

[180] D.A. Edwards, M.R. Prausnitz, R. Langer, J.C. Weaver, Analysis of enhanced transdermal transport by skin electroporation, Journal of Controlled Release 34(3) (1995) 211-221.

[181] J.D. Oliver, S. Anderson, J.L. Troy, B.M. Brenner, W.M. Deen, Determination of glomerular size-selectivity in the normal rat with ficoll, Journal of the American Society of Nephrology 3(2) (1992) 214-228.

[182] R. Lai, H. Liu, W.H. Lee, Y. Zhang, An anionic antimicrobial peptide from toad Bombina maxima, Biochemical and Biophysical Research Communications 295(4) (2002) 796-799.

[183] O.S. Belokoneva, H. Satake, E.L. Mal'tseva, N.P. Pal'mina, E. Villegas, T. Nakajima, G. Corzo, Pore formation of phospholipid membranes by the action of two hemolytic arachnid peptides of different size, Biochimica Et Biophysica Acta-Biomembranes 1664(2) (2004) 182-188.

[184] L. EhretSabatier, D. Loew, M. Goyffon, P. Fehlbaum, J.A. Hoffmann, A. vanDorsselaer, P. Bulet, Characterization of novel cysteine-rich antimicrobial peptides from scorpion blood, Journal of Biological Chemistry 271(47) (1996) 29537-29544.

[185] S.E. Blondelle, E. Takahashi, K.T. Dinh, R.A. Houghten, The antimicrobial activity of hexapeptides derived from synthetic combinatorial libraries, Journal of Applied Bacteriology 78(1) (1995) 39-46.

[186] P. Fehlbaum, P. Bulet, S. Chernysh, J.P. Briand, J.P. Roussel, L. Letellier, C. Hetru, J.A. Hoffmann, Structure-activity analysis of thanatin, a 21-residue inducible insect defense peptide with sequence homology to frog skin antimicrobial peptides, Proceedings of the National Academy of Sciences of the United States of America 93(3) (1996) 1221-1225.

[187] M. Frohm, B. Agerberth, G. Ahangari, M. StahleBackdahl, S. Liden, H. Wigzell, G.H. Gudmundsson, The expression of the gene coding for the antibacterial peptide LL-37 is induced in human keratinocytes during

inflammatory disorders, Journal of Biological Chemistry 272(24) (1997) 15258-15263.

[188] T. Miyata, F. Tokunaga, T. Yoneya, K. Yoshikawa, S. Iwanaga, M. Niwa, T. Takao, Y. Shimonishi, Antimicrobial Peptides, Isolated from horseshoe-crab hemocytes, Tachyplesin-II, and Polyphemusin-I and Polyphemusin-II: Chemical structures and biological-activity, Journal of Biochemistry 106(4) (1989) 663-668.

[189] C.B. Park, J.H. Lee, I.Y. Park, M.S. Kim, S.C. Kim, A novel antimicrobial peptide from the loach, Misgurnus anguillicaudatus, Febs Letters 411(2-3) (1997) 173-178.

[190] P.E.G. Thoren, D. Persson, M. Karlsson, B. Norden, The Antennapedia peptide penetratin translocates across lipid bilayers - the first direct observation, Febs Letters 482(3) (2000) 265-268.

[191] T. Nakamura, H. Furunaka, T. Miyata, F. Tokunaga, T. Muta, S. Iwanaga, M. Niwa, T. Takao, Y. Shimonishi, Tachyplesin, a class of antimicrobial peptide from the hemocytes of the horseshoe-crab (Tachypleus-Tridentatus): Isolation and chemical-structure, Journal of Biological Chemistry 263(32) (1988) 16709-16713.

[192] W.T. Heller, A.J. Waring, R.I. Lehrer, T.A. Harroun, T.M. Weiss, L. Yang, H.W. Huang, Membrane thinning effect of the beta-sheet antimicrobial protegrin, Biochemistry 39(1) (2000) 139-145.

[193] Y. Park, S.N. Park, S.C. Park, S.O. Shin, J.Y. Kim, S.J. Kang, M.H. Kim, C.Y. Jeong, K.S. Hahm, Synergism of Leu-Lys rich antimicrobial peptides and chloramphenicol against bacterial cells, Biochimica Et Biophysica Acta-Proteins and Proteomics 1764(1) (2006) 24-32.

[194] B. Agerberth, H. Gunne, J. Odeberg, P. Kogner, H.G. Boman, G.H. Gudmundsson, Fall-39, a putative human peptide antibiotic, is cysteine-free and expressed in bone-marrow and testis, Proceedings of the National Academy of Sciences of the United States of America 92(1) (1995) 195-199.

[195] I.H. Lee, C.Q. Zhao, Y. Cho, S.S.L. Harwig, E.L. Cooper, R.I. Lehrer, Clavanins, alpha-helical antimicrobial peptides from tunicate hemocytes, Febs Letters 400(2) (1997) 158-162.

[196] M.E. Selsted, M.J. Novotny, W.L. Morris, Y.Q. Tang, W. Smith, J.S. Cullor, Indolicidin, a novel bactericidal tridecapeptide amide from neutrophils, Journal of Biological Chemistry 267(7) (1992) 4292-4295.

[197] B. Schittek, R. Hipfel, B. Sauer, J. Bauer, H. Kalbacher, S. Stevanovic, M. Schirle, K. Schroeder, N. Blin, F. Meier, G. Rassner, C. Garbe, Dermcidin: a

novel human antibiotic peptide secreted by sweat glands, Nature Immunology 2(12) (2001) 1133-1137.

[198] I. Cornut, K. Buttner, J.L. Dasseux, J. Dufourcq, The Amphipathic alpha-helix concept - Application to the de-novo design of ideally amphipathic Leu, Lys peptides with hemolytic-activity higher than that of melittin, Febs Letters 349(1) (1994) 29-33.

[199] T.C. Terwilliger, D. Eisenberg, The structure of melittin. 2. Interpretation of the structure, Journal of Biological Chemistry 257(11) (1982) 6016-6022.

VITA

Yeu-chun Kim was born in Seoul, Korea on December 23, 1974. In 1993, he attended Yonsei University, Korea and was public service personnel to do military service from 1995 to 1996. He graduated from Yonsei University with a Bachelor of Science in Chemical Engineering in Feburary, 1999. In March, 1999, he attended the Korea Avanced in Science and Technology (KAIST) in Taejon, Korea and graduated in August, 2001 with a Master of Science in Chemical Engineering. He was a researcher at the Korea Research Institute of Bioscience and Biotechnology (KRIBB), Taejon, Korea joint program from 2000 to 2001. In August 2002, he attended the Georgia Institute of Technology in Atlanta, Georgia where he was accepted as a Ph.D. candidate in the School of Chemical and Biomolecular Engineering. His dissertation title was "TRANSDERMAL DRUG DELIVERY ENHANCED BY MAGAININ PEPTIDE." He defended his doctoral thesis on October 12, 2007 and obtained his Ph.D. in Chemical Engineering with a minor in Management in December 2007.